



U.S. Department
of Transportation

**National Highway
Traffic Safety
Administration**



DOT HS 812 919

April 2020

Investigation of Potential Design and Performance Criteria for Booster Seats Through Volunteer and Dynamic Testing

DISCLAIMER

This publication is distributed by the U.S. Department of Transportation, National Highway Traffic Safety Administration, in the interest of information exchange. The opinions, findings and conclusions expressed in this publication are those of the authors and not necessarily those of the Department of Transportation or the National Highway Traffic Safety Administration. The United States Government assumes no liability for its contents or use thereof. If trade or manufacturers' names are mentioned, it is only because they are considered essential to the object of the publication and should not be construed as an endorsement. The United States Government does not endorse products or manufacturers.

Suggested APA Format Citation:

Klinich, K. D., Jones, M. H., Manary, M. A., Ebert, S. H., Boyle, K. J., Malik, L., ... Reed, M. P. (2020, April). *Investigation of potential design and performance criteria for booster seats through volunteer and dynamic testing* (Report No. DOT HS 812 919). Washington, DC: National Highway Traffic Safety Administration.

Technical Report Documentation Page

1. Report No. DOT HS 812 919	2. Government Accession No.	3. Recipient's Catalog No.	
4. Title and Subtitle Investigation of Potential Design and Performance Criteria for Booster Seats Through Volunteer and Dynamic Testing		5. Report Date April 2020	
		6. Performing Organization Code	
7. Authors Klinich, Kathleen D., Jones, Monica H., Manary, Miriam A., Ebert, Sheila H., Boyle, Kyle J., Malik, Laura, Orton, Nichole R., Reed, Matthew P.,		8. Performing Organization Report No.	
9. Performing Organization Name and Address University of Michigan Transportation Research Institute 2901 Baxter Rd. Ann Arbor MI 48109		10. Work Unit No. (TRAIS)	
		11. Contract or Grant No. DTNH2215D00017	
12. Sponsoring Agency Name and Address National Highway Traffic Safety Administration 1200 New Jersey Avenue SE Washington, DC 20590		13. Type of Report and Period Covered January 2014-July 2018	
		14. Sponsoring Agency Code	
15. Supplementary Notes			
16. Abstract The purpose of this research was to explore candidate booster performance metrics that have the potential to identify less effective booster systems, since current FMVSS No. 213 booster performance requirements can be met without a booster. A combination of volunteer testing of belt fit and posture along with dynamic sled tests of booster seats was employed to achieve the project goals. Posture and belt fit were measured in 24 child volunteers 4 to 12 years old. Children were measured in three vehicles and three laboratory seating conditions selected to provide cushion lengths and belt geometries representing the range found in late model vehicle rear seats. Six different booster seats, as well as the no-booster condition, were evaluated. Test conditions were also evaluated using 6YO, 10YO, and small female anthropomorphic test devices (ATDs). Posture differences between children and ATDs were greater in the no-booster condition and the two lower backless boosters compared to the four boosters that raised the occupant by 75 mm or more, but the differences were not large enough to warrant recommendation of an alternate seating procedure. The shoulder belt tended to be closer to the ATD necks than those of child volunteers; the lap belt was always further below the ATD ASIS than the volunteer's belt. To provide a more realistic test environment, dynamic testing was performed using a surrogate seat belt retractor on the most recent preliminary design update for the FMVSS No. 213 seat assembly. Eleven booster products were evaluated, as well as the no-booster condition, with six tests performed using the Hybrid III 10YO and 33 tests run with the Hybrid III 6YO. Possible metrics associated with good ATD kinematics (no submarining or rollout) were the difference between knee and head excursion, maximum torso angle, as well as lumbar MomentZ and ForceY. Tests with the surrogate retractor were as repeatable as testing with current FMVSS No. 213 conditions.			
17. Key Word booster seats, occupant submarining, FMVSS No. 213, performance metrics		18. Distribution Statement Document is available to the public from the National Technical Information Service, www.ntis.gov .	
19. Security Classif. (of this report)	20. Security Classif. (of this page)	21. No. of Pages 148	22. Price

TABLE OF CONTENTS

List of Figures	iv
List of Tables	vii
Background	1
Objectives	2
Methods: Dynamic Testing.....	3
<i>First (2015) dynamic sled test series</i>	<i>3</i>
Overview	3
Test Bench	3
Booster Seat Selection	4
<i>Second (2018) Dynamic Test Series</i>	<i>5</i>
Test Bench	5
Booster Seats.....	6
<i>Overall Dynamic Testing.....</i>	<i>9</i>
Belt Geometry Comparison	9
ATDs and Instrumentation	10
Test protocols	10
Matrix.....	11
Analysis Techniques.....	13
METHODS: VOLUNTEER TESTING	15
<i>Subject Recruitment and Characteristics</i>	<i>31</i>
<i>Data Analysis.....</i>	<i>32</i>
RESULTS: DYNAMIC TESTING.....	34
<i>Overview.....</i>	<i>34</i>
<i>Qualitative Assessment.....</i>	<i>38</i>
Kinematics.....	38
Testing Issues	41
<i>Repeatability</i>	<i>41</i>
Sled Pulse	41
Performance Measures	42
<i>Candidate Booster Metrics.....</i>	<i>48</i>
Submarining Measures	51
Static measures	57
RESULTS: VOLUNTEER TESTING	61
<i>Qualitative Review.....</i>	<i>61</i>
<i>Child Versus ATD Posture.....</i>	<i>64</i>
Fore-Aft Hip Position Versus 6YO ATD	65
Vertical Hip Position Versus 6YO ATD.....	67
Lower Extremity Posture Versus 6YO ATD.....	71
Head CG Position Versus 6YO and 10YO ATD.....	73

Comparison Between Child and 6YO ATD Posture.....	76
Lap Belt Fit.....	78
Shoulder Belt Fit.....	83
Discussion and Conclusions.....	87
<i>Volunteer Testing</i>	87
<i>Dynamic Testing</i>	89
Testing Conditions	89
Repeatability	90
Candidate booster metrics.....	90
References	94
Appendix A	99
Appendix B	106
Appendix C.....	125

LIST OF FIGURES

Figure 1. The preliminary FMVSS No. 213 bench used for the 2015 test series.4

Figure 2. Booster seats used for testing in 2015 test series: (a) TurboBooster, (b) Amp, (c) Incognito, and (d) Bubble Bum.....5

Figure 3. The preliminary FMVSS No. 213 bench used for the 2018 test series.6

Figure 4. Belt anchorage locations in 2015 and 2018 versions of the 213 seat assembly.9

Figure 5. 2015 tests (left) used a locking latchplate for the inboard anchor mount, while 2018 tests (right) used a sliding latchplate.10

Figure 6. Exterior view of test vehicles: Chevy Malibu, Toyota Corolla, Jeep Compass.19

Figure 7. Toyota Corolla20

Figure 8. Chevy Malibu.....20

Figure 9. Jeep Compass.....21

Figure 10. Reconfigurable laboratory seating seat assembly22

Figure 11. Subject seated in three laboratory conditions, with (left) and without (right) a booster.....24

Figure 12. D-ring angles across vehicle and lab conditions, compared to fleet +/- 1STD.25

Figure 13. Inboard angles across vehicle and lab conditions, compared to fleet +/- 1STD.....25

Figure 14. Outboard angles across vehicle and lab conditions, compared to fleet +/- 1STD.26

Figure 15. Side view (left) and front view (right) belt geometries.26

Figure 16. Examples of standing and seated postures scanned for each subject.28

Figure 17. Hardseat used for measuring subject reference landmarks.....28

Figure 18. Compensation for adiposity at the PSIS flesh margin (A) and ASIS flesh margin (B) separating the depressed surface landmark from the underlying bone landmark29

Figure 19. Distribution of test subjects by height, weight, and group.32

Figure 20. Comparison between 2015 and 2018 tests run with the no-booster condition: peak excursion and initial shoulder belt fit.39

Figure 21. Design of the Evenflo Amp (left) offers some lateral head protection at peak excursion, compared to more typical kinematics provided by Aidia Pathfinder (right), where the head moves forward out of the sides of the booster.39

Figure 22. Shoulder belt loading ATD arm with Combi Kobuk.40

Figure 23. Kinematics of ATD using the Mifold device.....40

Figure 24. Comparison of peak head excursion for 6YO (top row) and 10YO (bottom row) in no-booster (left), Cosco Easy Elite (center), and Baby Trend Hybrid 3-in-1 (right).41

Figure 25. Sled pulse overlay of 33 tests with 6YO ATD42

Figure 26. Sled pulse overlay of six tests with 10YO ATD.....42

Figure 27. Overlap of head resultant acceleration for tests with 6YO ATD.....45

Figure 28. Overlay of chest resultant acceleration for tests with 6YO ATD.46

Figure 29. Overlay of change in chest angle for tests with 6YO ATD.47

Figure 30. HIC(36) versus HIC(15).....49

Figure 31. Peak head resultant acceleration versus 3 ms chest clip acceleration.50

Figure 32. Head excursion versus knee excursion.51

Figure 33. Side view peak of action images for test with (left) and without (right) occupant submarining.....52

Figure 34. Change in thorax angle versus knee-head excursion.....53

Figure 35. Maximum thorax angle versus knee-head excursion.53

Figure 36. Neck axial load for 6YO tests.....54

Figure 37. Lumbar MomentZ for 6YO Tests.....	55
Figure 38. Lumbar ForceY for 6YO tests.....	56
Figure 39. Lumbar MomentZ for 10YO tests.....	56
Figure 40. Lumbar ForceY for 10YO tests.....	57
Figure 41. Lap belt score versus knee-head excursion.....	58
Figure 42. Shoulder belt score versus knee-head excursion.....	58
Figure 43. Boost amount versus knee-head excursion.....	59
Figure 44. IIHS rating versus knee-head excursion.....	60
Figure 45. Comparison of fore-aft hip position (relative to H36YO) in seat assembly conditions: Z, B, and L. Negative values indicate that the child volunteer is forward of the 6YO ATD.....	66
Figure 46. Comparison of fore-aft hip position (relative to H36YO) in vehicle conditions: Toyota, Jeep, and Malibu. Negative values indicate that the child volunteer is forward of the 6YO ATD.....	67
Figure 47. Comparison of vertical hip position (relative to H36YO) in seat assembly conditions: Z, B, and L. A positive value indicates that the child’s hip position is above the 6YO ATD.....	69
Figure 48. Comparison of vertical hip position (relative to H36YO) in vehicle conditions: Toyota, Jeep, and Malibu. A positive value indicates that the child’s hip position is above the 6YO ATD.....	70
Figure 49. Difference in knee position (fore-aft X position, vertical Z position).....	72
Figure 50. Distribution of the included knee angle. Box plots illustrate the distribution of the child lower extremity postures and color-coded filled circles overlay the included knee angle for the 6YO ATD installed in each booster, across the mockup and vehicle configurations.....	73
Figure 51. Location of the HeadCG of child participants and ATDs (6YO and 10YO) across all booster and mockup configurations. ATDs are coded by both booster and ATD.....	74
Figure 52. Location of the HeadCG of child participants and ATDs (6YO, 10YO, 5 th , 50 th) across all booster and vehicle configurations. ATDs are coded by both booster and ATD...74	74
Figure 53. 6YO, 10YO, and 5 th ATDs on the Britax (A) (left to right) in Toyota.....	75
Figure 54. 5 th on Britax (A) and 50 th on seat in Toyota (better view of roof).....	75
Figure 55. 6YO, 10YO, 5 th ATDs on the Britax (A) and 50 th on vehicle seat (left to right) in Jeep (vehicle with taller ceiling height).....	76
Figure 56. Association between the mean child head CG location and the 6YO ATD head CG location. Data points show the mean child head CG X and Z positions for each booster and package configuration.....	76
Figure 57. Association between the mean child hip X and Z position and the 6YO ATD hip. Data points show the mean child hip X and Z positions for each booster and package configuration.....	77
Figure 58. Box plots of fore-aft lap belt position in mockup conditions: B-Z, B-B, and B-L.....	79
Figure 59. Box plots of fore-aft lap belt position in vehicle conditions: Toyota, Jeep, and Malibu.....	80
Figure 60. Box plots of the vertical lap belt position across all the boosters in mockup conditions: B-Z, B-B, and B-L.....	81
Figure 61. Box plots of the vertical lap belt position in vehicle conditions: Toyota, Jeep, and Malibu. A positive value indicates that the lap belt is above ASIS bone.....	82

Figure 62. Lap belt position of volunteers relative to ASIS compared to 6YO ATD (filled circles).....	83
Figure 63. Lap belt position of volunteers relative to ASIS compared to 10YO ATD (filled squares).....	83
Figure 64. Distribution of the shoulder belt score (mm) across all the boosters in mockup conditions: B-Z, B-B, and B-L.....	85
Figure 65. Distribution of the shoulder belt score (mm) across all the boosters in vehicle conditions: Toyota, Jeep, and Malibu.....	86
Figure 66. Head CG vertical location versus subject stature, relative to target zone defined by locations of small female and midsize male ATDs.....	88
Figure 67. No-booster condition with 6YO (left) and 10YO (right) shows submarining tendencies on 2018 version of the bench.....	92

LIST OF TABLES

Table 1. Boosters used in 2018 dynamic testing series.....	8
Table 2. Test Matrix.....	12
Table 3. Proposed repeatability criteria.....	14
Table 4. Belt anchorage coordinates used in ATD belt fit evaluation.....	16
Table 5. Range of LBS and SBS for each booster; photos show the 30 degree lap belt position with the fore shoulder belt position.....	17
Table 6. Boosters used in volunteer testing, with designations and color codes for each booster.....	18
Table 7. Vehicle belt geometries compared to fleet dimensions.....	19
Table 8. Laboratory belt geometries compared to fleet measurements.....	23
Table 9. Anthropometry.....	27
Table 10. Landmarks digitized in hardseat.....	29
Table 11. Volunteer test matrix for Subject Groups I, II, and III*.....	30
Table 12. Points and streams digitized in the mockup.....	30
Table 13. Points and streams digitized in the vehicle.....	31
Table 14. Anthropometry summary for each group.....	32
Table 15. Anthropometry summary for all subjects.....	32
Table 16. Summary of dynamic test results.....	35
Table 17. Range of ATD measures across test with same booster.....	43
Table 18. Child posture laboratory seating conditions.....	61
Table 19. Child posture in vehicle conditions.....	63
Table 20. N, mean, and standard deviation of fore-aft hip position for each booster.....	66
Table 21. N, mean, standard deviation of fore-haft hip position for each booster.....	68
Table 22. Regression results predicting mean child head CG position from 6YO ATD head CG.....	77
Table 23. Regression results predicting mean child hip position from 6YO ATD hip position.....	78
Table 24. Current and proposed allowable occupant height ranges for optimal head vertical location.....	88

BACKGROUND

Belt-positioning booster seats are recommended for use by children who have outgrown forward-facing harnessed child restraint systems (CRS), but are too small to achieve good belt fit using vehicle lap-shoulder belts. The latest national estimates of booster seat use indicate that 45 percent of children 4 to 7 years old use booster seats (Li et al. 2016), although to achieve good belt fit, most children under age 11 would benefit from using boosters (Klinich et al. 2016). Field data indicates that children 4 to 8 using boosters are 45 percent less likely to sustain injury in crashes compared to children using seat belts alone (Arbogast, Jermakian, Kallan, & Durbin, 2009, Durbin., Elliott, & Winston, 2003).

Several studies of child posture and belt fit (Reed et al. 2008, 2009, Bilston & Sagar, 2007) have identified how boosters reduce injury risk by improving belt fit. First, the booster repositions the child's body upward to achieve a skeletal position similar to that of an adult, for whom the seat belt system, air bags, and interior padding requirements are nominally designed. Historically, products have achieved this by boosting the child's seated position upward by at least 75 to 100 mm, so the lap belt crosses the body at the top of the thigh close to the pelvic bone, and the shoulder belt crosses the clavicle, the center of the sternum, and the opposite hip near the greater trochanter of the femur. This vertical shift also produces a more advantageous side view lap belt angle that prevents the lap belt from shifting upward during a crash. Second, boosters may have lap and shoulder belt guides to help establish and maintain good belt fit for the entire duration of travel. Third, a booster that raises the child effectively shortens the cushion length, allowing the child to sit more upright and maintain a comfortable bent-leg posture throughout a trip, which also contribute to better belt fit.

The most recent revision to FMVSS No. 213 protocols included an updated seating procedure that places the anthropomorphic test device (ATD) slightly forward in the booster (using a positioning pad) relative to prior versions of the standard; the seating procedure was developed from studies of volunteer posture in boosters. Some current commercial boosters do not significantly raise the child's body upward. Since the ATD seating procedures are based on prior studies that evaluated boosters that provided at least 75 mm of boost, there are concerns that the seating procedures developed for taller boosters may not be suitable for positioning ATDs in a realistic manner on lower boosters.

The measures currently used to assess dynamic performance in FMVSS No. 213 include head excursion, knee excursion, head injury criteria (HIC) (36 ms), and 3 ms chest clip acceleration. The dynamic requirements of FMVSS No. 213 can currently be met on the existing bench without using any booster, raising concerns that the FMVSS No. 213 criteria for boosters are not demanding enough to prevent ineffective boosters from entering the US market.

The current FMVSS No. 213 seat assembly uses fixed anchors to mount the lap and shoulder portions of the belt. In vehicles, children use boosters with production seat belt systems that includes shoulder belt retractors. A shoulder belt retractors allow some initial spool-out of the belt, letting the occupant rotate forward to allow better engagement of the belt system with the shoulder and pelvis. Manary et al. (2018) developed a surrogate seat belt retractor that produced occupant kinematics similar to a production seat belt system. Using a more realistic belt system during dynamic testing of boosters may be able to help

identify less effective boosters. In addition, NHTSA has published preliminary changes to the bench of the FMVSS No. 213 seat assembly, as well as the belt anchorage geometry (NHTSA, 2015, 2018), such that the test setup more closely resembles the stiffness and geometry seen in more recent vehicles.

Previous research has shown that some aspects of the Hybrid III family of ATD's pelvic and shoulder designs have limited biofidelity with which the dummies can assess the risk of submarining of real children (Rouhana et al., 1990). More specifically, the front edge of the ATD pelvic block has been shown to be higher and more prominent than the anterior superior iliac spine (ASIS) of seated children, which are usually located at the same height as the top of the child thigh in automotive seating postures (Reed et al., 2009). In addition, the ATDs do not measure abdominal loading. Several research efforts have attempted to develop a more biofidelic pelvis and abdomen with improved instrumentation to assess submarining potential (Klinich et al. 2010, Hagedorn & Stammen 2015), but these tools are not yet available for regulatory booster assessment.

Despite the biofidelity issues with the Hybrid III pediatric ATDs, there are some candidate criteria with potential to improve the assessment of submarining. Klinich et al. (2010) found that the difference between knee and head excursion, as well as the amount of forward torso rotation, were associated with ATD kinematics that did and did not exhibit submarining kinematics characterized by minimal forward head motion coupled with substantial knee excursion. Hagedorn and Stammen (2015) monitored ASIS loads to characterize abdomen loading. Beck et al. (2015) assessed pelvic rotation as a candidate measure for differentiating submarining, but found knee excursion to be a better measure. Jermakian and Edwards (2017) used abdominal penetration, ASIS loads, knee minus head excursion and forward torso rotation to detect submarining potential in a range of boosters using the H3-6YO with and without the modified pelvis/abdomen hardware. The Insurance Institute for Highway Safety rates boosters on their ability to provide good static belt fit under belt geometries representing the range found in the vehicle fleet rear seat (IIHS 2017). Canadian child restraint regulations include a stiffness requirement based on compression testing (Transport Canada, 2010).

OBJECTIVES

The purpose of this research was to explore candidate booster performance metrics that may have the potential to identify less effective booster systems. A combination of volunteer testing of belt fit and posture and dynamic sled tests of booster seats was employed to achieve the project goals. Dynamic testing was performed using a surrogate seat belt retractor to provide a more realistic restraint system, as well as the most recent preliminary design update for the FMVSS No. 213 seat assembly.

METHODS: DYNAMIC TESTING

First (2015) dynamic sled test series

Overview

The initial series of dynamic tests to develop booster performance metrics was conducted in 2014 and 2015. In this series, exploring booster metrics was a secondary goal to developing a procedure for using a surrogate seat belt retractor that provides a more realistic shoulder belt performance compared to the static shoulder belt currently used in FMVSS No. 213. Test results summarizing the development of the surrogate retractor are found in Manary et al. (2018). Tests from this previous research program used the initial prototype retractor design (SR1) and the bench design and belt anchorage locations from the August 2015 drawings of the FMVSS No. 213 test bench. The surrogate retractor settings were set to provide approximately 50 mm of shoulder belt spool-out from the retractor, which best matched results from production seat belt retractors.

Test Bench

The initial set of tests was performed using a preliminary version of the updated FMVSS No. 213 test bench (shown in Figure 1 and hereafter referred to as the 2015 bench) that has been developed as a potential replacement for the current FMVSS No. 213 frontal impact bench implemented in 2005. The 2015 bench consists of the vehicle seat portion of the seat assembly referenced in NHTSA's Docket NHTSA-2013-0055-0002 (Summers, 2015a)], except the height of the lower anchors was reduced by 40 mm (per NHTSA's directive). The bench also differs from the May 2015 drawings in that the seat back has been extended upwards by 50 mm to create a longer/taller seat back support surface. In addition, between the tests run in 2014 (not included in this report) and 2015, the shoulder belt upper anchor point was moved to the location on drawings posted in Docket No. NHTSA-2013-0055-0008 (Summers, 2015b.) This bench was mounted facing forward on the impact sled at the University of Michigan Transportation Research Institute (UMTRI). It was positioned and defined with an origin so excursion measurements of ATDs with this bench would be consistent with those measured in tests performed on the current FMVSS No. 213 bench. To accomplish this, the location of the Z point was established by using the SAE J826 manikin to define the H-point-to-Z-point relationship on the current FMVSS No. 213 bench and then used to establish the same Z-point relative to the measured H-point on the 2015 bench.



Figure 1. The preliminary FMVSS No. 213 bench used for the 2015 test series.

Booster Seat Selection

The booster seats selected for the 2015 series include the backless version of the Graco TurboBooster, the Evenflo Amp, the Safety 1st Incognito, and the Bubble Bum inflatable, all shown in Figure 2. The TurboBooster and the Amp were selected because they provide both vertical boosting of the occupant and have rigid physical features to guide the lap belt onto the child's pelvis. The Incognito and the Bubble Bum were selected because they provide a lower level or, in the case of the inflatable product, variable level of vertical boost (the Bubble Bum passes FMVSS No. 213 requirements while completely deflated) and they have flexible pelvic belt guides. All boosters selected for the initial phase of testing were backless so that no booster feature would interfere with the evaluation of the surrogate retractor. All booster seats were used per the manufacturers' instructions. The TurboBooster and Amp have a shoulder belt positioning clip, but since the shoulder belt was initially routed well on the ATD's shoulder, use of the clip was not necessary per the manufacturers' instructions.



Figure 2. Booster seats used for testing in 2015 test series:
a) TurboBooster, b) Amp, c) Incognito, and d) Bubble Bum

Second (2018) Dynamic Test Series

Test Bench

The second test series was performed on an updated version of the preliminary FMVSS No. 213 bench constructed in 2018 and shown in Figure 3. This seat assembly was constructed using drawings dated July 2017 provided by NHTSA; the final version of these drawings was dated August 2018 and published in NHTSA Docket 2013-0055-0015 (Summers, 2015c). The main differences between the 2015 and 2018 seating assemblies were a change in the three-point belt anchoring geometry and the use of a sliding latchplate at the inboard lap belt anchor, as well as an even taller seat back. Of note, the mounting fixture for the 2018 upper shoulder belt D-ring was more rigid than the D-ring mounting fixture used in the 2015 series. When reviewing overhead video, the D-ring fixture in the 2015 series has some visible deflection, which is not present in the D-ring fixture in the 2018 series.



Figure 3. The preliminary FMVSS No. 213 bench used for the 2018 test series.

Booster Seats

To choose eleven boosters for the 2018 dynamic test series, we first reviewed the 2017 list of booster seats that is compiled on the American Academy of Pediatrics (AAP, 2017) website. Based on the types of products listed, the following distribution of different booster styles reflects the proportions available on the market: three backless, three highback-to-backless, one highback only, two 3-in-1, and two combination.

The next step was to review the booster ratings of the Insurance Institute for Highway Safety (IIHS 2017). Most boosters currently receive a “best bet” rating. Therefore, we chose to also consider products that were rated by IIHS as “not recommended”, “good bet”, and “check fit”, to determine if less than “best bet” ratings of belt fit were associated with adverse dynamic testing outcomes. This led us to include the Cosco Easy Elite (not recommended), Baby Trend 3n1 (good bet), Combi Kobuk Air Thru (good bet), and Evenflo Big Kid Amp Highback (check fit).

Another goal of this study was to examine the posture of children and ATDs in boosters that did not “boost” as much as traditional booster products. We reviewed

product photos of boosters and chose the Lil Fan backless (best bet), Mifold¹ (not rated), and Safety 1st Incognito (not rated) using this criterion.

The last four boosters were chosen to fill in the targeted distribution of booster styles while trying to vary manufacturers and belt-routing features. Within a manufacturer, lower cost options were preferred. The remaining four boosters, all rated as “best bets”, were Graco 4ever, Britax Pioneer, Graco TurboBooster highback, and Cybex Solution X-Fix. After the initial selection process, the Cybex Solution X-Fix appears to be discontinued for sale in the US, so the AIDIA Pathfinder, also rated as a Best Bet by IIHS, was substituted. Table 1 shows photos of each booster seat as well as the style.

¹ While the Mifold may not be a “booster” under FMVSS No. 213, with NHTSA’s approval, UMTRI included the product in this study as it had features, such as a very low profile and different belt routing, that were of interest to this research project.

Table 1. Boosters Used in 2018 Dynamic Testing Series

Backless			
	Lil Fan Backless Box Seat	Mifold Grab and Go	Safety 1 st incognito
Highback to backless			
	Graco TurboBooster Highback	Evenflo Amp High Back	Combi Kobuk
3-in-1			
	Graco 4Ever 4in 1	Cosco Easy Elite	
Combination			
	Baby Trend Hybrid 3N1	Britax Pioneer Harness2Booster	
		Highback only	

Overall Dynamic Testing

Belt Geometry Comparison

Figure 4 shows differences in belt anchor locations between the 2015 and 2018 editions of the FMVSS No. 213 seat assembly, using the bench Z-point as the origin. In the 2018 version, the D-ring is higher and further back compared to tests performed with the 2015 version of the seat assembly, and the distance between the lower belt anchors is smaller. This results in a change in front-view angle from about 55 to 59 degrees, which generally brings the belt closer to the ATD's neck. The other key difference in belt systems is that our 2015 tests with the surrogate retractor used a fixed inboard anchor mount, while the 2018 version uses a sliding latchplate, as shown in Figure 5.

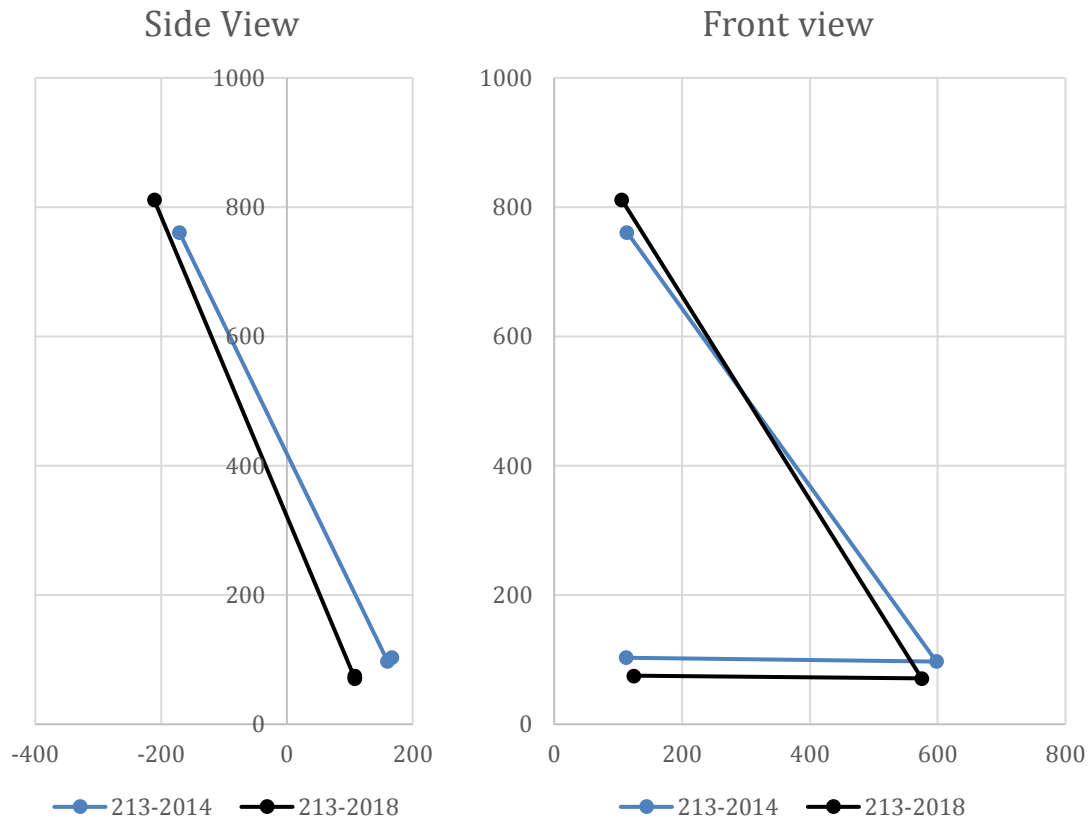


Figure 4. Belt anchorage locations in 2015 and 2018 versions of the 213 seat assembly.



Figure 5. 2015 tests (left) used a locking latchplate for the inboard anchor mount, while 2018 tests (right) used a sliding latchplate.

Testing performed in the 2015 series used the initial surrogate retractor design (SR1), described by Manary et al. (2018). The surrogate retractor used in the 2018 tests (SR2) includes improvements of roller bearings to the spindle and revised framing elements developed by NHTSA.

ATDs and Instrumentation

The Hybrid III 6YO ATD (part 572 subpart S) was used in both series tests to represent a child occupant using a booster seat. In the 2018 series of tests, six tests were also performed with the Hybrid III 10YO ATD (part 572 subpart T). The ATDs were instrumented with head, chest and pelvic accelerometers, upper neck and lumbar 6-axis load cells, torso and pelvic angular rate sensors, along with upper and lower ASIS load cells. Lap belt loads were measured in all tests. Shoulder belt loads were measured using an instrumented belt anchorage only in the 2015 series of tests to avoid shifting of the effective belt anchorage location and interference with the retractor performance. Head and knee excursion were measured using ImageJ using the Z-point as the reference. A silicone lap shield was used to prevent the lap belt from dropping into the gap at the front of the ATD pelvis and engaging the ATD in a nonbiofidelic manner.

Belt spool-out was measured using the overhead camera view and ImageJ digitizing software. The location where the belt webbing exited the D-ring was marked so it was visible on the camera. The location of this mark was digitized at time zero and peak excursion; the linear distance between these was calculated to be the belt spool-out. For the 2018 series of tests, additional targets were added to the belt webbing above the retractor and a camera was focused on the belt to allow an alternate method of spool-out measurement. Using the sideview camera, the amount of spool-out was calculated by digitizing the movement of both the upper and lower targets relative to fixed targets and averaging the displacement results using ImageJ. There was no substantial differences in the spool-out measured with the top and bottom targets (~3mm or less).

Test protocols

The current FMVSS No. 213 test protocol was used to place the booster on the bench and the Hybrid III 6YO or 10YO ATD in the seat using the current FMVSS No. 213 dummy positioning process (TP-213). Two high contrast targets were placed on each moving part

of each CRS. A FARO Arm 3D coordinate measurement system was used to document the position of the ATD, booster, belt anchorage locations and belt fit in each test. In tests with the surrogate retractor, the belt tension was dictated by the retractor spring.

In the 2015 series of tests, one set of seat pan foam was used for all tests and the tests were timed to run at least one hour apart to allow foam recovery. In the 2018 series, the seat pan foam was switched out every test, alternating between two sets of foam. During the 2018 series, the foam components were checked using the IFD (indentation force deflection) test twice throughout the series and showed minimal change in stiffness characteristics. For the 2018 test series, coarse sand paper was mounted to the metal seat back and seat pan to minimize foam movement. In addition, tests using the J826 manikin to determine the H-point of the 2018 bench showed minimal geometric differences (< 5 mm for all key measures) between the two sets of foam used in the 2018 test series.

In the 2015 series of tests, setting the belt retractor to allow approximately 50 mm of spool-out provided a dynamic response that was similar to one of the production belts being used for comparison. The desired amount of spool-out was set by measuring 50 mm of webbing payout at the top of the retractor during setup. The 2018 series of tests used an updated and enhanced retractor (SR2) provided by NHTSA. In tests run by NHTSA to assess the updated prototype, they shared a new procedure of setting the spool-out with a half turn release of the spindle. In an attempt to create consistency with the VRTC tests, this protocol was used in the first six tests run in the 2018 series. However, in the initial UMTRI tests the ATD was experiencing head contact with legs/torso and the resulting HIC values were substantially higher than those from the UMTRI 2015 series, as well as the HIC values reported from the VRTC series, and dynamic retractor spool-out measured ~80 mm. Some of the high HIC values resulted from the head contacting the chest or legs and had less relationship with booster performance, which was the focus of the work. To understand the difference in results, we performed additional check out runs, varying the retractor slack used as well as modifying the sled pulse. We found that using a quarter turn of slack and a less severe FMVSS No. 213 pulse provided results that were more consistent with the 2015 series of tests and better suited to evaluating the differences between booster performance. Thus, all remaining tests were conducted with the quarter turn of slack and the pulse at the less severe end of the FMVSS No. 213 corridor. Because of the different test conditions, results from the first six tests are included in the data summary, but not considered in analysis of repeatability or development of potential booster metrics. Appendix A contains updated instructions on using the surrogate retractor.

Matrix

The full sled matrix from both series is shown in Table 2. SR1 refers to the surrogate retractor prototype developed in 2014, while SR2 refers to the improved surrogate retractor prototype developed in 2018. The Q or H refers to setting a quarter or half turn of slack in the retractor. For the belt, LLP refers to the locking latch plate used in the 2015 tests, while SLP refers to the sliding latch plate used in the 2018 tests. The belt geometry refers to the drawing package of August 2015 or July 2017.

Table 2. Test Matrix

Test ID	ATD	Bench	Retractor/ Setting	Belt	Booster Model	Booster Style
NT1508	6YO	2015	SR1/Q	LLP, 815	Graco TurboBooster	Backless
NT1509	6YO	2015	SR1/Q	LLP, 815	Graco TurboBooster	Backless
NT1510	6YO	2015	SR1/Q	LLP, 815	BubbleBum	Backless
NT1511	6YO	2015	SR1/Q	LLP, 815	BubbleBum	Backless
NT1512	6YO	2015	SR1/Q	LLP, 815	Evenflo Amp	Backless
NT1513	6YO	2015	SR1/Q	LLP, 815	Incognito	Backless
NT1514	6YO	2015	SR1/Q	LLP, 815	None	None
NT1515	6YO	2015	SR1/Q	LLP, 815	Graco TurboBooster	Backless
NT1801	6YO	2018	SR2/H	SLP, 717	Graco TurboBooster	Backless
NT1802	6YO	2018	SR2/H	SLP, 717	Cosco Easy Elite	3-in-1
NT1803	6YO	2018	SR2/H	SLP, 717	Britax Pioneer	Combination
NT1804	6YO	2018	SR2/H	SLP, 717	Graco 4ever	3-in-1
NT1805	6YO	2018	SR2/H	SLP, 717	None	None
NT1806	6YO	2018	SR2/H	SLP, 717	Graco TurboBooster	Backless
NT1807	6YO	2018	SR2/Q	SLP, 717	Evenflo BK Amp	Highback
NT1808	6YO	2018	SR2/Q	SLP, 717	Combi Kobuk	Highback
NT1809	6YO	2018	SR2/Q	SLP, 717	Aidia Pathfinder	Highback
NT1810	6YO	2018	SR2/Q	SLP, 717	BT Hybrid 3n1	Combination
NT1811	6YO	2018	SR2/Q	SLP, 717	Graco TurboBooster	Highback
NT1812	6YO	2018	SR2/Q	SLP, 717	Cosco Easy Elite	3-in-1
NT1813	6YO	2018	SR2/Q	SLP, 717	Britax Pioneer	Combination
NT1814	6YO	2018	SR2/Q	SLP, 717	Graco 4ever	3-in-1
NT1815	6YO	2018	SR2/Q	SLP, 717	Aidia Pathfinder	Highback
NT1816	6YO	2018	SR2/Q	SLP, 717	Evenflo BK Amp	Highback
NT1817	6YO	2018	SR2/Q	SLP, 717	Combi Kobuk	Highback
NT1818	6YO	2018	SR2/Q	SLP, 717	BT Hybrid 3n1	Combination
NT1819	6YO	2018	SR2/Q	SLP, 717	Cosco Easy Elite	3-in-1
NT1820	6YO	2018	SR2/Q	SLP, 717	Graco TurboBooster	Highback
NT1821	6YO	2018	SR2/Q	SLP, 717	Britax Pioneer	Combination
NT1822	6YO	2018	SR2/Q	SLP, 717	Graco 4ever	3-in-1
NT1823	6YO	2018	SR2/Q	SLP, 717	Combi Kobuk	Highback
NT1824	6YO	2018	SR2/Q	SLP, 717	Aidia	Highback
NT1825	6YO	2018	SR2/Q	SLP, 717	Evenflo BK Amp	Highback
NT1826	6YO	2018	SR2/Q	SLP, 717	BT Hybrid 3n1	Combination
NT1827	6YO	2018	SR2/Q	SLP, 717	Graco TurboBooster	Highback
NT1828	6YO	2018	SR2/Q	SLP, 717	Lil Fan	Backless

Test ID	ATD	Bench	Retractor/ Setting	Belt	Booster Model	Booster Style
NT1829	6YO	2018	SR2/Q	SLP, 717	Lil Fan	Backless
NT1830	6YO	2018	SR2/Q	SLP, 717	Incognito	Backless
NT1831	6YO	2018	SR2/Q	SLP, 717	Lil Fan	Backless
NT1832	6YO	2018	SR2/Q	SLP, 717	Incognito	Backless
NT1833	6YO	2018	SR2/Q	SLP, 717	Mifold	Backless
NT1834	6YO	2018	SR2/Q	SLP, 717	Incognito	Backless
NT1835	6YO	2018	SR2/Q	SLP, 717	Mifold	Backless
NT1836	6YO	2018	SR2/Q	SLP, 717	Mifold	Backless
NT1837	6YO	2018	SR2/Q	SLP, 717	None	None
NT1838	6YO	2018	SR2/Q	SLP, 717	None	None
NT1839	6YO	2018	SR2/Q	SLP, 717	None	None
NT1840	10 YO	2018	SR2/Q	SLP, 717	Cosco Easy Elite	3-in-1
NT1841	10 YO	2018	SR2/Q	SLP, 717	Graco TurboBooster	Backless
NT1842	10 YO	2018	SR2/Q	SLP, 717	Combi Kobuk	Highback
NT1843	10 YO	2018	SR2/Q	SLP, 717	BT Hybrid 3n1	Combination
NT1844	10 YO	2018	SR2/Q	SLP, 717	Incognito	Backless
NT1845	10 YO	2018	SR2/Q	SLP, 717	None	None

Analysis Techniques

NHTSA has traditionally used coefficient of variation (standard deviation divided by the mean) to assess the repeatability of an ATD or test protocol, with values of <5 rated as Excellent, 5 to ≤ 8 Good, 8 to ≤ 10 Marginal, and >10 Poor (Rhule et al. 2005). One of our objectives is to assess repeatability of current and new booster metrics under test conditions using the surrogate retractor relative to the repeatability of current booster metrics using the current regulatory procedures. However, the repeatability we can obtain using current regulatory procedures for some booster measures is far better than an allowable CV score of 10.

Instead, we propose that the criteria shown in Table 3 be used to assess repeatability in the current test series. The thresholds are based on past UMTRI experience using the current regulatory protocols. The range of values (maximum minus minimum) among tests run under the same condition is used rather than the standard deviation. An advantage of the proposed criteria is that ATD head and chest acceleration measures are assessed using the same ranges, regardless of the value of the measure; the same is true for head and knee excursion.

Table 3. Proposed Repeatability Criteria

	units	Range			
		Excellent	Good	Marginal	Poor
Sled accel	g	<0.2	0.2-<0.5	0.5-<0.7	0.7+
Sled velocity	mi/hr	<0.2	0.2-<0.5	0.5-<0.7	0.7+
Head, chest, pelvis accelerations	g	0-<4	4-<8	8-<12	12+
Chest & pelvis angles	deg	0-<4	4-<8	8-<12	12+
Neck and lumbar moments	Nm	0-<4	4-<8	8-<12	12+
HIC		0-60	61-120	121-180	>180
Force (peaks < 1000)	N	0-60	61-120	121-180	>180
Force (peaks > 1000)	N	0-120	121-240	241-360	>360
Head, knee excursion; spool-out	mm	0-<7	7-<14	14-<21	21+

Several dynamic candidate measures of booster performance were calculated. Current FMVSS No. 213 measures of booster performance that include peak resultant head acceleration, 3 ms chest clip acceleration, HIC (36 ms), head excursion, and knee excursion were evaluated. As previously proposed by Klinich et al. (2010), the difference between peak knee excursion and peak head excursion was calculated. The amount of chest rotation was calculated using integrated data from the chest angular rate sensor. The change in angle and the final angle were calculated. The maximum angle was calculated by adding the initial torso angle of the ATD (based on FARO arm measurements of H-point and the head of the shoulder-head-socket-screw.) Based on recent work by Belwadi, A., Duong, N., Fein, S., Maheshwari, J., & Arbogast, (2018), upper neck forces and moments (particularly y-force) were also considered. Lumbar and ASIS measurements were considered as well.

Several static measures of booster performance were also assessed. The amount of “boost” provided by each booster was calculated by subtracting the z-coordinate of the H-point when the ATD was seated on the test bench without a booster (mean of three repeats) from the z-coordinate of the H-point when the ATD was seated on the test bench with a booster. The lap belt score (LBS) and shoulder belt score (SBS) previously developed at UMTRI (Reed et al. 2008, 2016) were also calculated for each test condition.

METHODS: VOLUNTEER TESTING

Booster selection

The volunteer portion of the project tested child volunteers with six of the eleven boosters used for dynamic testing. To evaluate how the belt fit provided by these boosters varies, we performed belt fit measurements using the Hybrid III 6YO ATD. Using a laboratory seat assembly developed for previous volunteer tests (Reed et al. 2017), we evaluated lap belt fit and shoulder belt fit in four conditions. After reviewing the range of rear seat belt anchorage locations documented in the rear seat (Reed and Ebert, 2013), as well as the belt anchorage conditions used by IIHS in assessing belt fit (IIHS 2018), we chose lap belt angles representing 30 and 75 degree angles crossed with shoulder belt positions representing fore and aft locations. Locations of the belt anchorages and angles in the XZ and YZ planes are shown in Table 4. All locations are referenced to the seat H-point. Testing was performed with cushion length set to 465 mm (SAE J2732, 2008), approximately the mean value of measured rear seats.

Table 4. Belt anchorage coordinates used in ATD belt fit evaluation

Dring	X	Y	Z	XZ angle	YZ angle
Fleet -1 STD	309	210	510	26	20
Fleet +1 STD	513	298	652	44	28
Used: fore	310	300	580	28	27
Used: aft	510	210	580	41	20
Inboard	X	Y	Z	XZ angle	YZ angle
Fleet -1 STD	39	-149	-107	36	30
Fleet +1 STD	201	-233	-173	60	44
Used: min	47	280	-90	30	18
Used: max	156	280	-174	75	32
Outboard	X	Y	Z	XZ angle	YZ angle
Fleet -1 STD	54	214	-83	40	18
Fleet +1 STD	164	320	-207	66	38
Used: min	47	280	-90	30	18
Used: max	156	280	-174	75	32

Table 5 shows the range of measured lap belt scores (LBS) and shoulder belt scores (SBS) measured across the four belt anchorage conditions. Pictures are of the 30 degree lap belt position with the fore shoulder belt position. Six boosters were selected to maximize differences in booster style, manufacturer, and belt fit scores. Boosters selected for testing with volunteers were the Britax Pioneer, Lil Fan Noback Booster, Graco 4Ever, Graco TurboBooster, Dorel Incognito, and Combi Kobuk AirThru. The Cybex Solution was considered, but seems to be no longer available for purchase in the US. Table 6 shows more detailed images of the boosters tested with the volunteers, as well as the color coding used throughout the project and report to designate each booster.

Table 5. Range of LBS and SBS for each booster; photos show the 30 degree lap belt position with the fore shoulder belt position

40 Britax Pioneer	B41 Cosco Easy Elite	B42 Mifold GrabNGo	B43 Lil Fan Noback booster seat	B44 Graco 4Ever	B45 Graco Turbo Booster
					
LBS: 6:12	LBS: -12:6	LBS:33-41	LBS: 22-33	LBS:-5:10	LBS: 13:21
SBS: 4:11	SBS: -7: -18	SBS: -30:1	SBS: 1-33	SBS: -5:8	SBS: -1:10
B46 BabyTrend Hybrid LX	B47 Evenflo Big Kid Sport	B48 Combi Kobuk Air Thru	B49 Cybex Solution XFix	B50 Dorel Incognito	None
					
LBS: 9:13	LBS: 9:19	LBS: 9:18	LBS: 19:32	LBS: -1:13	LBS: -29:13
SBS: 14:20	SBS: 20:25	SBS: 18:54	SBS: 4:9	SBS: -20: -66	SBS: -65: -81

Table 6. Boosters used in volunteer testing, with designations and color codes for each booster.

A	B	C
 <p data-bbox="224 695 570 783">Combination Highback only Britax Pioneer Harness2Booster</p>	 <p data-bbox="667 695 956 783">Booster Backless Only Lil Fan Backless Box Seat</p>	 <p data-bbox="1105 695 1341 783">Combination Highback to Backless Graco 4Ever 4in 1</p>
D	E	F
 <p data-bbox="232 1234 565 1320">Booster Highback to Backless Graco TurboBooster Highback</p>	 <p data-bbox="691 1234 927 1320">Booster Highback to Backless Combi Kobuk</p>	 <p data-bbox="1117 1234 1333 1320">Booster Backless Only Safety 1st incognito</p>

Vehicle Selection

For the vehicle testing portion of the volunteer study, the objective was to measure volunteers in three vehicles that provide a range of belt geometries and cushion lengths. Past data on rear seat geometry were reviewed, and vehicle interior pictures from manufacturer websites were checked to identify potential candidate vehicles. Researchers performed preliminary measurements on available candidate vehicles at a rental agency, and the three vehicles shown in Figure 6 were selected to provide a range of belt geometries and cushion lengths: Toyota Corolla, Jeep Compass, and Chevy Malibu. Standard procedures to document vehicle interior dimensions using the J826 manikin and belt fit with the Hybrid III 6YO ATD were then performed at UMTRI. Table 7 summarizes the key dimensions for the three vehicles relative to the fleet measurements reported by Reed and Ebert (2013). The Corolla, Jeep and Chevy had seat back angles of 26°, 22.5° and 23° and seat cushion angles of 15°, 4° and 13° respectively (SAE J826).



Figure 6. Exterior view of test vehicles: Chevy Malibu, Toyota Corolla, Jeep Compass.

Table 7. Vehicle Belt Geometries Compared to Fleet Dimensions

Dring	X	Y	Z	XZ angle	YZ angle
Fleet -1 STD	309	210	510	26	20
Fleet +1 STD	513	298	652	44	28
Corolla	512	-234	499	46	25
Compass	209	-317	548	21	30
Malibu	443	-289	546	39	28

Inboard	X	Y	Z	XZ angle	YZ angle
Fleet -1 STD	39	-149	-107	36	30
Fleet +1 STD	201	-233	-173	60	44
Corolla	153	187	-146	44	38
Compass	198	102	-169	40	59
Malibu	84	189	-113	53	31

Outboard	X	Y	Z	XZ angle	YZ angle
Fleet -1 STD	54	214	-83	40	18
Fleet +1 STD	164	320	-207	66	38
Corolla	45	-261	-108	67	22
Compass	79	-243	-192	68	38
Malibu	18	-245	-86	79	19

The Corolla was selected because it had the shortest cushion length of those available (455 mm) and inboard anchor located close to the bight.



Figure 7. Toyota Corolla

The Chevy Malibu had the longest cushion length of available vehicles (475 mm), a D-ring that was further rearward and higher than other choices, and nonsymmetric lower anchors. The seat also includes a bightline waterfall.



Figure 8. Chevy Malibu

The Jeep Compass has a relatively low and forward D-ring and its cushion length is in the middle of the range available (468 mm).



Figure 9. Jeep Compass

Laboratory Seat Conditions

Volunteers were also tested in a reconfigurable laboratory seating seat assembly shown in Figure 10. When selecting the cushion lengths and belt geometries for the seating seat assembly, the intent was to choose three conditions that complement the vehicle geometries to provide a range of conditions representative of the vehicle fleet. In addition, since this project includes evaluation of boosters using volunteers and ATDs statically, as well as dynamic testing of the same boosters, we chose to set one of the conditions for the laboratory seating bench to match the belt locations of the 2018 revision to the FMVSS No. 213 seat assembly.

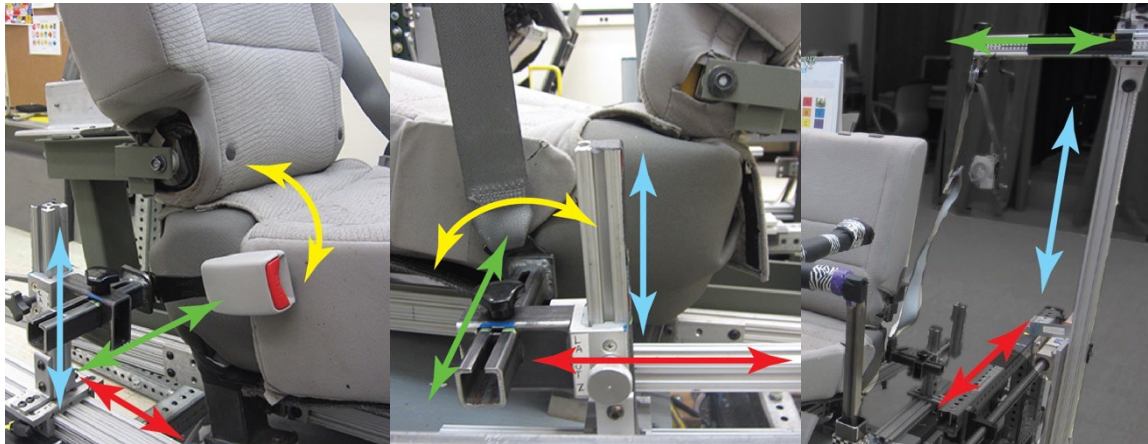


Figure 10. Reconfigurable laboratory seating seat assembly

For the three vehicles, cushion lengths are 455, 468, and 475 mm; all of the eight candidate vehicles fell within this range. The range in the Huang and Reed (2006) study was 420 through 520, with a median of 460 mm for minivans, 470 for cars, and 465 overall; the overall mean value was 495 mm. In a past study to examine the effect of cushion length on child ATD kinematics, cushion length was adjusted to 350, 400, and 450 mm (Klinich et al. 2012). For the volunteer portion of the study, we chose cushion lengths of 465 (B), 495 (Z) mm, and 523 mm (L) to represent the median, mean, and max from the Huang and Reed study.

Table 8 lists the belt anchorage locations and angles used in the laboratory seating seat assembly. Condition L has belt geometry that matches the 2018 version of the FMVSS No. 213 seat assembly. Geometries for conditions B and Z were selected to produce XZ and YZ

angles not found in the three vehicles, but within the most common range in the fleet. Figure 11 shows a subject seated in each laboratory condition.

Table 8. Laboratory belt geometries compared to fleet measurements

Dring	X	Y	Z	XZ angle	YZ angle
Fleet -1 STD	309	210	510	26	20
Fleet +1 STD	513	298	652	44	28
Lab L	474	244	588	39	23
Lab B	410	200	540	37	20
Lab Z	350	270	610	30	24

Inboard	X	Y	Z	XZ angle	YZ angle
Fleet -1 STD	39	-149	-107	36	30
Fleet +1 STD	201	-233	-173	60	44
Lab L	155	-225	-137	41	31
Lab B	120	-190	-145	50	37
Lab Z	70	-225	-160	66	35

Outboard	X	Y	Z	XZ angle	YZ angle
Fleet -1 STD	54	214	-83	40	18
Fleet +1 STD	164	320	-207	66	38
Lab L	155	225	-137	41	31
Lab B	130	250	-160	51	37
Lab Z	60	220	-200	73	42

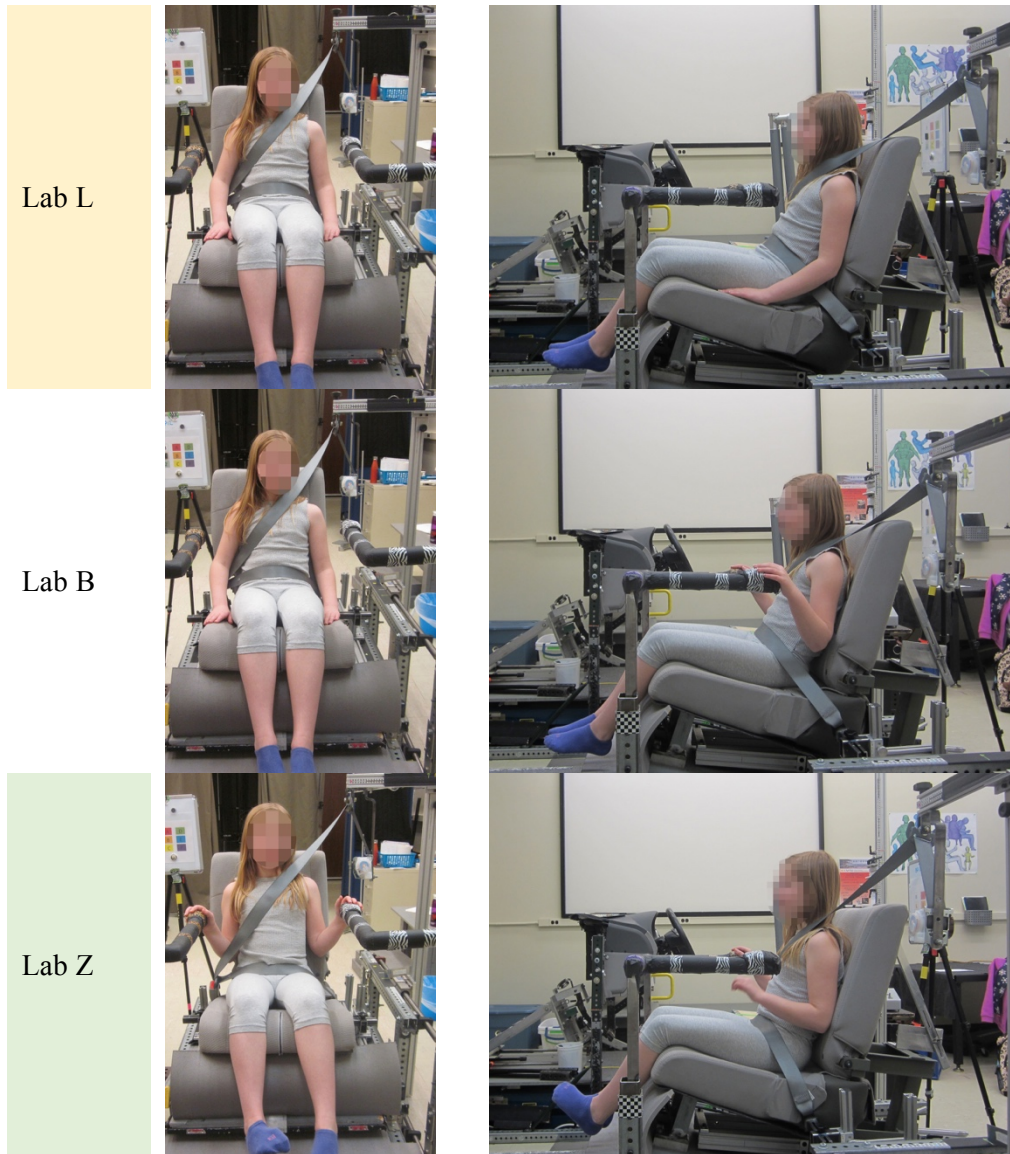


Figure 11. Subject seated in three laboratory conditions, with (left) and without (right) a booster.

Figure 12 through Figure 15 show the range of belt angles and belt anchorage locations experienced by each subject across the three laboratory and three vehicle conditions. Shaded rectangles on each plot show the mean \pm STD from the vehicle fleet.

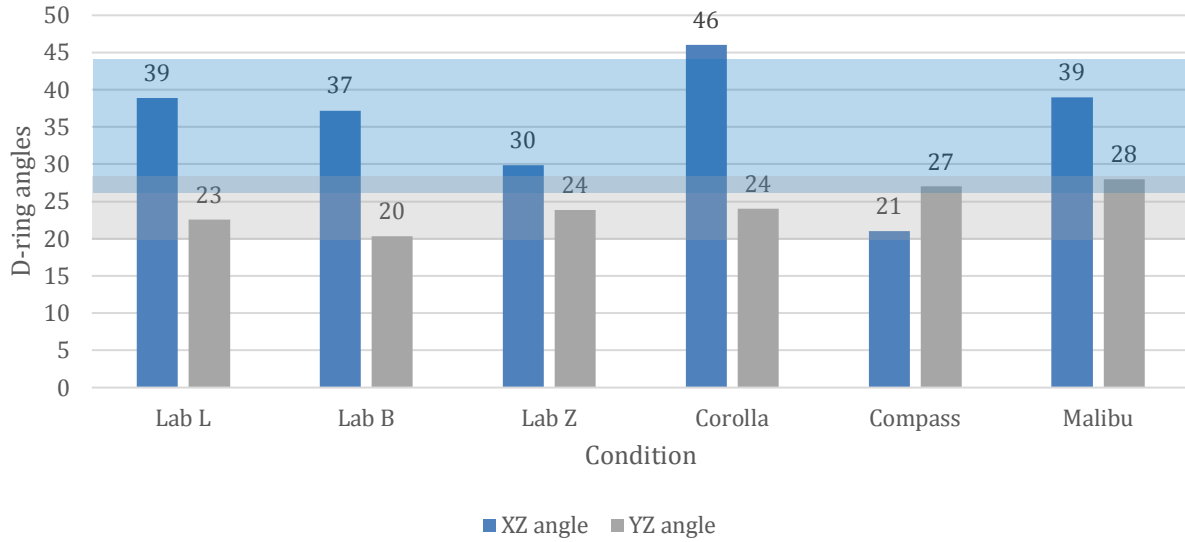


Figure 12. D-ring angles across vehicle and lab conditions, compared to fleet +/- 1STD.

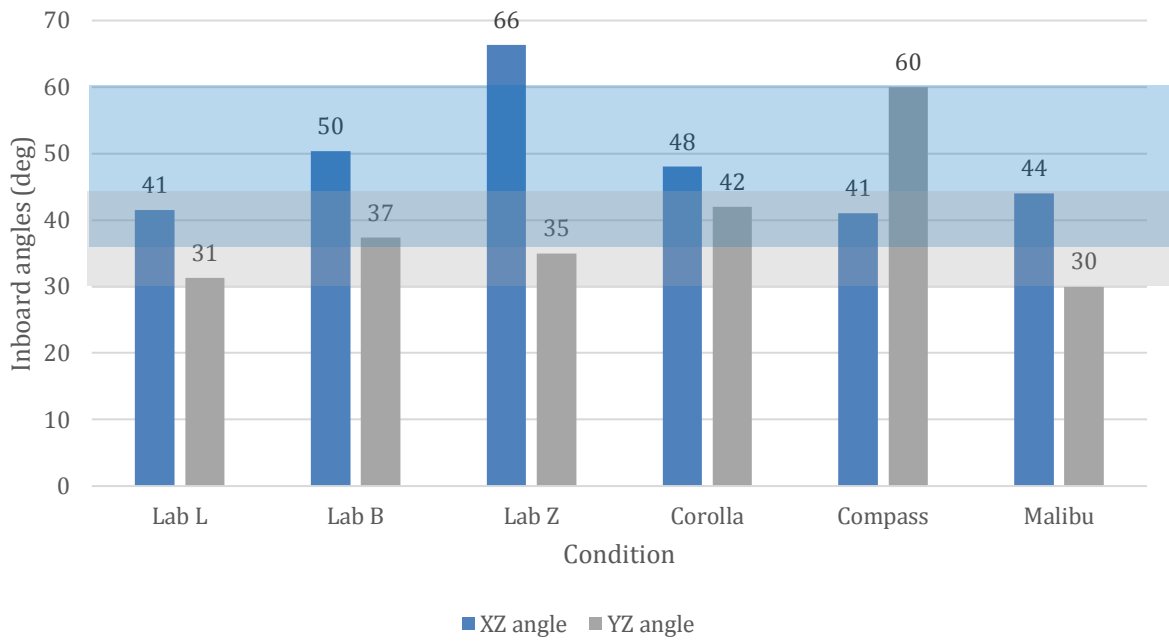


Figure 13. Inboard angles across vehicle and lab conditions, compared to fleet +/- 1STD.

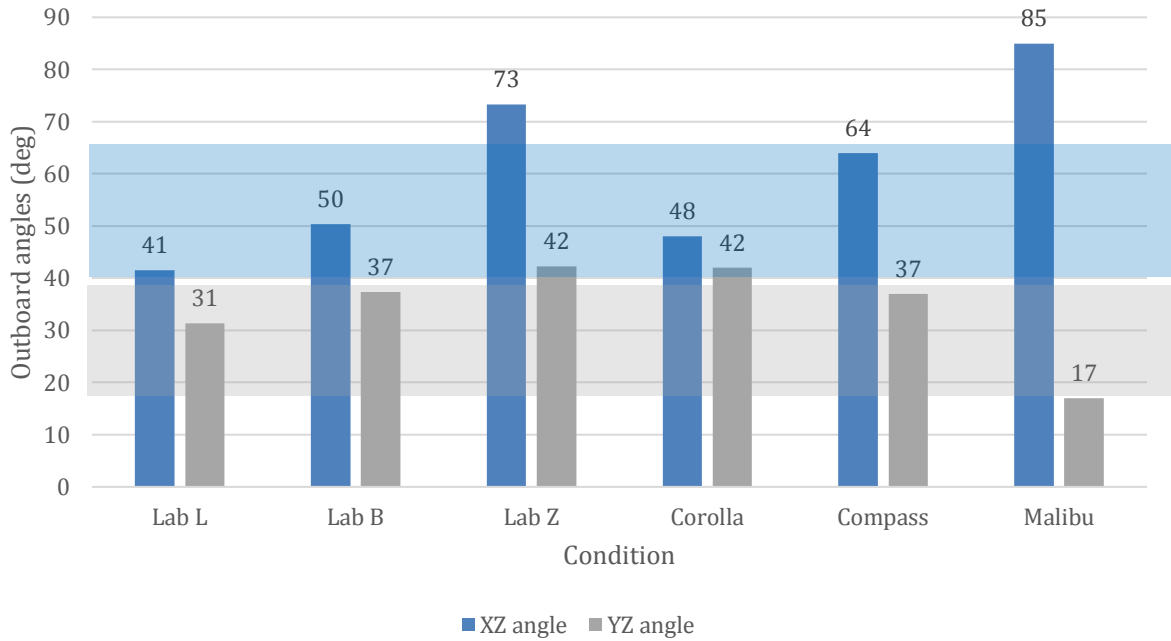


Figure 14. Outboard angles across vehicle and lab conditions, compared to fleet +/- 1STD.

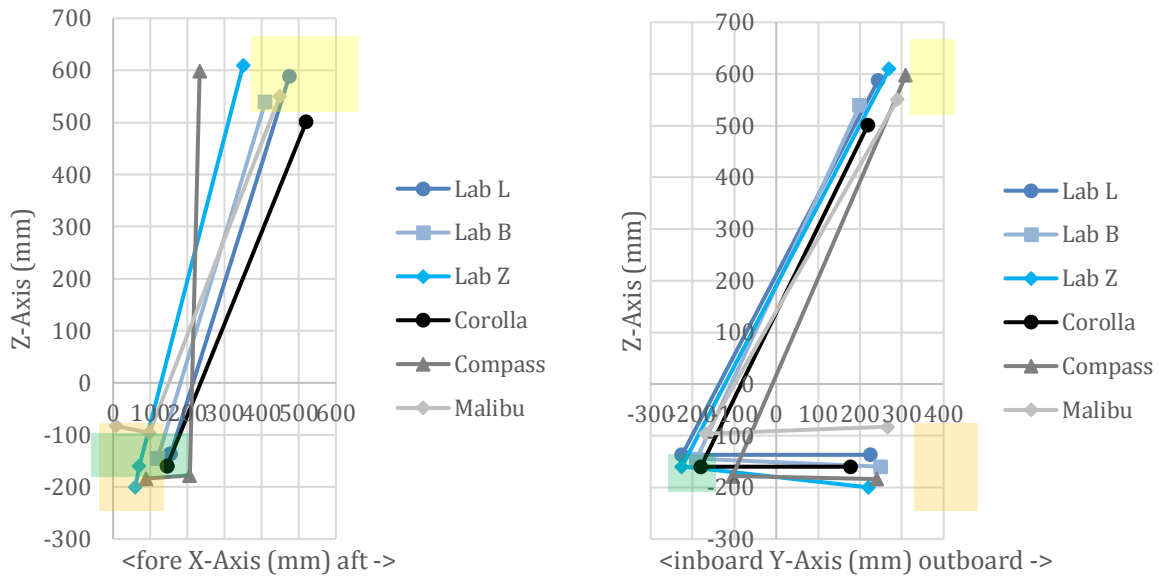


Figure 15. Side view (left) and front view (right) belt geometries.

Test Protocol

Data collection was conducted at UMTRI by research staff experienced with the body shape, posture and belt fit measurement protocols that have been used in several previous UMTRI studies with children (Reed et al. 2005, 2006, 2009, 2013, Jones et al. 2015, Kim et al. 2015, Ebert, Klinich, Manary, Malik, & Reed, 2018). After reviewing procedures and obtaining consent from subjects, body landmarks were marked on the child's skin using washable marker or stickers.

Standard anthropometric dimensions, including stature, body weight, and linear breadths and depths were gathered from each participant to characterize the overall body size and shape. All measurements were obtained from the participants while wearing snug-fitting test clothing. Table 9 contains a complete list of measurements.

Table 9. Anthropometry

Gender	Buttock-knee length
Date of birth	Buttock-popliteal length
Stature (with shoes)	Chest depth
Stature (without shoes)	Abdomen depth
Weight (without shoes)	Pelvic depth
Erect sitting height	Abdomen breadth
Eye height (sitting)	Bideltoid breadth
Shoulder height (sitting)	Bi-acromial breadth
Acromion height (sitting)	Shoulder breadth
Knee height	Maximum hip breadth
Tragion to top of head	Bi-ASIS breadth
Head breadth	
Head length	

Body shape and surface contours were recorded using a Vitronic Vitus XXL full-body laser scanner and Scanworx software by HumanSolutions. The VITUS XXL records hundreds of thousands of data points on the surface of the body in about 12 seconds by sweeping four lasers vertically. The two cameras on each of the four scanning heads pick up the laser light contour projected on the participant and translate the images into accurate three-dimensional data. As illustrated in Figure 16, the participants were scanned in two postures: standing and seated unsupported.

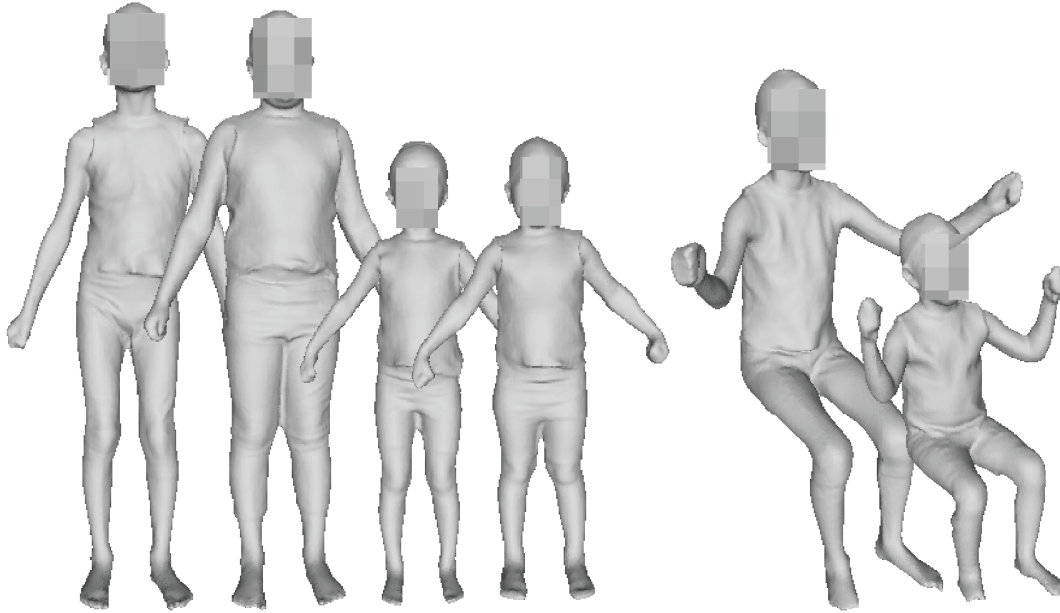


Figure 16. Examples of standing and seated postures scanned for each subject.

Body landmark locations were recorded in the laboratory hardseat shown in Figure 17. The hardseat allows access to posterior spine and pelvis landmarks that are inaccessible in the automotive seat. Figure 18 references the adjustment for adiposity described in Reed et al. (2013) that was applied to the points recorded on the pelvis. Table 10 lists the landmarks recorded in the hardseat.



Figure 17. Hardseat used for measuring subject reference landmarks.

Table 10. Landmarks digitized in hardseat

Back of head	Lateral femoral epicondyle, Lt and Rt	C7
Top of head (vertex)	Medial femoral epicondyle, Lt and Rt	T4
Tragion, Rt and Rt	Suprapatella, Lt and Rt	T8
Ectoorbitale, Lt and Rt	Infrapatella, Lt and Rt	T12
Infraorbitale at pupil center, Lt and Rt	Heel, Lt	L1
Glabella	Lateral malleolus, Lt	L2
Anterior acromion, Lt and Rt	Medial malleolus, Lt	L3
Lateral humeral epicondyle, Lateral, Lt	Lateral ball of foot, Lt	L4
Ulnar styloid process, Lt	Medial ball of foot, Lt	L5
Suprasternale	Toe (longest tibiale), Lt	ASIS, Lt and Rt
Substernale		PSIS, Lt and Rt

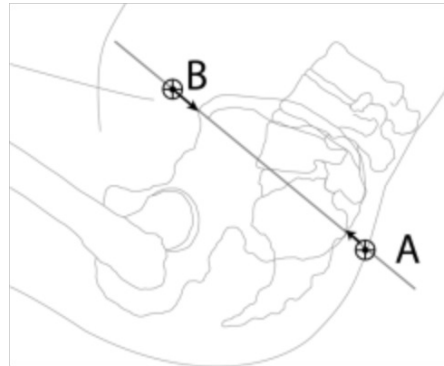


Figure 18. Compensation for adiposity at the PSIS flesh margin (A) and ASIS flesh margin (B) separating the depressed surface landmark from the underlying bone landmark

The laboratory and vehicle test conditions for the study are listed in Table 11. Subjects were assigned to three test groups (I, II, and III), with the goal of each group having a similar mean and range of stature and body weight. Each subject is tested in each vehicle and seat assembly condition once without a booster, as well as in two different boosters. Each subject is tested once with each booster in the vehicles and in the lab conditions.

Table 11. Volunteer Test Matrix for Subject Groups I, II, and III*

	Booster A	Booster B	Booster C	Booster D	Booster E	Booster F	None
Vehicle 1	I	II	III	I	II	III	I, II, III
Vehicle 2	II	III	I	II	III	I	I, II, III
Vehicle 3	III	I	II	III	I	II	I, II, III
Lab L	III	I	II	III	I	II	I, II, III
Lab B	I	II	III	I	II	III	I, II, III
Lab Z	II	III	I	II	III	I	I, II, III

For each vehicle and laboratory test condition, the child sat in the selected seating configuration. The experimenter palpated body landmarks on the head, chest, pelvis, and extremities and recorded the landmark locations in three dimensions using a FARO Arm. The FARO Arm was also used to collect streams of data to define the belt path. Table 12 lists the points collected in the mockup, while Table 13 lists those collected in the vehicles.

Table 12. Points and streams digitized in the mockup

<u>Participant</u>	<u>Seat</u>
C7 (Cervicale)	Seat pan reference points
Back of head (max rearward)	Seat back reference point
Top of head (max height)	
Tragion, Rt	<u>Restraint System</u>
Ectoorbitale, Rt	D-ring reference point
Infraorbitale at pupil center, Rt	Lower anchorages reference points
Glabella	
Suprasternale	<u>Shoulder Belt</u>
Substernale	Inboard and outboard edge on clavicle
Medial clavicle, Rt	Top and bottom edge at participant's
Lateral clavicle, Rt	midline
Anterior of acromion, Rt	Inboard edge at participant's
Lateral humeral epicondyle, Rt	Suprasternale height
Lateral ulnar styloid process, Rt	
ASIS, Lt and Rt	<u>Lap Belt</u>
Suprapatella, Lt and Rt	Top edge and bottom edge at ASIS
Infrapatella Lt	lateral position (Lt and Rt) and at
Lateral femoral epicondyle Rt	participant's midline
Medial femoral epicondyle Lt	
Toe (bottom edge of sole, longest shoe point), Rt	<u>Seat Belt Streams</u>
Heel (bottom edge of sole at midline), Rt	Top/ inboard edge of the shoulder belt
Lateral malleolus, Rt	Top edge of the lap belt from latch

Table 13. Points and streams digitized in the vehicle

<u>Participant</u>	<u>Vehicle</u>
C7 (Cervicale)	3 Points on door opening frame
Back of head (max rearward)	
Top of head (max height)	<u>Shoulder Belt</u>
Tragion, Lt	Inboard and outboard edge on clavicle
Ectoorbitale, Lt	Top and bottom edge at participant's
Infraorbitale at pupil center, Lt	midline
Glabella	Inboard edge at participant's
Suprasternale	Suprasternale height
Substernale	
Anterior of acromion, Lt and Rt	<u>Lap Belt</u>
Lateral humeral epicondyle, Lt	Top edge and bottom edge at ASIS
Lateral ulnar styloid process, Lt	lateral position (Lt and Rt) and at
ASIS, Lt and Rt	participant's midline
Suprapatella, Lt and Rt	
Infrapatella Lt and Rt	<u>Seat Belt Streams</u>
Lateral femoral epicondyle Lt	Top/ inboard edge of the shoulder belt
Medial femoral epicondyle Rt	Top edge of the lap belt
Toe (bottom edge of sole, longest shoe point), Lt	
Heel (bottom edge of sole at midline), Lt	
Lateral malleolus, Lt	

Subject Recruitment and Characteristics

Twenty-four children between the ages of 4 and 12 years were recruited to participate in the study. Subjects were selected to span a large range of stature and age with an approximately equal distribution of boys and girls. Volunteers were recruited by word of mouth, online advertising, flyers, and the University of Michigan Human Research Recruiting Registry website (www.UMHealthResearch.org). Informed consent was obtained in writing from the parent or guardian and orally from the child. All subject forms and test protocols were approved by the University of Michigan Institutional Review Board.

As subjects were recruited, they were assigned to three groups with the goal of each group having similar characteristics in terms of gender, stature, and weight distribution. Figure 19 shows the distribution of subjects by group, height, and weight. Table 14 summarizes the mean, minimum, and maximum of key anthropometry measures for each group, while Table 15 summarizes the measures for all subjects.

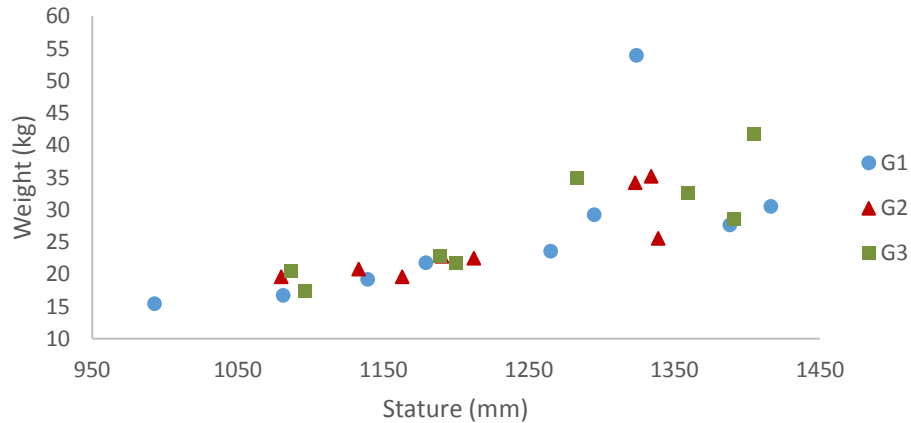


Figure 19. Distribution of test subjects by height, weight, and group.

Table 14. Anthropometry summary for each group

Measurement *	Group 1 (4 boys, 5 girls)			Group 2 (4 boys, 4 girls)			Group 3 (5 boys, 3 girls)		
	Mean	Min	Max	Mean	Min	Max	Mean	Min	Max
Age (yr)	7	4	9	7	4	10	7	4	11
Stature	1241	993	1416	1222	1080	1339	1251	1087	1405
Weight (kg)	26.9	15.5	53.9	25.0	19.5	35.2	27.5	17.4	41.7
BMI (kg/m ²)	17.1	14.3	30.7	16.6	14.2	19.8	17.2	14.5	21.2
Erect Sitting Height	666	567	765	651	594	693	664	592	726
Shoulder Height	419	334	475	407	370	444	413	376	463
Buttock-Popliteal Length	338	270	381	334	289	371	339	280	407
Bi-deltoid Breadth	306	242	408	304	273	358	311	257	351
Hip Breadth	214	175	264	223	196	296	209	178	251

*mm unless noted

Table 15. Anthropometry Summary for All Subjects

Measurement *	Mean	Min	Max
Age (yr)	7	4	11
Stature	1235	993	1416
Weight (lb)	58.1	34.1	118.8
BMI (kg/m ²)	16.9	14.2	30.7
Erect Sitting Height	660	567	765
Shoulder Height	412	334	475
Buttock-Popliteal Length	336	270	407
Bi-deltoid Breadth	305	242	408
Hip Breadth	213	175	296

*mm unless noted

Data Analysis

All data were expressed with the origin at the seat H-point. For the highback booster conditions the child data were then aligned to the ATD data using the booster reference points. Therefore the comparison of posture would be relative to the same seating surface, the booster. Due to differences in seating surface created by the fore-aft positioning of the backless booster, the child backless booster data were not aligned to the ATD booster position.

Posture analysis focused on the vertical and fore-aft locations the hip joint center (HJC) and the knee location. To compare the posture of the child volunteers to the ATDs, we

calculate the location of the anatomical landmark, and plot the difference between the child and ATD, calculated by subtracting the ATD value from the child value. Comparisons of mean value across all booster conditions were evaluated for statistical significance using both paired t-tests and the non-parametric Wilcoxon signed rank test. Included knee angle was calculated using landmarks corresponding to the HJC, knee joint, and ankle joint. For these plots, values for the ATD in each booster are directly compared to the angles measured in subjects. Plots of head CG directly compare the location of the ATD and children in each booster, aligning vehicle seat H-points. Linear regression was used to model the relationship between ATD and volunteer HJC and head CG location.

For belt fit, the distance from the top of the lap belt to the ASIS was separated into fore-aft and vertical components. Right and left side measures were averaged. For plots, belt fit measures for the ATDs are directly overlaid on the belt fit measures of the volunteers. For shoulder belt, the lateral location of the inboard edge of the shoulder belt is calculated relative to the top of the sternum.

RESULTS: DYNAMIC TESTING

Overview

Table 16 summarizes key dynamic response measures for each test. Test IDs beginning with NT15 are from the 2015 test series, while the remaining NT18 coded tests were conducted in 2018. The six tests with crossed-out IDs were run with a larger belt spool-out setting and more severe pulse (as explained in the methods section); results are summarized here and included in data submissions but not included in further analysis of repeatability or booster metrics. Test IDs NT1840 through NT1045 were run with the 10Y0; remaining tests were run with the 6Y0. Text colors for each test match the colors used to represent each booster product on subsequent plots.

Appendix B contains example images for each booster and ATD combination. The results include initial position and maximum excursion on the overhead and right-side cameras, as well as the pre-test photos highlighting the initial position of the shoulder and lap belt.

Table 16. Summary of dynamic test results

Test ID	Head Resultant Peak (g)	HIC(36)	HIC(15)	3.0 msClip (G)	Upper Neck Resultant Force(N)	Upper Neck Resultant Moment (N)	Total Chest Rotation	SBS	L LBS	R LBS	Boost Z	Retractor Payout	Head Ex	Knee Ex	Knee-Head	Lumbar FY	Lumbar MZ
NT1508	84	860	669	55.6	2585	40.6	53	12	27	29	100	102	608	627	19	834	-11.4
NT1509	98	795	605	56.4	2272	36.9	42	9	24	27	102	87	565	621	56	691	-11.6
NT1510	88	574	270	46.2	2138	38.3	29	-8	17	19	84	42	483	625	142	34	-1
NT1511	106	789	386	50.2	3007	46.4	21	4	23	30	90	63	508	630	122	40	-2.9
NT1512	100	883	631	53.6	2308	44	29	6	23	22	109	65	517	614	97	347	-7.2
NT1513	114	981	638	54.6	2719	55.1	22	-17	9	11	52	61	518	598	80	93	-2.7
NT1514	81	847	601	55.1	2293	43.4	33	-37	7	10	0	63	540	581	41	40	-0.8
NT1515	82	724	539	54.1	2160	35.9	40	9	24	27	102	70	560	620	60	662	-11.6
NT1801	181	1415	948	58.2	2920	60.0	56	28	13	9	115	85	646	656	90	943	-9.3
NT1802	120	2480	1544	55.0	8137	134.3	27	11	11	12	127	78	640	807	167	78	-1.4
NT1803	133	875	618	57.4	2329	42.0	53	39	5	3	145	83	666	702	36	893	-12.7
NT1804	84	1126	880	54.7	Na	52.9	41	15	11	9	176	80	588	717	129	423	-10.4
NT1805	73	822	527	57.9	3348	41.8	15	-32	6	9	0	55	445	592	147	62	-0.3
NT1806	87	1164	893	55.4	2794	48.3	41	7	13	11	113	53	576	648	72	848	-9.1
NT1807	80	985	759	51.1	2514	51.1	47	25	27	23	121	54	599	670	71	797	-8
NT1808	73	829	596	57.3	2416	49.3	51	42	16	14	96	52	623	643	20	1428	-11
NT1809	78	892	698	55.1	2522	47.7	39	17	14	15	118	57	595	646	51	593	-9
NT1810	81	873	665	47.5	2357	43.0	41	26	14	15	103	51	568	664	96	851	-8.1
NT1811	80	969	729	55.2	2543	48.0	47	26	17	15	109	51	603	644	41	970	-9
NT1812	88	1717	900	49.0	5959	97.6	21	0	7	8	124	46	597	777	180	105	-2
NT1813	70	701	494	50.1	2207	45.7	51	20	23	21	149	45	609	684	75	647	-7

Test ID	Head Resultant Peak (g)	HIC(36)	HIC(15)	3.0 msClip (G)	Upper Neck Resultant Force(N)	Upper Neck Resultant Moment (N)	Total Chest Rotation	SBS	L LBS	R LBS	Boost Z	Retractor Payout	Head Ex	Knee Ex	Knee-Head	Lumbar FY	Lumbar MZ
NT1814	81	986	713	51.7	3009	60.69	34	8	18	16	177	49	568	712	144	435	-7
NT1815	80	955	731	54.4	2517	49.1	41	19	16	15	119	52	598	656	58	733	-8
NT1816	77	845	677	52.8	2409	42.5	38	23	23	25	121	48	585	670	85	826	-8.1
NT1817	73	745	512	58.5	2213	46.8	55	40	18	18	95	51	621	640	19	1337	-11.8
NT1818	77	917	679	48.3	2462	46.5	42	23	13	12	102	47	578	663	85	905	-8
NT1819	88	1687	930	51.5	5540	87.5	21	0	2	3	121	48	594	779	185	167	-2.4
NT1820	79	989	747	53.4	2531	47	40	25	18	19	111	51	588	646	58	737	-8.9
NT1821	75	808	608	50.5	2323	52.4	50	19	23	21	152	55	605	689	84	652	-8.4
NT1822	80	877	657	49.5	2426	49.5	38	11	14	13	178	54	571	707	136	581	-8.4
NT1823	74	745	527	57.2	2248	46.5	55	37	19	13	95	51	626	634	8	1434	-13.3
NT1824	75	824	618	51.7	2390	46.5	37	20	14	14	121	48	587	657	70	749	-9
NT1825	79	910	711	51.7	2523	51.1	48	23	25	23	123	54	596	669	73	923	-7.9
NT1826	78	946	696	45.7	2509	47.7	42	27	15	17	103	54	575	662	87	958	-8.2
NT1827	82	952	722	54.3	2550	49.5	47	23	21	18	108	55	593	639	46	846	-8.6
NT1828	88	975	668	56.4	2508	48.8	32	10	23	24	72	48	505	609	104	563	-7.9
NT1829	103	1029	668	54.6	2484	52.7	33	9	23	22	64	47	503	607	104	573	-8.5
NT1830	68	749	485	41.8	2693	32.5	13	-25	10	8	46	47	456	590	134	42	-1.7
NT1831	92	950	661	54.9	2543	49.3	35	9	24	21	66	46	507	604	97	602	-9.1
NT1832	69	720	481	54.1	2744	30.8	13	-24	11	12	44	48	453	587	134	49	-2.8
NT1833	134	839	397	45.9	3422	43.3	36	9	52	50	27	45	457	665	208	32	9.2
NT1834	71	755	515	50.7	2708	33.3	13	-24	12	11	46	47	459	586	127	40	-2.7
NT1835	115	857	431	46.3	3558	46.2	35	7	48	44	26	47	460	660	200	36	8.9
NT1836	91	904	475	44.7	3372	44	36	9	48	44	24	50	469	671	202	29	8.2

Test ID	Head Resultant Peak (g)	HIC(36)	HIC(15)	3.0 msClip (G)	Upper Neck Resultant Force(N)	Upper Neck Resultant Moment (N)	Total Chest Rotation	SBS	L LBS	R LBS	Boost Z	Retractor Payout	Head Ex	Knee Ex	Knee-Head	Lumbar FY	Lumbar MZ
NT1837	84	574	374	54.1	3058	38.5	15	-38	8	7	1	43	451	587	136	51	-1.9
NT1838	92	561	367	55.4	3120	36	17	-35	7	5	-1	43	445	586	141	66	-1.4
NT1839	90	573	364	55.4	2979	36.4	14	-34	5	5	-1	49	452	594	142	77	-1.3
NT1840	133	2091	1495	49.1	6263	64.3	31	5	11	14	122	49	630	889	259	430	-5.6
NT1841	181	975	552	51.1	3391	54.6	40	30	39	39	87	49	571	696	125	919	-17.9
NT1842	75	912	558	55.8	2619	53.4	43	44	25	27	93	56	630	709	79	1417	-24
NT1843	84	1146	735	49.9	3572	50.9	31	36	27	24	108	51	612	772	160	840	-14.9
NT1844	265	1121	1121	48.2	3340	44.1	27	-24	16	15	44	48	512	698	186	95	-1.3
NT1845	75	787	559	49.2	3755	47.6	20	-23	3	5	0	44	501	704	203	42	-0.4

Qualitative Assessment

Kinematics

The no-booster condition was the only test scenario run on both the 2015 and 2018 seat assembly. Figure 20 shows a comparison of the peak head excursions, as well as the initial position of the shoulder belt. Although both tests had similar shoulder belt scores (-37 and -35), the different y-z angle of the shoulder belt resulting from the anchor geometry changes (Figure 4) is visible when comparing the initial position of the belt on the ATD. Head excursion is 540 mm in the 2015 test, but measures about 450 mm in the 2018 tests; torso rotation is about 16 degrees less with the new geometry. The changes in the seat assembly between the two iterations resulted in an increased propensity for submarining kinematics without a booster, suggesting that the 2018 changes may create a seat assembly that is more effective at differentiating between boosters that prevent submarining and those that allow it. Because of the substantial differences in kinematics in this condition resulting from changes between the 2015 and 2018 versions of the test bench, results from the other 2015 tests run with the surrogate retractor may no longer be relevant. However, they are included on subsequent plots for reference.

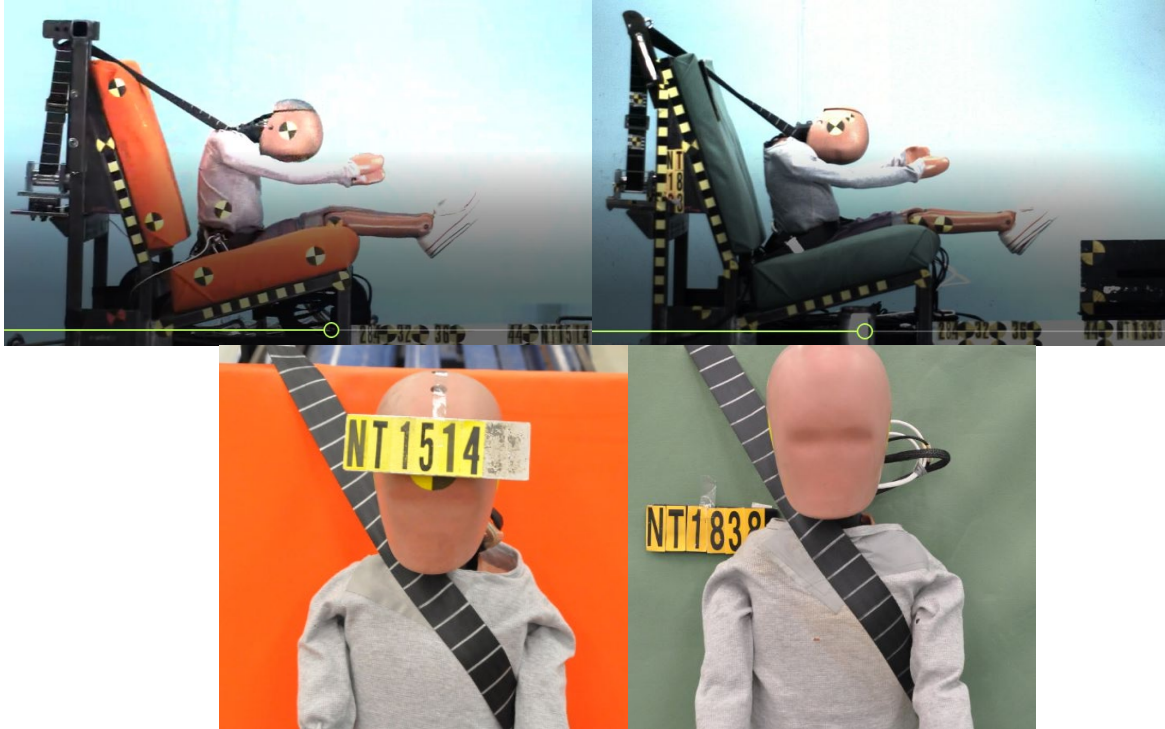


Figure 20. Comparison between 2015 and 2018 tests run with the no-booster condition: peak excursion and initial shoulder belt fit.

As shown in Figure 21, among all of the boosters tested, the Evenflo Amp in highback mode was the only product in which the head restraint portion of the booster moved forward with the ATD's head. This behavior may allow the side wings on the product to offer some head protection in crashes with non-frontal components.



Figure 21. Design of the Evenflo Amp (left) offers some lateral head protection at peak excursion, compared to more typical kinematics provided by Aidia Pathfinder (right), where the head moves forward out of the sides of the booster.

Among all of the boosters tested, the Combi Kobuk was the only one in which the shoulder belt loaded the ATD's upper arm rather than the shoulder (Figure 22). This loading occurred in tests run with both the 6YO and 10YO ATDs. This booster had the highest shoulder belt scores, indicating an initial outboard placement on the ATD's shoulder.



Figure 22. Shoulder belt loading ATD arm with Combi Kobuk.

With the Mifold device shown in Figure 23, the initial placement of the belt using the shoulder belt guide places it on the center of the shoulder. However, the guide does not keep the belt centered on the shoulder during the test, and the belt moves to load the ATD against the neck. The lap belt guides place the belt forward of the pelvis on the tops of the ATD thighs. This combination of belt loading allows the pelvis to move forward while the torso is prevented from rotating; the abdomen insert is released from the ATD in every test.

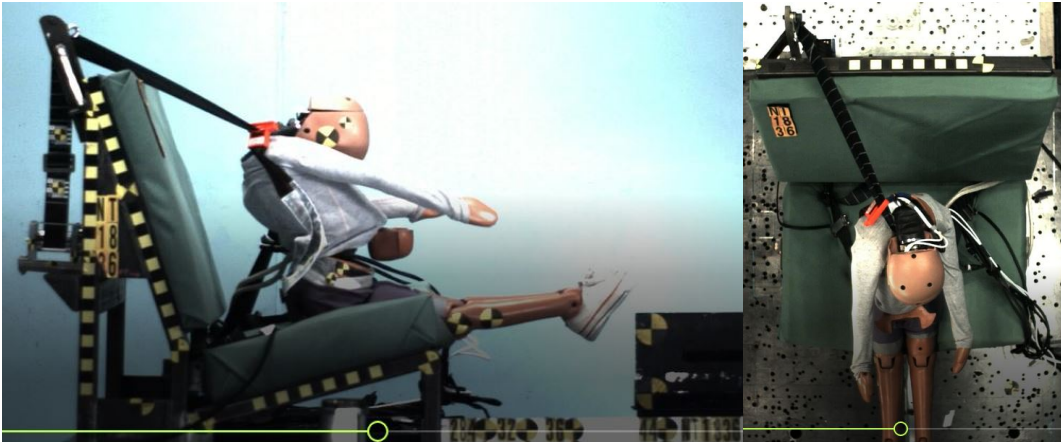


Figure 23. Kinematics of ATD using the Mifolddevice.

For the six conditions run with both the 6YO and 10YO ATD, the mean excursions for the 10YO averaged 25 mm more for the head and 93 mm more for the knee excursion. Figure 24 compares the ATD kinematics for the no-booster condition, the Cosco Easy Elite, and the Baby Trend Hybrid 3-in-1.

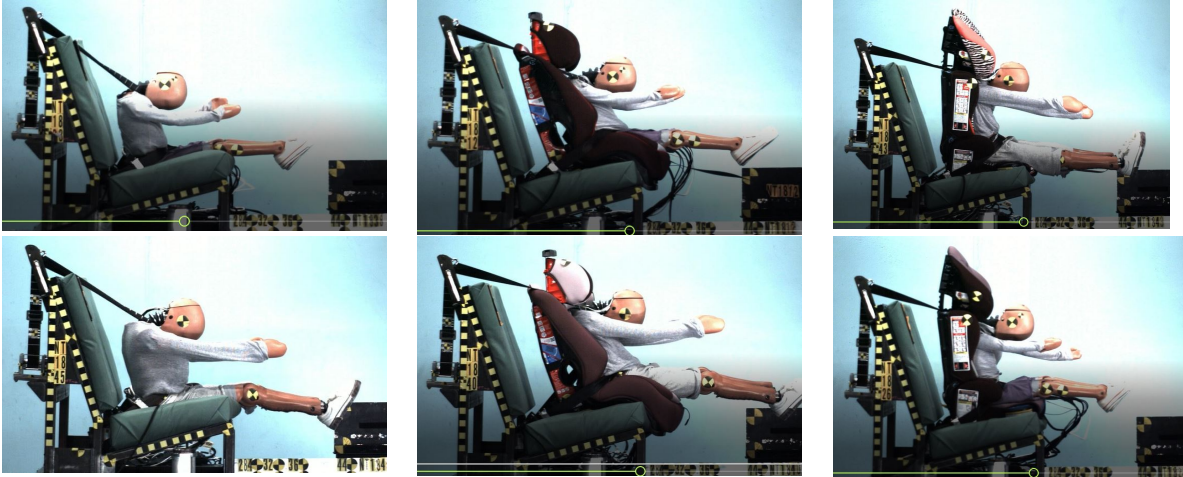


Figure 24. Comparison of peak head excursion for 6YO (top row) and 10YO (bottom row) in no-booster (left), Cosco Easy Elite (center), and Baby Trend Hybrid 3-in-1 (right).

Testing Issues

During an initial check out run, the shoulder belt slid into the gap on the right side of the ATD neck and tore the ATD's chest bib. The part was swapped out. The spring in the surrogate retractor broke during the setup of test NT1828. It was replaced with a spare spring, which lasted for the remainder of the test series.

Repeatability

Sled Pulse

An overlay of the sled pulses for tests NT1807-NT1839 (all run with the H3-6YO ATD) is shown in Figure 25, while the sled pulse for the tests run with the H3-10YO ATD are shown in Figure 26. The FMVSS No. 213 corridor is shown in yellow for reference.

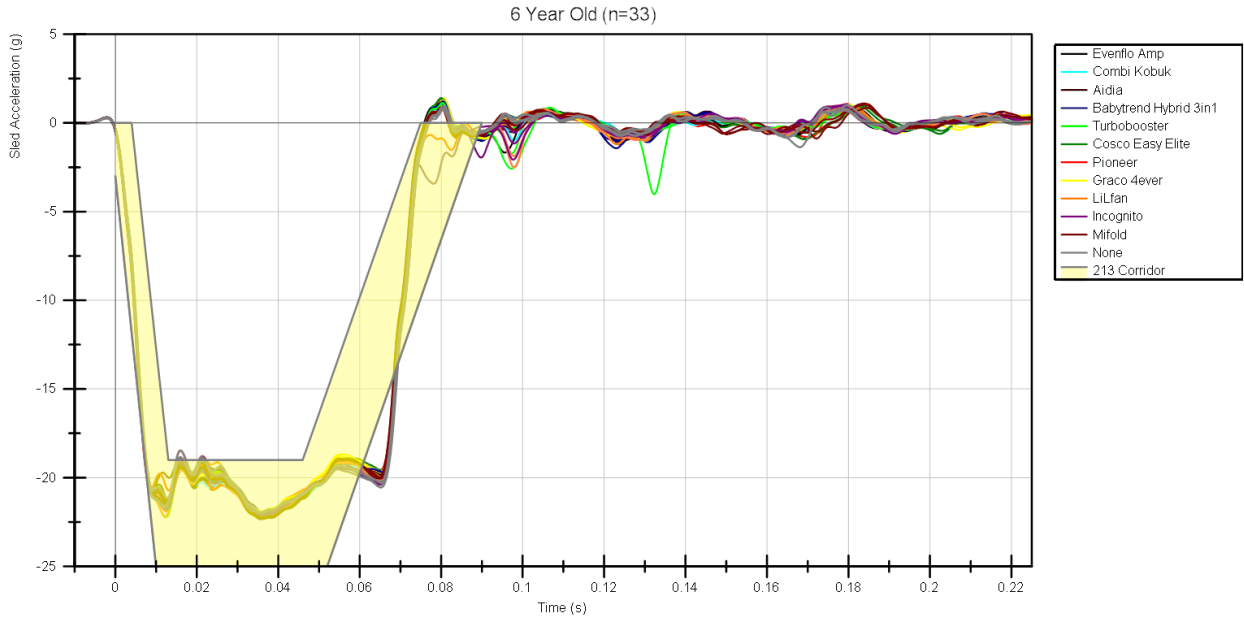


Figure 25. Sled pulse overlay of 33 tests with 6YO ATD

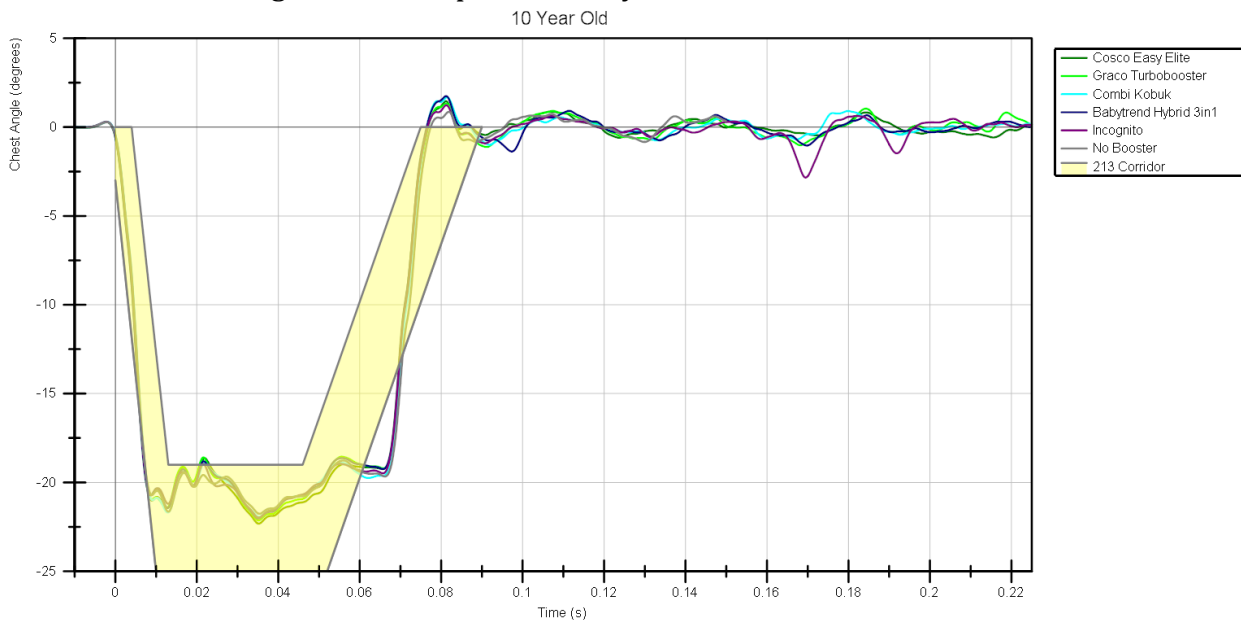


Figure 26. Sled pulse overlay of six tests with 10YO ATD

Performance Measures

Two or three tests were performed with each booster. Table 17 lists the range across all tests with each booster condition for key performance measures. Each cell is shaded according to the proposed repeatability criteria listed in the methods, with dark green=excellent, light green=good, yellow=marginal, and orange=poor. Most ATD measures had good or excellent repeatability for each set of booster tests, but repeatability of some measures varied with booster model.

Table 17. Range of ATD measures across test with same booster

Booster		Evenflo BK Amp	Combi Kobuk	Aidia	BT Hybrid 3n1	Graco TB HB	Cosco EE	Brtiax Pioneer	Graco 4ever	Lil Fan	Incognito	Mifold	No booster
number of tests		3	3	3	3	3	2	2	2	3	3	3	3
Test Velocity		0.1	0.1	0.1	0.0	0.1	0.0	0.2	0.1	0.1	0.0	0.0	0.2
Peak Acceleration (G)		0.1	0.1	0.1	0.0	0.0	0.2	0.0	0.0	0.0	0.1	0.1	0.0
Average Acceleration (G)		0.1	0.0	0.1	0.1	0.1	0.1	0.3	0.2	0.3	0.1	0.1	0.0
Head Acceleration	Resultant Peak (G)	3.0	0.9	4.6	3.9	2.3	0.8	5.3	1.2	14.7	2.3	43.2	8.6
	H.I.C. (UN)	159.7	84.2	139.0	78.1	65.6	27.4	118.6	115.0	114.8	34.2	60.7	23.3
	H.I.C. (36)	140.1	84.2	131.1	73.1	37.8	30.0	106.6	108.7	79.4	35.3	65.0	13.3
	H.I.C. (15)	82.1	83.7	112.2	31.0	25.5	30.0	114.5	56.3	61.7	33.8	78.5	10.4
	3.0 ms Clip (G)	1.7	1.3	3.4	2.6	1.8	2.5	0.4	2.2	1.8	12.3	1.6	1.3
Upper Neck Moment	Resultant Peak (Nm)	8.6	2.8	2.6	4.7	2.5	10.1	6.7	11.2	3.9	2.5	2.9	2.5
Lumbar Moment		1.8	2.4	5.7	3.6	6.9	5.1	3.1	1.6	2.2	2.7	9.5	2.8
Lumbar Moment	Peak Z (Nm)	0.5	1.9	1.0	0.2	0.3	0.0	1.3	1.2	1.2	1.1	1.0	0.6
Upper Neck Force**	Resultant Peak (N)	114.3	203.1	131.9	151.8	18.5	418.6	116.5	583.6	58.9	51.5	185.7	141.1
Lumbar Force**		188.8	122.4	163.9	124.5	214.0	337.4	6.9	37.8	137.8	87.4	183.6	54.3
Left ASIS Upper Force*		51.5	62.8	20.8	29.9	33.2	67.7	40.0	34.8	32.5	53.2	42.3	61.7
Left ASIS Lower Force *		74.9	125.5	93.9	12.1	94.7	1.8	69.0	17.5	63.5	73.5	21.9	27.1
Right ASIS Upper Force *		64.3	102.3	38.7	66.4	6.6	0.9	13.2	59.1	43.4	11.3	20.9	41.6
Right ASIS Lower Force *		94.7	67.8	38.6	90.9	1094.8	6.6	8.3	7.9	96.2	70.5	48.0	38.5
Lumbar Force*	Y (N)	126	97	156	108	234	62	4	146	39	9	7	26

Booster		Evenflo BK Amp	Combi Kobuk	Aidia	BT Hybrid 3n1	Graco TB HB	Cosco EE	Briaax Pioneer	Graco 4ever	Lil Fan	Incognito	Mifold	No booster
Pelvis Acceleration	Resultant Peak (G)	3.1	1.9	13.1	2.9	3.5	4.8	2.8	3.2	4.9	5.0	2.2	2.2
Pelvis Angle	Peak Forward Rotation (deg)	1.7	10.2	1.3	3.7	5.4	0.7	4.4	0.3	2.1	1.2	1.4	3.8
	Peak Rear Rotation (deg)	2.2	0.3	3.7	6.1	3.0	0.4	4.4	7.2	5.6	3.0	0.1	2.1
Chest Angle	Peak Forward Rotation (deg)	4.3	4.2	5.5	0.8	6.7	1.6	1.3	5.1	6.1	0.9	2.3	2.7
	Initial	2.0	1.2	2.2	1.8	1.6	2.7	0.3	0.8	0.7	1.2	0.9	0.3
Chest Angle	Initial + Abs (Peak Fwd)	4.6	5.2	7.7	1.3	7.4	1.1	1.6	5.9	6.8	2.1	2.6	2.9
Left Lap Load**	Resultant Peak (N)	135.8	43.1	166.7	56.7	392.3	90.2	33.0	213.5	228.7	188.8	376.3	147.2
Right Lap Load**		329.2	140.0	277.2	160.6	450.8	149.4	213.3	67.9	151.2	213.9	226.4	102.6
Retractor Payout	Peak (mm)	6.0	1.5	9.0	6.8	4.6	2.0	9.8	4.9	2.0	0.8	5.3	6.4
Excursion	Head (mm)	14.0	5.0	11.0	10.0	15.0	3.0	4.0	3.0	4.0	6.0	12.0	7.0
	Knee (mm)	1.0	9.0	11.0	2.0	7.0	2.0	5.0	5.0	5.0	4.0	11.0	8.0
	Knee-head (mm)	14.0	12.0	19.0	11.0	17.0	5.0	9.0	8.0	7.0	7.0	8.0	6.0

* Uses peak < 1000 N criteria ** Uses peak >1000 N criteria

Overlay plots of the head resultant acceleration, chest resultant acceleration, and change in chest rotation are found in Figure 27 through Figure 29. Each color corresponds to a different booster model. The differences between boosters are larger than differences within boosters and distinctive characteristics of the pulses, such as the bimodal character of the Easy Elite pulse (shown in dark green) were repeatable between runs.

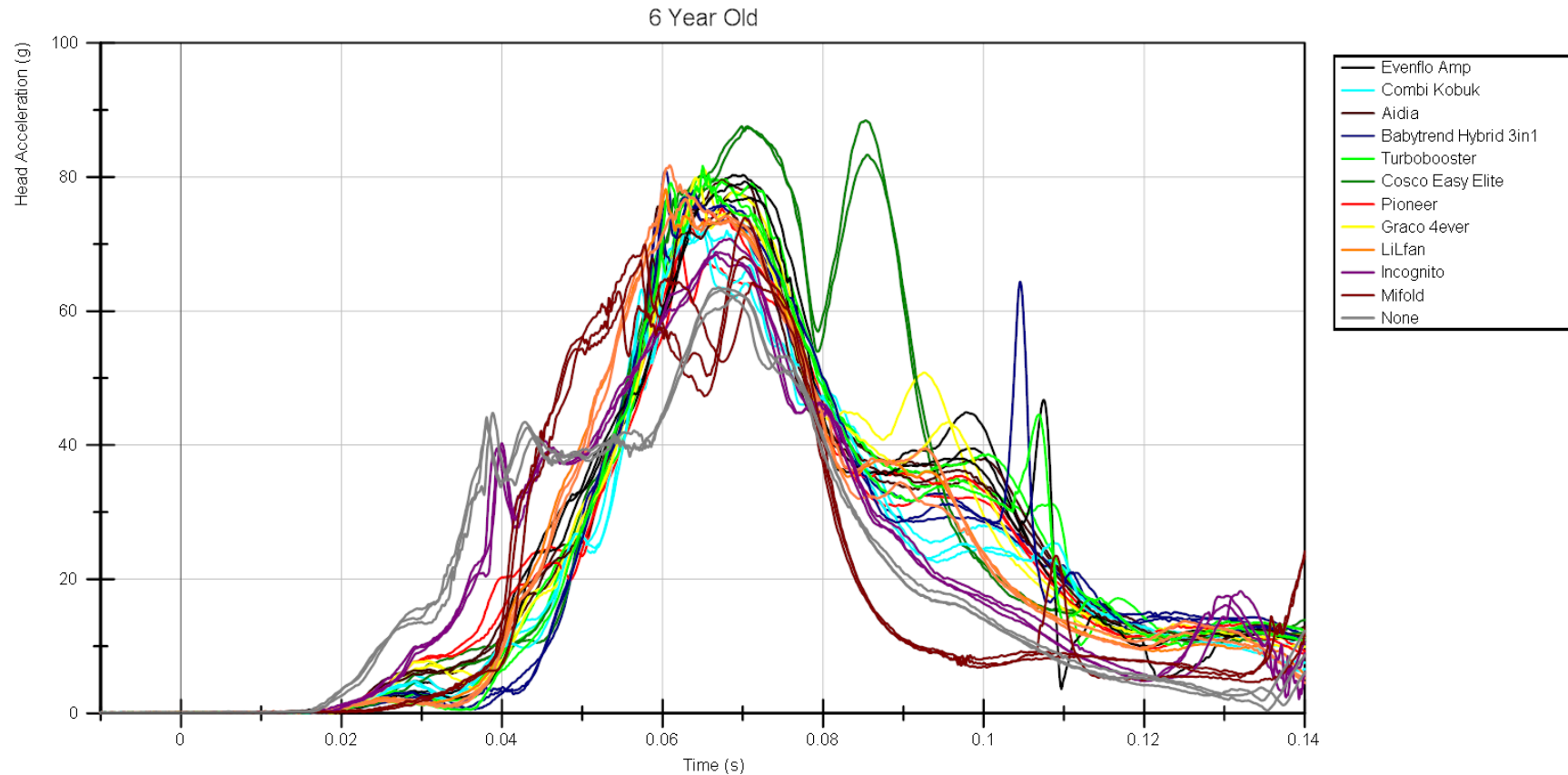


Figure 27. Overlap of head resultant acceleration for tests with 6YO ATD.

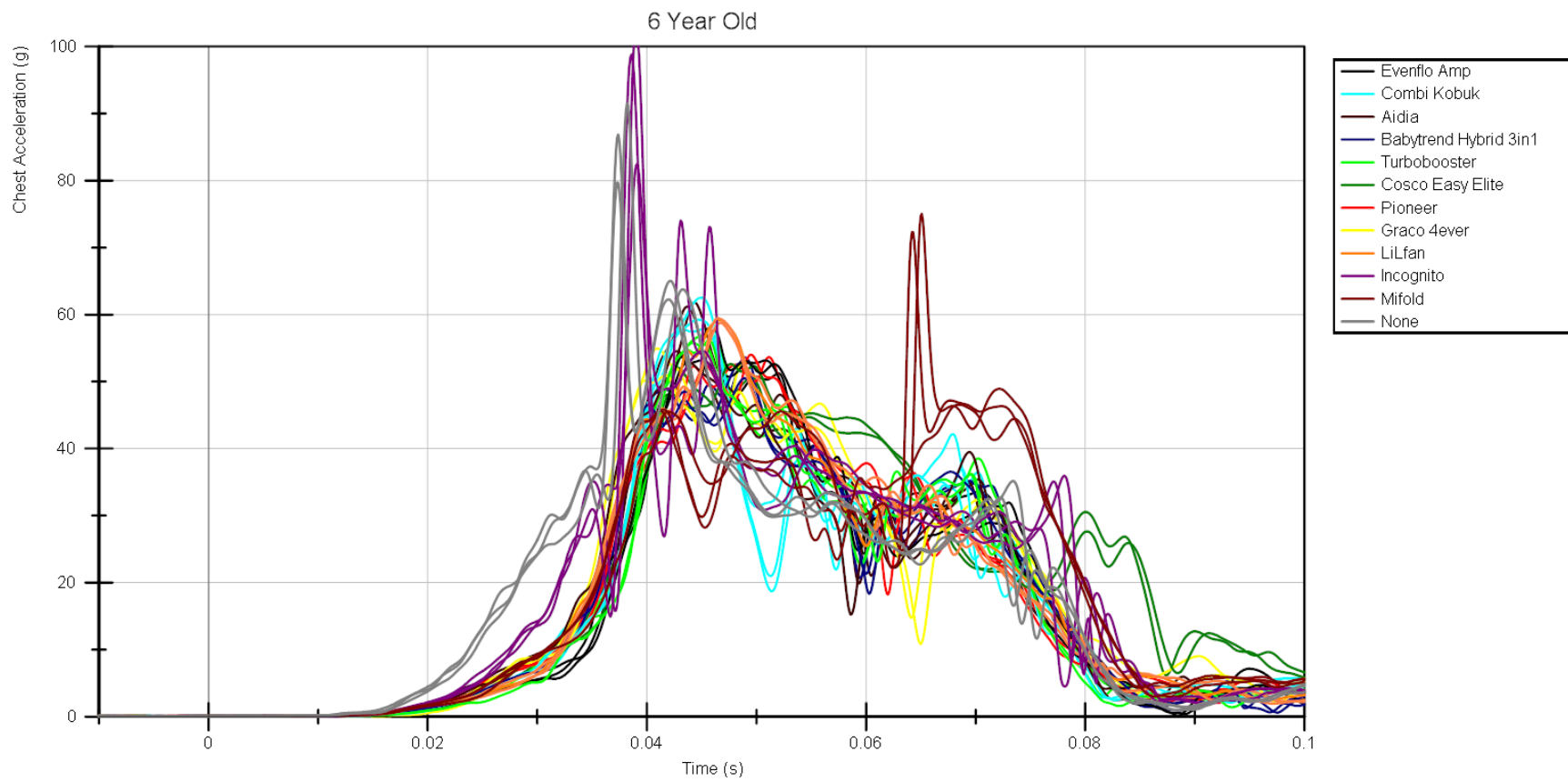


Figure 28. Overlay of chest resultant acceleration for tests with 6YO ATD.

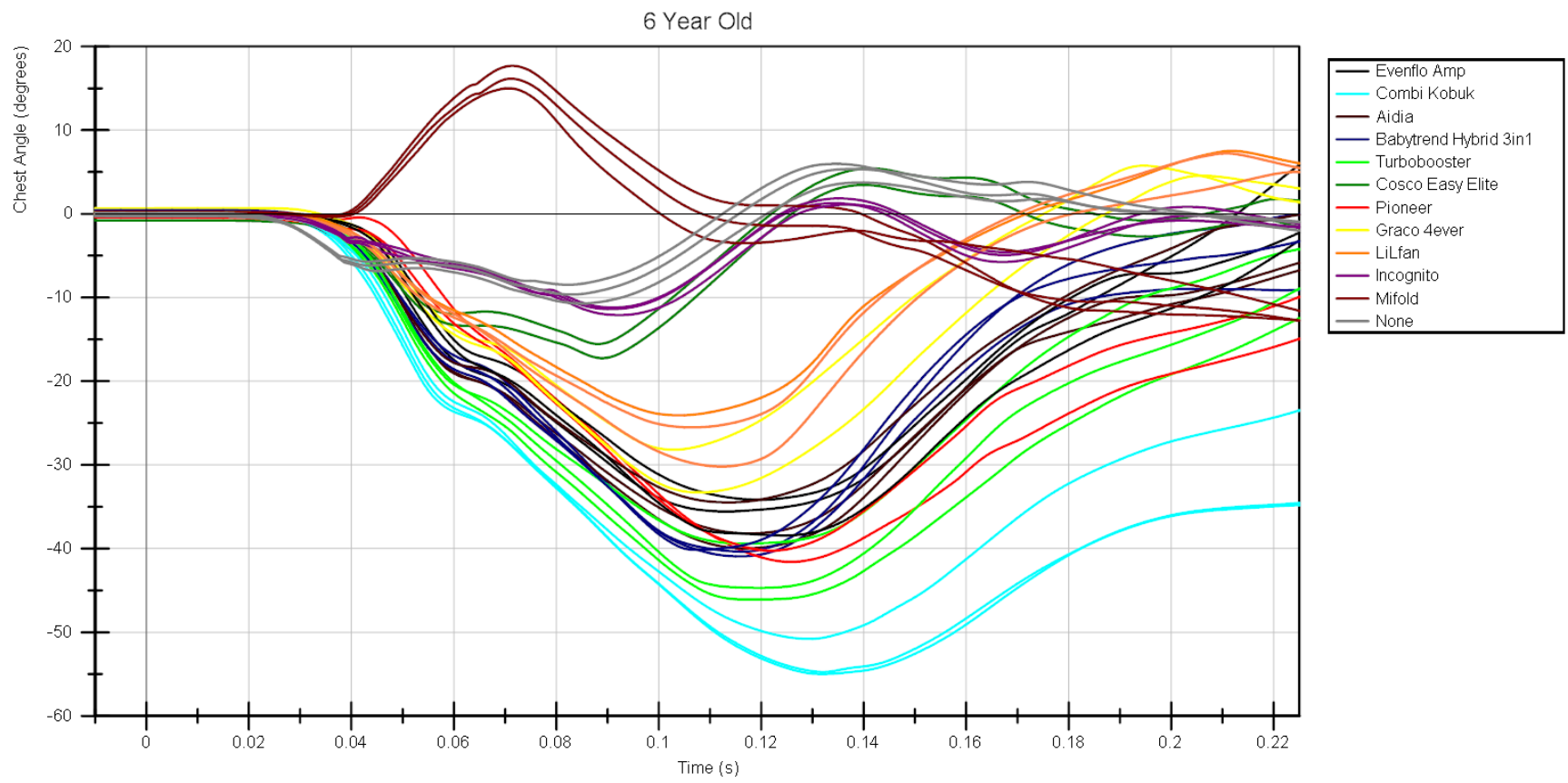


Figure 29. Overlay of change in chest angle for tests with 6YO ATD.

Candidate Booster Metrics

For the plots in this section, each color corresponds to a different booster model; colors are consistent with the color schemes used in the volunteer portion of the study. Symbol shapes correspond to different categories of boosters, with circles indicating highback, squares indicating backless, triangles indicating 3-in-1, and diamonds indicating no booster. Larger symbols indicate data from tests performed with the H3-10YO ATD, while small symbols are those run with the H3-6YO ATD. Filled symbols are tests performed with the 2018 version of the test bench, while open symbols are those run with the 2015 version of the test bench. On each plot, lines in navy blue indicate current thresholds for performance criteria, either from current FMVSS No. 213 requirements or from alternate injury reference values (Irwin et al. 1999). Lines in gray indicate the possible threshold values based on the goal of performance that is at least 10 percent better than the no booster condition. Here solid lines are used to denote the targets for tests run with the H3-10YO and dotted lines are used for tests using the H3-6YO. On some plots, gray corridors indicate suggested thresholds corresponding to good kinematics.

Current Measures

A goal of this project is to identify thresholds for candidate booster metrics that are related to good occupant protection and cannot be met without using a booster. To begin, we review the currently used FMVSS No. 213 metrics to assess booster performance: HIC (36ms), 3ms chest clip acceleration, head excursion, and knee excursion. Review of current booster metrics is relevant because the use of the surrogate retractor, new belt geometry, and new bench design may require reevaluation of traditional criteria. Because the repeatability data indicated that HIC (15ms) was more repeatable than HIC (36 ms), we also evaluated this measure.

Figure 30 shows HIC(36) plotted versus HIC (15) for each test. Tests run without boosters pass current criteria, and actually perform better than almost all tests run with boosters. This is logical because the ATD is best coupled to the bench with no booster but suggests that neither HIC(36) nor HIC(15) are the best measures for differentiating booster performance.

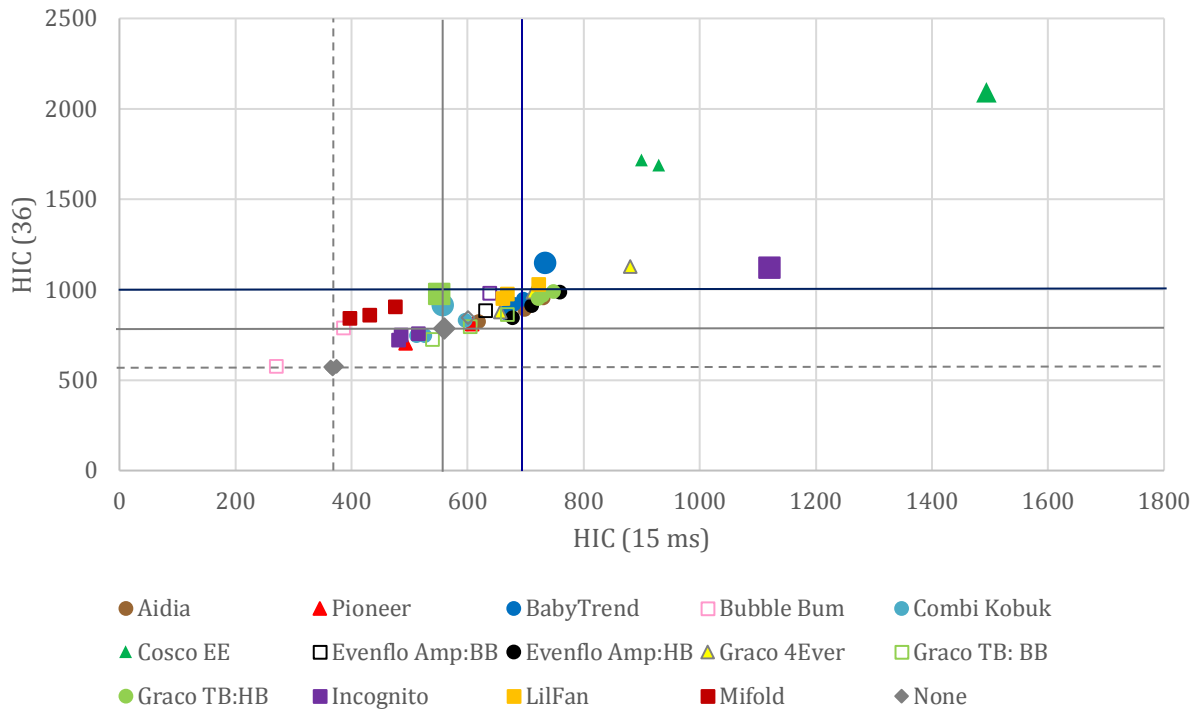


Figure 30. HIC(36) versus HIC(15).

Figure 31 plots peak resultant head acceleration versus 3 ms chest clip acceleration. A 3-ms clip head acceleration with an 80 g cutoff threshold (as used in the Canadian Motor Vehicle Safety Standard [CMVSS] 213) was also calculated but shows less differentiation among boosters than peak value. All of the boosters tested meet the existing 3-ms chest clip limit of 60 g; the no booster conditions measure about 55 g for the 6YO and 49 g for the 10YO. For peak head resultant acceleration, the 10YO test value was 75 g and the 6YO just over 80 g.

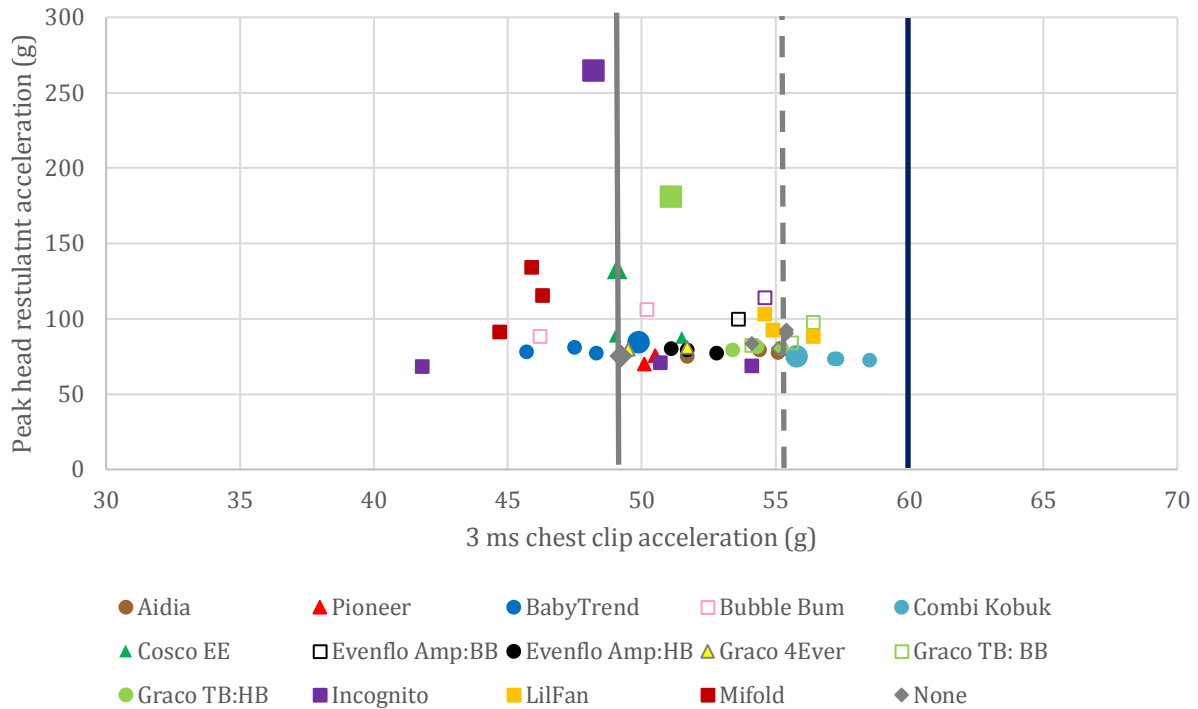


Figure 31. Peak head resultant acceleration versus 3 ms chest clip acceleration.

Head excursion is plotted against knee excursion in Figure 32. The measures for the 10YO are always higher than those for the 6YO, because the ATD is physically larger. This measure is not a displacement but rather an excursion, so if the ATD begins the test seated further forward relative to the seat assembly origin, the excursions tend to be larger. Consequently, the no-booster condition has among the lowest knee excursions, followed by the backless boosters with the exception of the Mifold. The highback boosters generally have the next greatest knee excursions, with the largest knee excursions seen in the 3-in-1 products. With regard to head excursion, the no-booster, Incognito, and Mifold had the lowest head excursions, followed by the rest of the backless boosters. Head excursions for the highback and 3-in-1 products were similar. Since the no-booster condition generally has among the lowest values of head and knee excursion compared to the booster conditions, these measures also do not adequately correspond with the improvements in safety provided by boosters observed in field data (Arbogast, Jermakian, Kallan, & Durbin, 2009, Durbin, Elliott, & Winston, 2003).

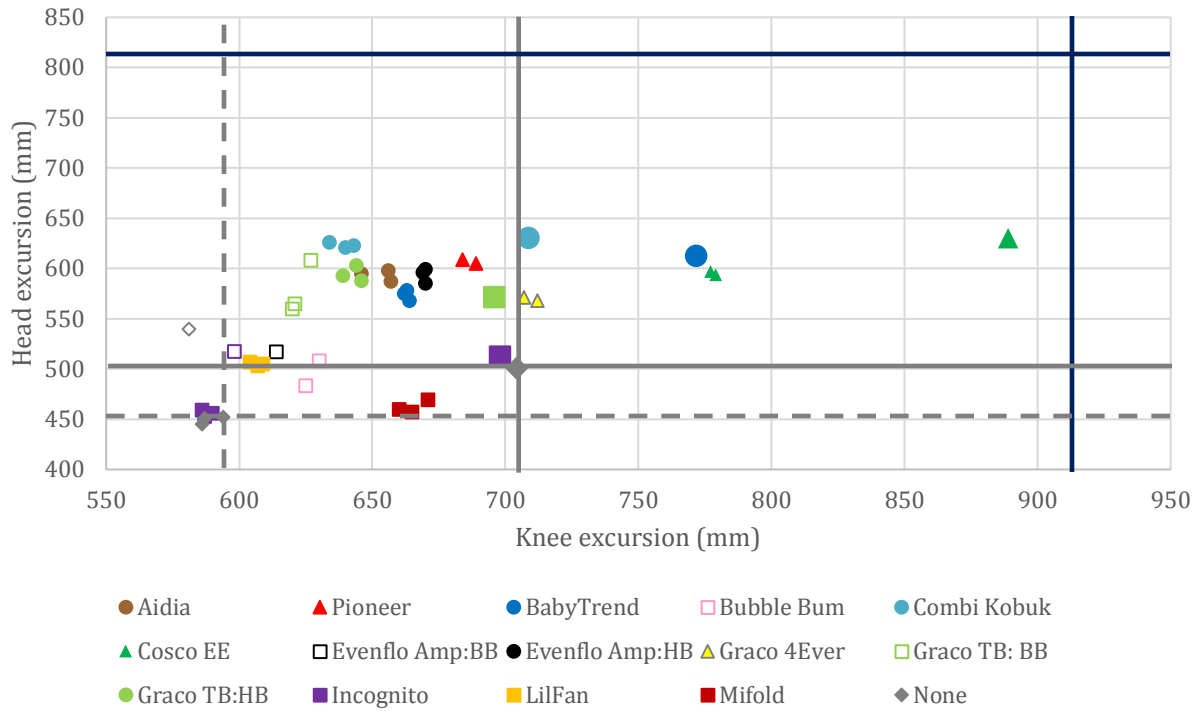


Figure 32. Head excursion versus knee excursion.

Submarining Measures

Submarining kinematics occur when the pelvis slides below the lap belt, allowing the lap belt to load the abdomen. A criterion that limits difference in head and knee excursion is based on concept that the classic submarining kinematics involve increased knee excursion and decreased head excursion. Figure 33 shows the head-knee excursion difference for non-submarining and submarining conditions. A properly used booster should keep the child in a raised position and direct the lap belt to the top of the thigh to eliminate submarining. Past research to identify quantitative measures of submarining have involved assessment of ASIS loads, calculating the difference between peak head excursion and knee excursion, and measuring forward torso rotation (Klinich et al. (2008, 2010, 2011, 2013, 2014a, 2014b.)

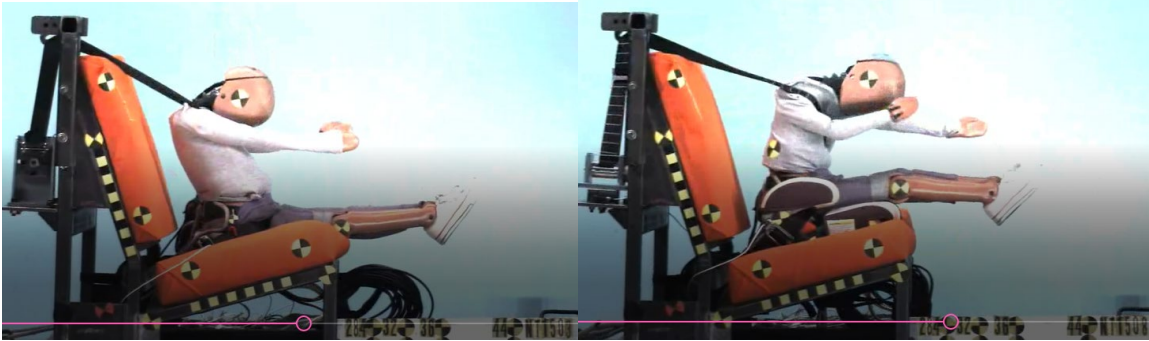


Figure 33. Side view peak of action images for test with (left) and without (right) occupant submarining.

The change in thorax angle (degrees of forward rotation) versus the knee-head excursion difference is plotted in Figure 34, while the maximum thorax angle (initial thorax angle+ degrees of forward rotation) versus knee-head excursion is plotted in Figure 35. The maximum thorax angle shows a stronger agreement with the knee-head excursion difference, because it accounts for the different initial positions of the ATD provided by different booster designs. Some past efforts found similar agreement using either change in angle or maximum angle (Klinich et al. 2010), but did not test as wide a variety of products. For the no-booster condition, the 6YO difference is approximately 140 mm, while the 10YO difference is just over 200 mm. To ensure that a booster actually performs better (not just the same) as the no-booster condition, we propose knee-head thresholds about 10 percent below these values, about 125 mm for the 6YO and 180 mm for the 10YO. For the no-booster condition, both the 6YO and 10YO have final torso angles of about -5 degrees, indicating that they do not rotate past vertical. Several other tests also indicate that the ATD did not rotate past vertical; these tests also had knee-head excursion differences greater than 140 mm.

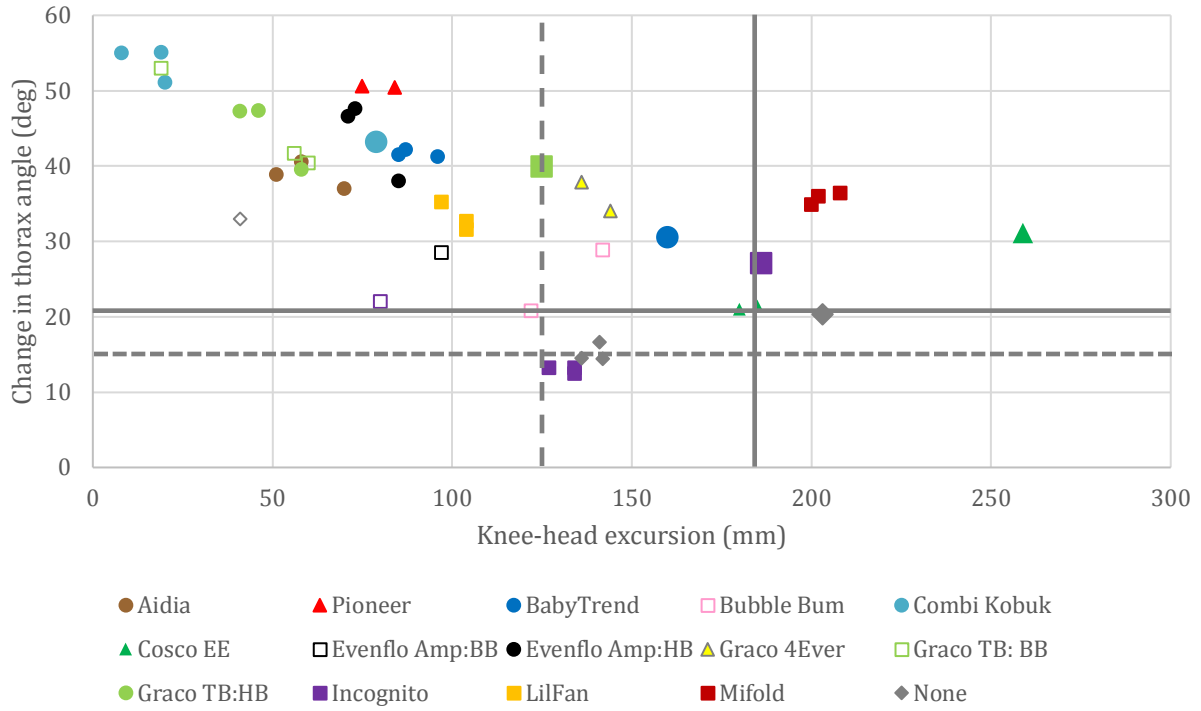


Figure 34. Change in thorax angle versus knee-head excursion.

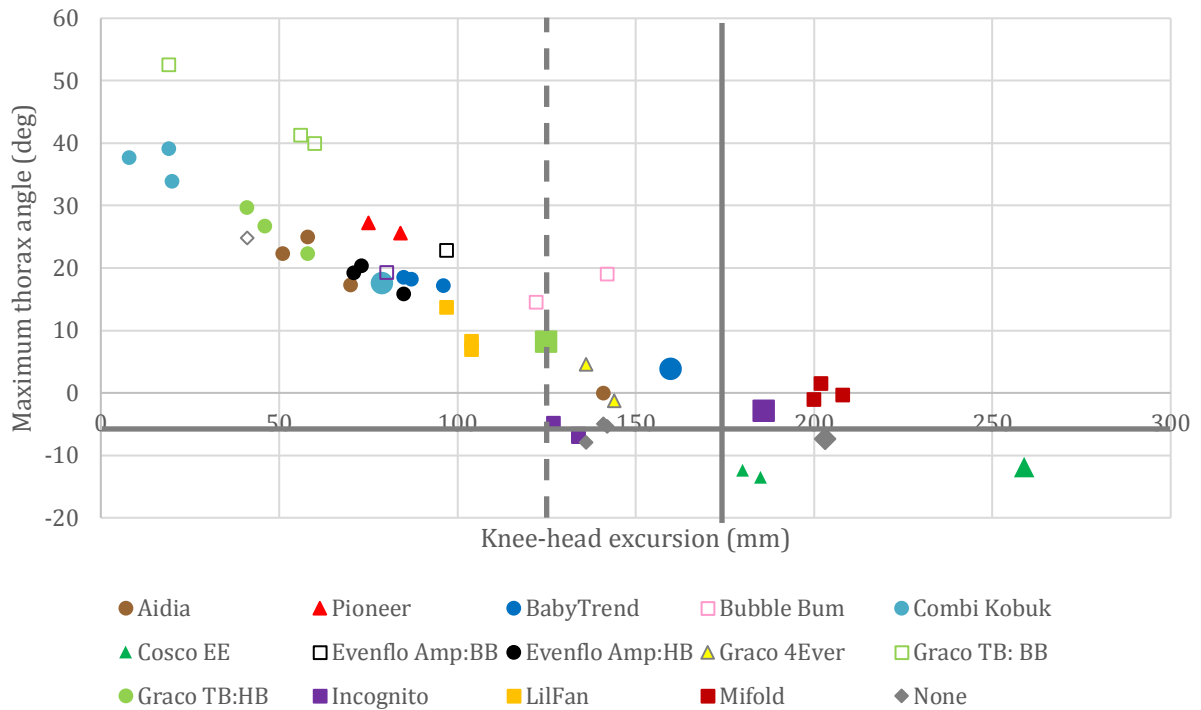


Figure 35. Maximum thorax angle versus knee-head excursion.

The upper neck and lumbar loads and moments, as well as the ASIS forces, were reviewed to identify if any measures or their resultants were correlated with kinematics. While the patterns of shifting loads between the upper and lower ASIS loadings can identify whether the belt tends to load the lower or upper part of the pelvis and how it shifts during a test, the ASIS load cells do not really identify the worst case belt loading scenarios of the belt loading entirely on the abdomen or forward on the thighs.

The axial neck loading force, shown in Figure 36 for the 6YO tests, could potentially differentiate the boosters having the largest knee-head differences using a threshold of about 2700 N (value of 3000 for no-booster condition minus 10%). However, published injury reference values for the 6YO axial neck tension are about 1800 N (Irwin et al. 1999); by this measure all boosters should produce serious neck injuries under these crash severities though this is not seen in field data (Arbogast, Jermakian, Kallan, & Durbin, 2009, Durbin, Elliott, & Winston, 2003).

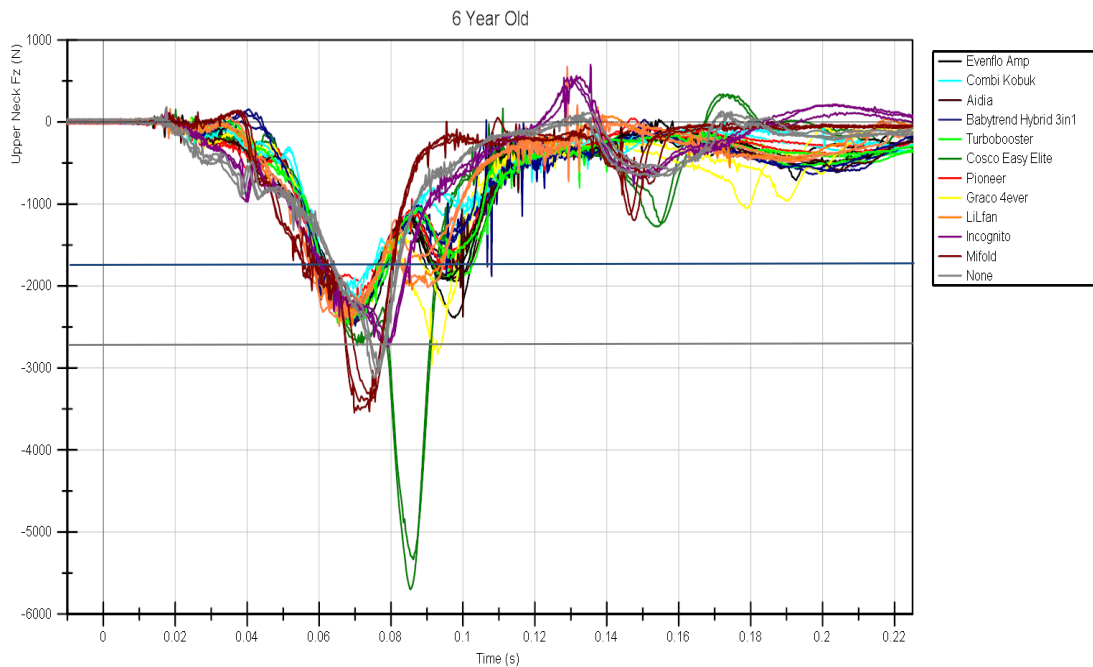


Figure 36. Neck axial load for 6YO tests.

Two lumbar measures, the MomentZ and ForceY, have the potential to differentiate between submarining, acceptable, and rollout kinematics. Results for the 6YO are shown in Figure 37 and Figure 38, while results for the 10YO are shown in Figure 39 and Figure 40. Results for the Combi Kobuk have the largest negative values of MomentZ and the highest values of ForceY, reflecting the greatest amount of twisting about the lumbar spine allowed when the shoulder belt loads the arm rather than the shoulder. The test conditions that prevented rotation of the lumbar spine by the shoulder belt loading the ATD close to the neck (no booster, Mifold, Incognito, and Easy Elite), have values near zero (or positive) for MomentZ and negative values for LumbarY. (Note that these measures would need to account for position of the shoulder belt in a passenger or driver side configuration.)

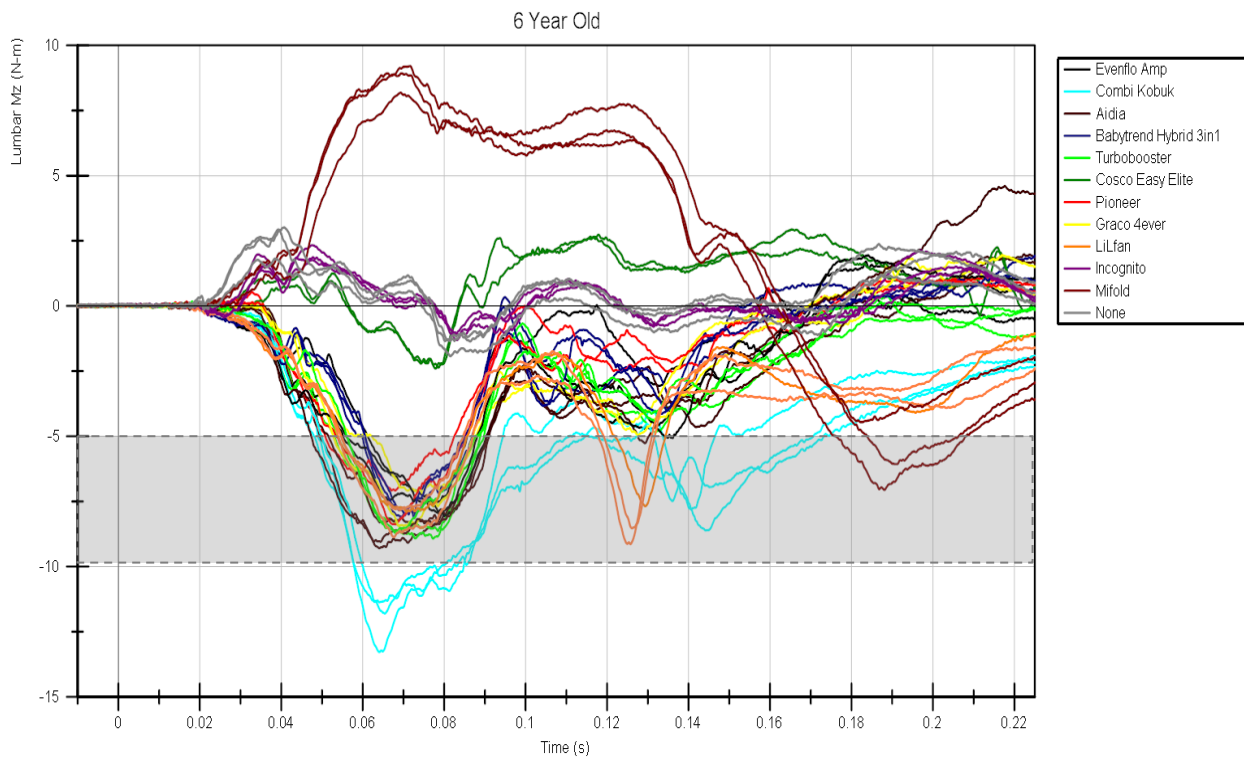


Figure 37. Lumbar MomentZ for 6YO Tests.

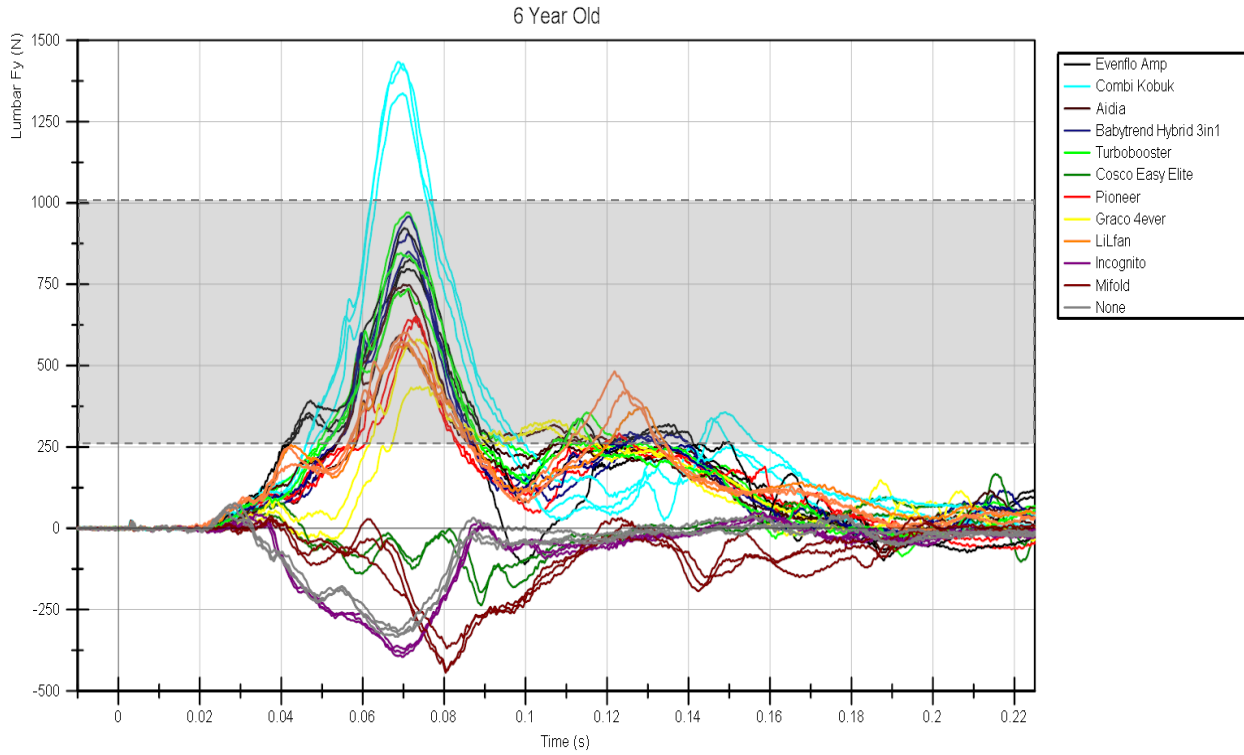


Figure 38. Lumbar ForceY for 6YO tests.

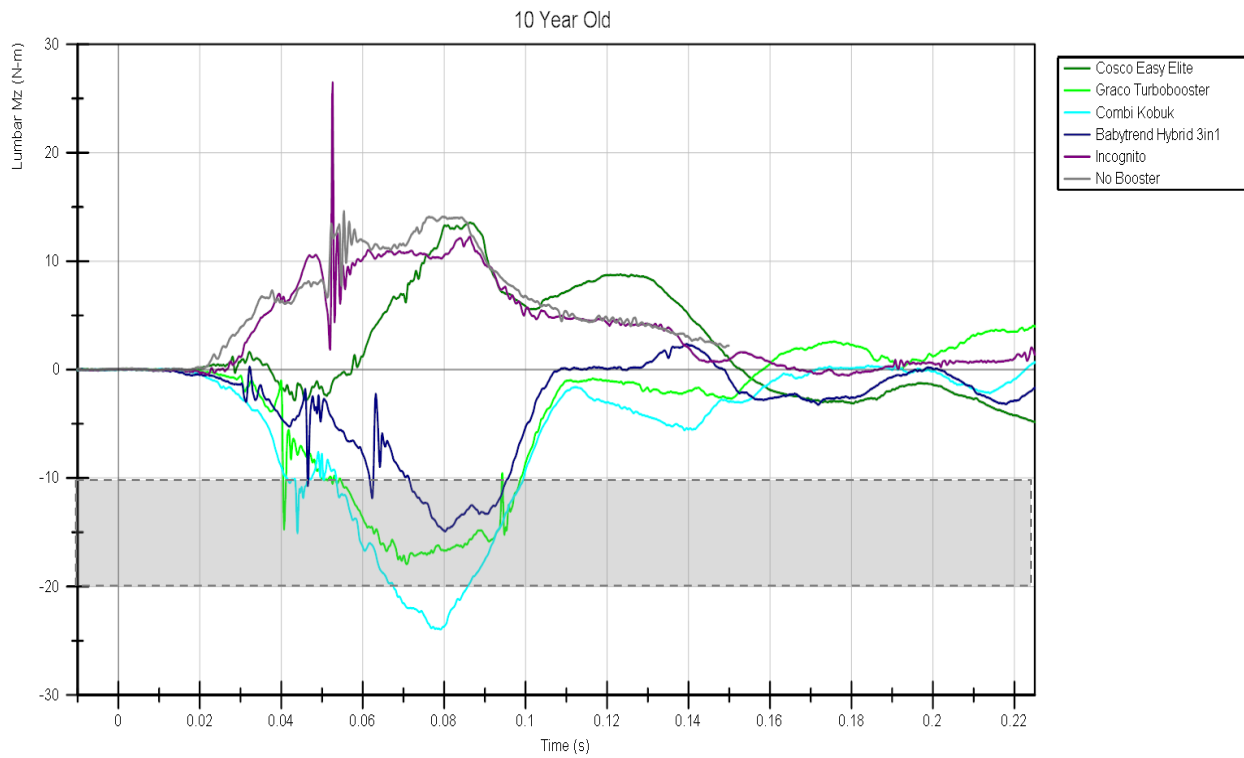


Figure 39. Lumbar MomentZ for 10YO tests.

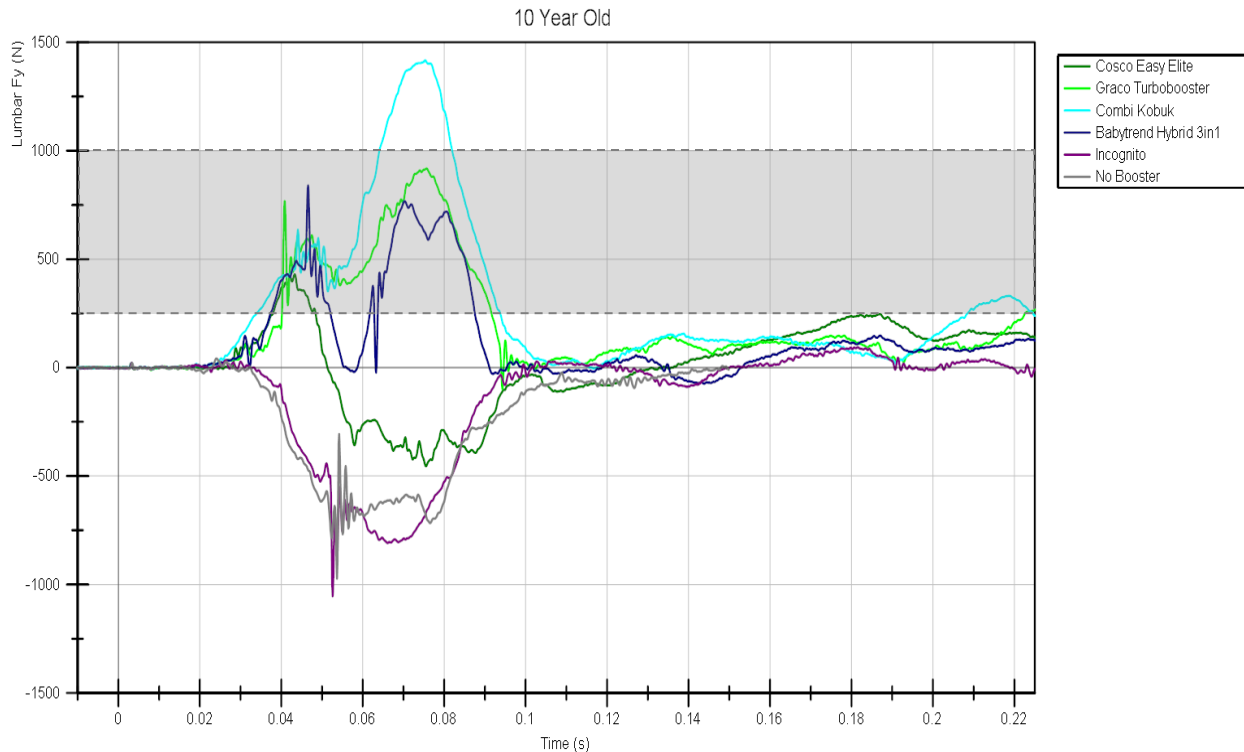


Figure 40. Lumbar ForceY for 10YO tests.

Static measures

Two measures of belt fit, lap belt score (LBS) and shoulder belt score (SBS), are plotted versus knee-head excursion in Figure 41 and Figure 42. The shaded green boxes on each plot correspond to the LBS and SBS ranges considered to be in the desirable range by the IIHS booster seat belt fit metric (IIHS 2018). These ranges are included for reference rather than a recommendation; belt fit scores may differ between the IIHS procedure and our measurements because of differences in seat geometry, belt geometry, and presence of test clothing.

For the LBS, shown in Figure 41, the no-booster condition has a LBS near 12 mm, while the 10YO value is 15 mm. Two boosters with scores close to these values also have knee-head excursions near or above the proposed threshold of 140 mm. Five boosters have LBS in the range of 12-20 mm but knee-head excursions below 100 mm. The booster with the highest LBS has knee-head excursions near 200 mm.

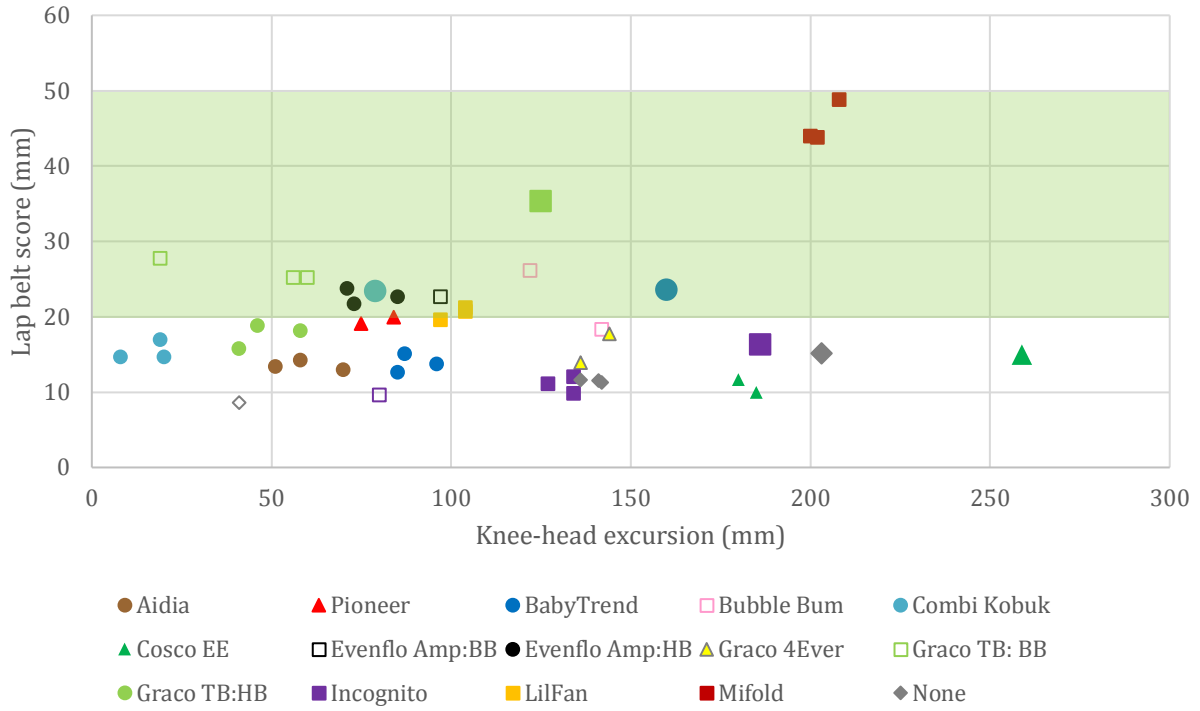


Figure 41. Lap belt score versus knee-head excursion.

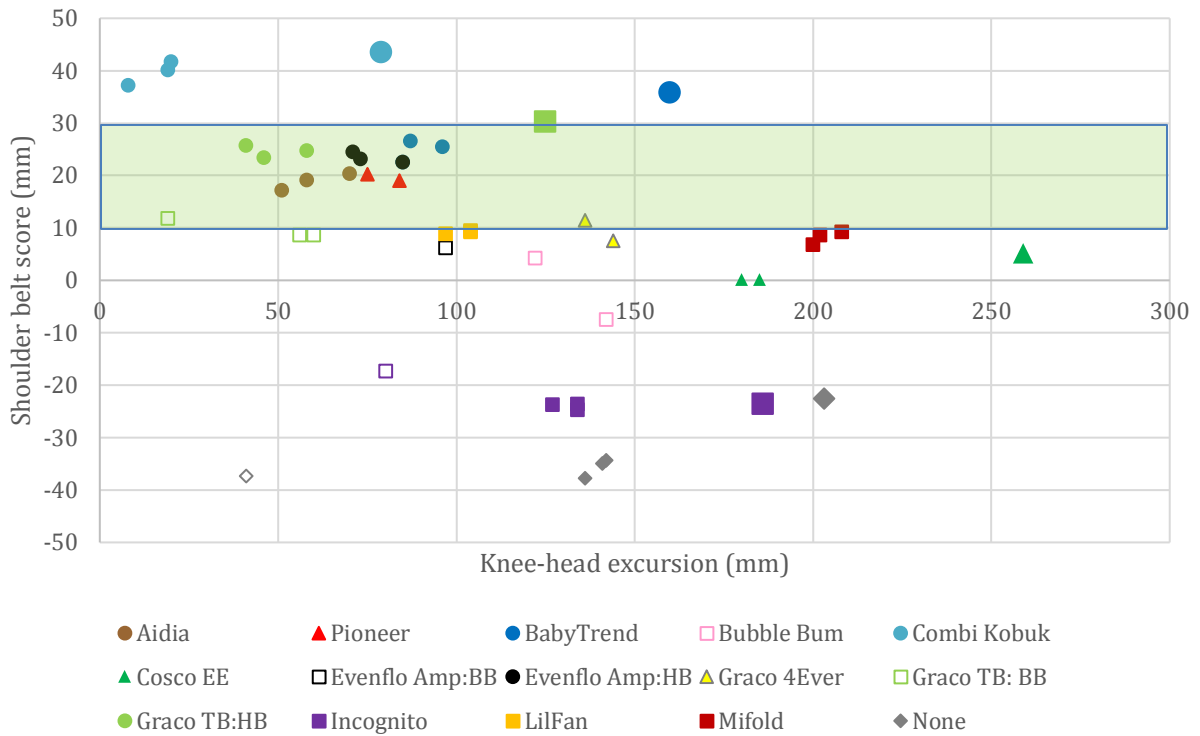


Figure 42. Shoulder belt score versus knee-head excursion.

The ability of the boosters to raise the seated occupant was quantified by the average of the right and left ATD H-point heights, measured with the FARO Arm during test setup. The zero level was defined as the average ATD H-point height when no booster was used. The amount of boost is plotted against knee-head excursion in Figure 43. While two of the products with knee-head excursions near or exceeding the no-booster values near 125 have the lowest amount of boost, the other boosters that exceed this level have boost values above 100 mm.

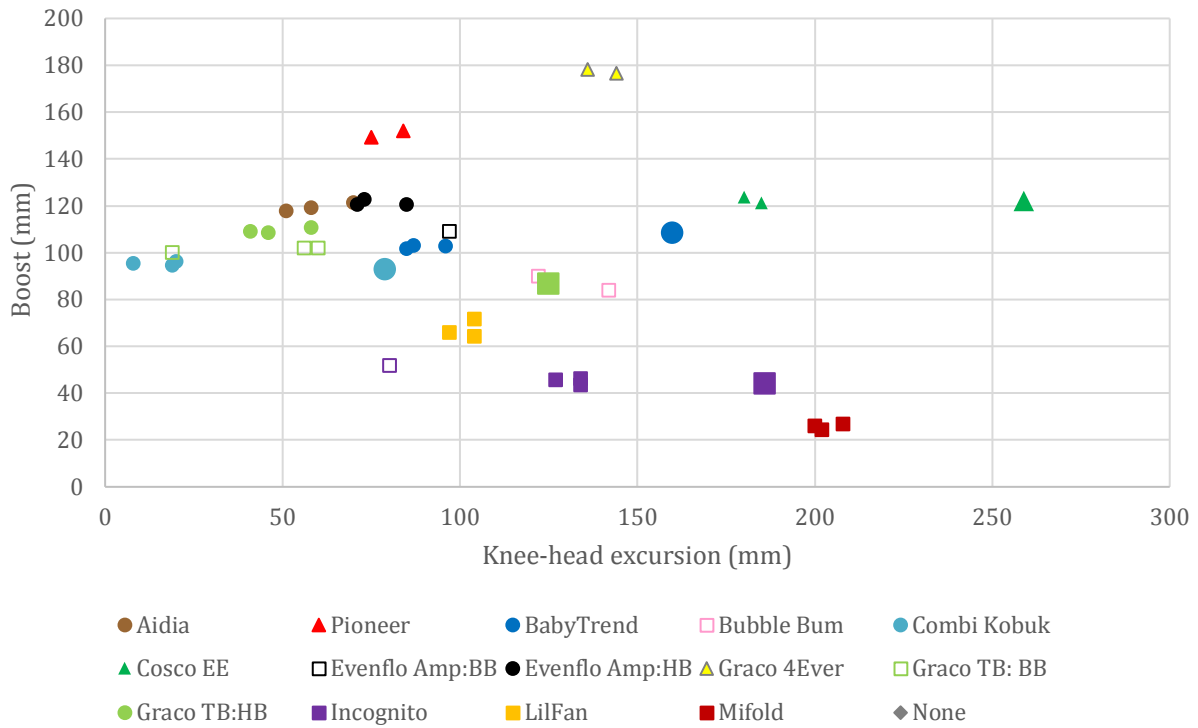


Figure 43. Boost amount versus knee-head excursion.

The IIHS booster seat ratings are based on the lap and shoulder belt fit provided by a booster under a variety of simulated vehicle belt geometries. The latest version of the procedure uses a simplified version of the H3-6YO to improve repeatability. Figure 44 shows the IIHS rating for each model versus the knee-head excursion. On this plot, 0 indicates not rated, 1 not recommended, 2 check fit, 3 good bet, and 4 best bet. The products that were not evaluated and the one receiving the “not recommended” rating were among the worst performers in terms of knee-head excursion.

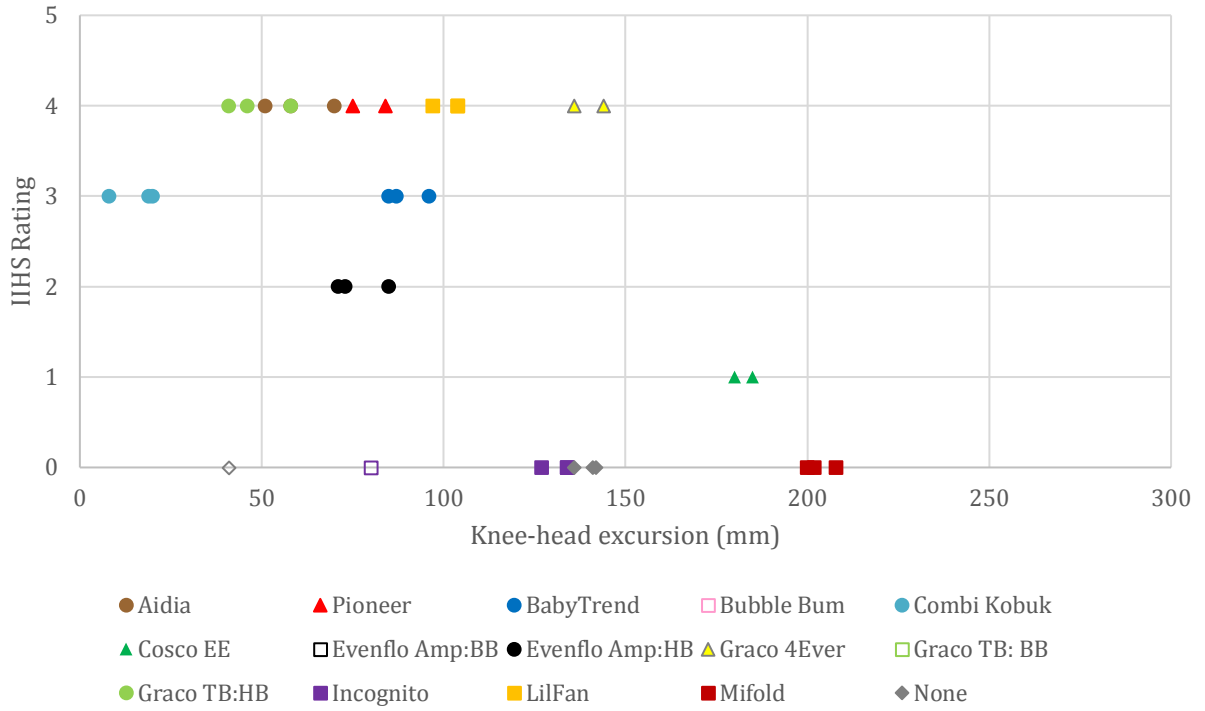


Figure 44. IIHS rating versus knee-head excursion.

RESULTS: VOLUNTEER TESTING

Qualitative Review

Sample photos of children whose height approximates that of the H3 6YO ATD are shown in Table 18 for the laboratory conditions and Table 19 for the vehicle conditions. Even in boosters, several volunteers chose to place their feet on the seat cushion or cross their lower extremities.

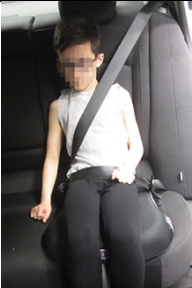
Table 18. Child posture laboratory seating conditions.

	B_L	B_B	B_Z
A			
B			
C			
D			

	B L	B B	B Z
E			
F			
None			
G1 Stature 1179 mm			
None			
G2 Stature 1190 mm			
None			
G3 Stature 1189 mm			

Table 19. Child posture in vehicle conditions.

	Corolla	Compass	Malibu
A			
B			
C			
D			
E			

	Corolla	Compass	Malibu
F			
None			
None			
None			

Child Versus ATD Posture

Appendix C contains plots that compare the individual child postures to those of the ATDs. On these plots, the ATD postures are shown in black and the color of the child postures varies with each booster seat. When reviewing these plots, the orange (B) and purple (F) backless boosters are vertically shorter than the other four products.

Detailed presentation of posture differences between the child volunteers and ATDs focuses on the 6YO ATD since all but two subjects were smaller than the 10YO ATD. However, the postural representations of the 10YO and small female ATDs are overlaid with those of the child volunteers in Appendix C.

Fore-Aft Hip Position Versus 6YO ATD

Figure 45 illustrates the fore-aft difference between the child and ATD hip position for all of the mockup conditions. Increasing negative indicates that the child volunteer is forward of the 6YO ATD. The mean forward shift of the child relative to 6YO ranged from 10-46 mm in seat assembly condition Z. Trends were similar in seat assembly condition L except that the range of the mean increased to 16-52 mm, the largest fore-aft difference across the mockup conditions. The two lower height boosters (Lil Fan [B] and Incognito [F]) resulted in child postures that were ~40 and ~52 mm forward of the 6YO ATD for both the L and Z seat assembly mockup test conditions, respectively. This difference was significant for the Incognito [F] versus all high-back boosters and for the Lil Fan [B] versus the Graco high-back boosters [C, D] in both package configurations and the Britax Pioneer [A] in the Z seat assembly mockup ($p < 0.01$).

For mockup condition B, the average hip position of the volunteers in the four taller boosters ranged from 10-24 mm forward of the hip location of the 6YO for all boosters, with the exception of the Graco 4Ever 4in1 HB [C], in which there was minimal difference between the 6YO and children. The two lower height boosters did not differ significantly from the other high-back boosters or no-booster conditions.

Figure 46 illustrates the fore-aft difference between the child and ATD hip position for all of the vehicle conditions. The position of child volunteers relative to the 6YO ATD ranged from 4-25 and 0-24 mm for the Toyota and Malibu vehicle configurations, respectively. In the Jeep vehicle configuration, the mean shift of hip position in the two lower height boosters was greater, resulting in child postures that were 23-50 mm forward of the 6YO ATD versus a mean range of fore-aft hip position of 6-15 mm for the high-back boosters. These differences were significant for the Incognito [F] versus all high-back boosters in the Jeep, and all high-back boosters with the exception of the Combi Kobuk [E] in the Malibu vehicle ($p < 0.01$). Although the Safety 1st Incognito demonstrated a trend towards a more forward seated child posture, these differences were not significant.

Table 20 lists the means and standard deviations of the difference in (delta) child-ATD fore-aft hip X position across boosters, collapsed across the mockup and vehicle conditions, including the no-booster conditions, for all subjects. Using both paired t-tests and the non-parametric Wilcoxon signed rank test, comparisons of mean value among the conditions were statistically different between the two lower height boosters (Lil Fan [B] and Incognito [F]) and all high-back boosters ((Britax Pioneer [A], Graco 4Ever 4in1 [C], Graco TurboBooster [D] and Combi Kobuk [E]) ($p < 0.01$).

Table 20. N, Mean, and standard deviation of fore-aft hip position for each booster

Booster	n	Mean	Std Dev
Britax Pioneer HB [A]	47	-14.942	17.3375
Graco 4Ever 4 in 1 HB [C]	36	-6.924	13.9259
Graco TurboBooster HB [D]	43	-8.497	18.9754
Combi Kobuk HB [E]	36	-18.478	16.632
Lil Fan BB [B]	46	-28.591	21.0019
Safety 1 st Incognito BB [F]	48	-36.911	23.9037
None	142	-25.689	26.9709

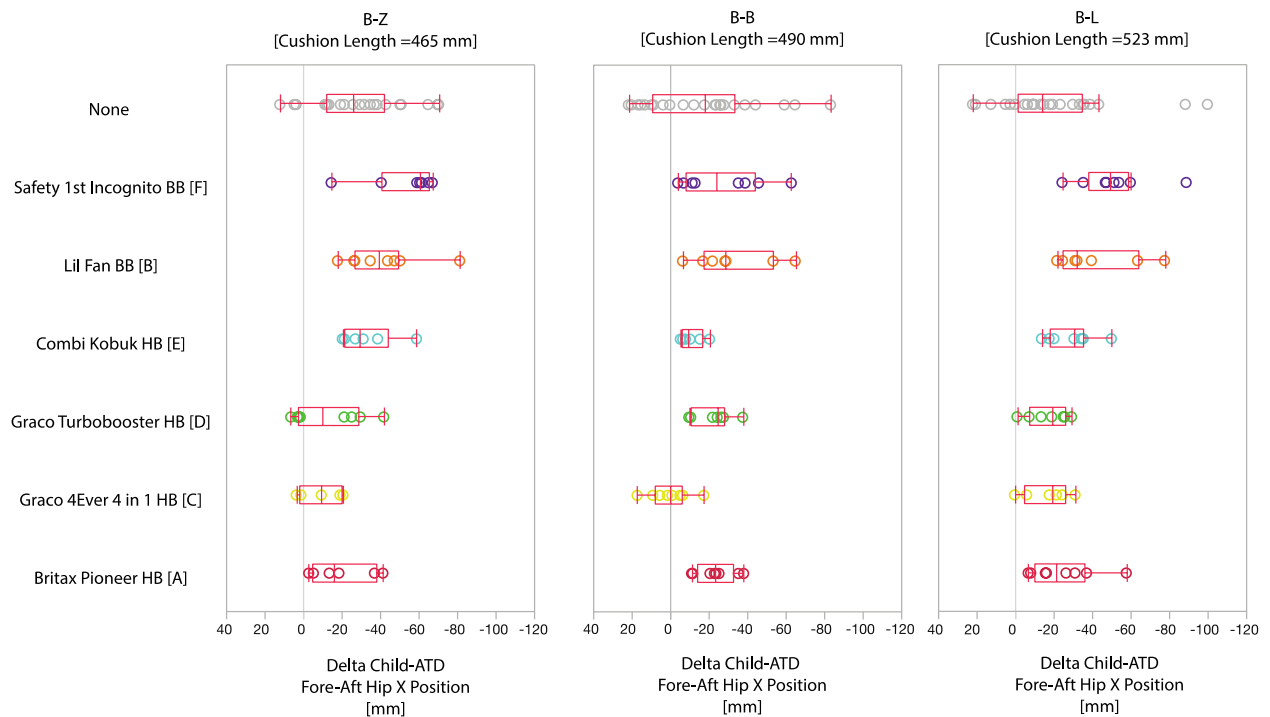


Figure 45. Comparison of fore-aft hip position (relative to H36YO) in seat assembly conditions: Z, B, and L. Negative values indicate that the child volunteer is forward of the 6YO ATD.

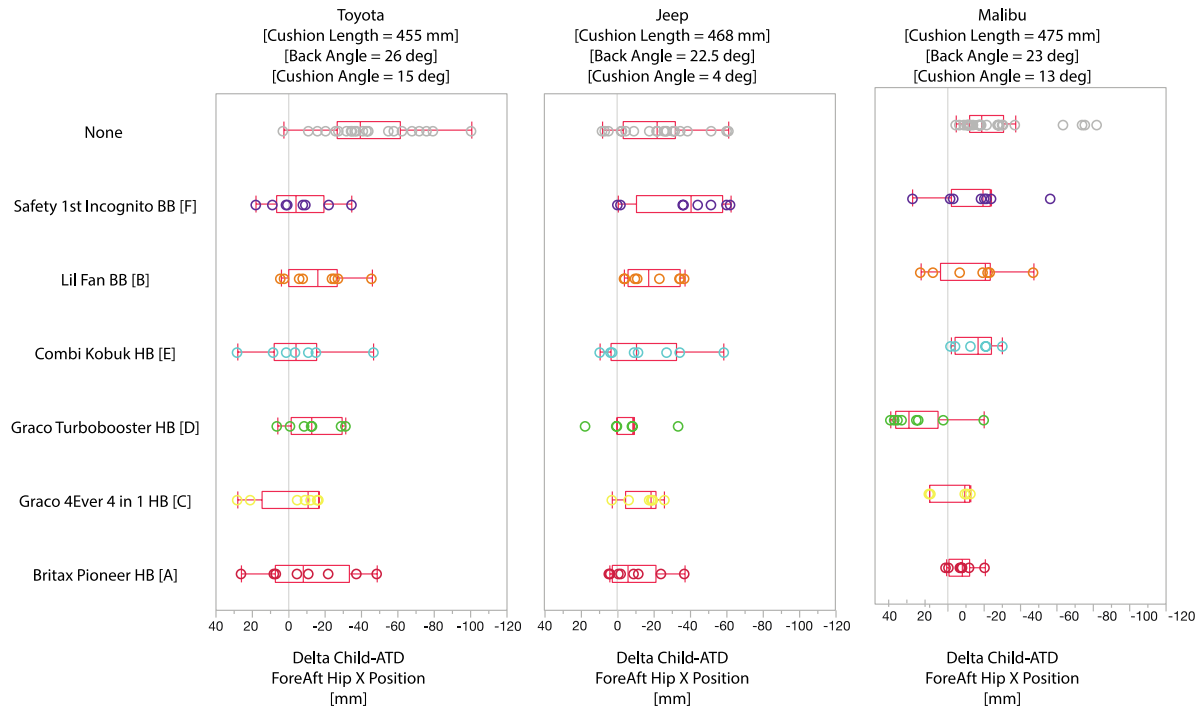


Figure 46. Comparison of fore-aft hip position (relative to H36YO) in vehicle conditions: Toyota, Jeep, and Malibu. Negative values indicate that the child volunteer is forward of the 6YO ATD.

Vertical Hip Position Versus 6YO ATD

Figure 47 and Figure 48 illustrate the vertical difference between the child and ATD hip position for the mockup and vehicle configurations, respectively. A positive value indicates that the child’s hip position is above the 6YO ATD. Across the conditions, the overall mean differences in the child’s vertical hip location relative to 6YO ATD were relatively small, indicating that the vertical location of the ATD hip position is representative of the child volunteers. Average hip position of the volunteers ranged from 14 mm above and 16 mm below the average 6YO ATD hip location. Trends were inconsistent across the combination of boosters in mockup and vehicle packages. The two lower height boosters did not differ meaningfully from the other high-back boosters. The only exception was a significant difference for the Incognito [F] versus Graco TurboBooster [D], Combi Kobuk [E] and Lil Fan [B] in the Jeep vehicle. Notably, the child’s hip position was significantly higher in comparison to the 6YO ATD for all no-boost conditions, across all package configurations.

Table 21 lists the means and standard deviations of the difference in (delta) child-ATD vertical hip Z position across boosters, collapsed across the mockup and vehicle conditions, including the no-booster conditions, for all subjects.

Table 21. N, Mean, standard deviation of fore-haft hip position for each booster

Booster	n	Mean	Std Dev
Britax Pioneer HB [A]	47	5.011	11.4042
Graco 4Ever 4 in 1 HB [C]	36	-1.078	9.1067
Graco TurboBooster HB [D]	43	-7.510	14.3148
Combi Kobuk HB [E]	36	-2.579	13.592
Lil Fan BB [B]	46	1.581	12.8432
Safety 1 st Incognito BB [F]	48	8.21	13.3907
None	142	18.65	18.0604

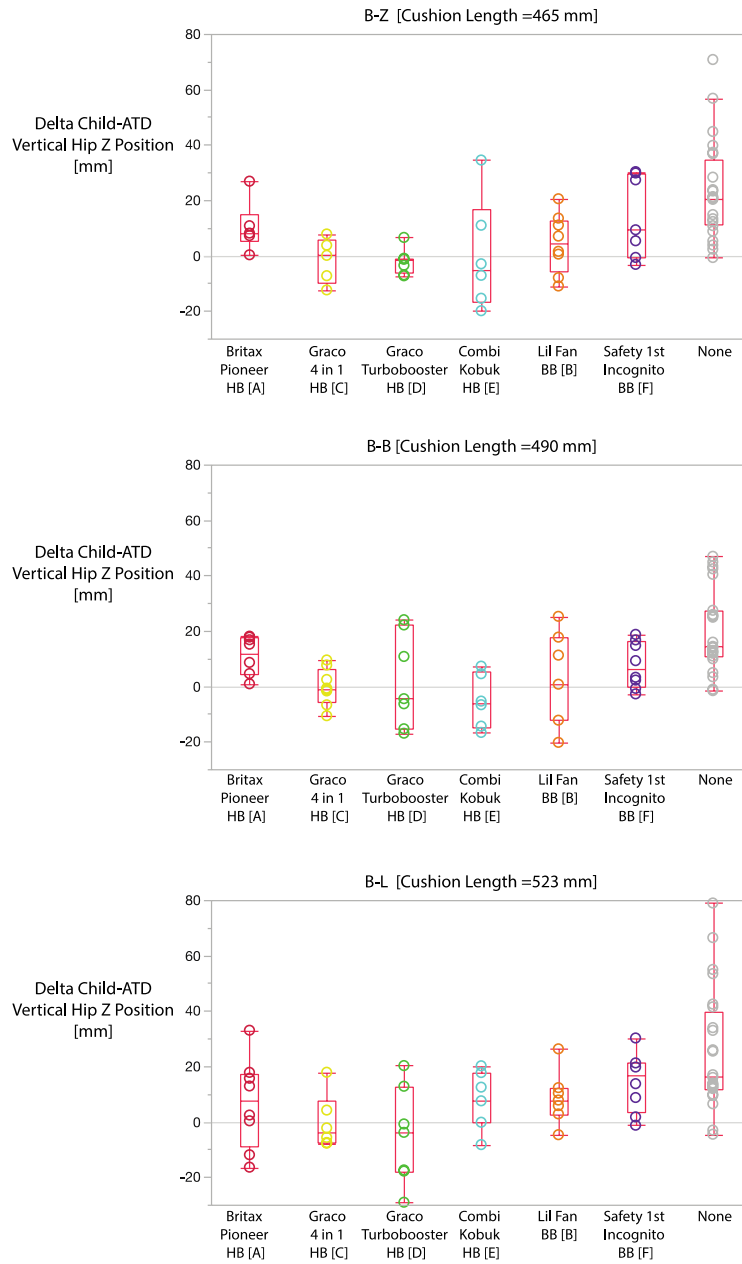


Figure 47. Comparison of vertical hip position (relative to H36YO) in seat assembly conditions: Z, B, and L. A positive value indicates that the child's hip position is above the 6YO ATD.

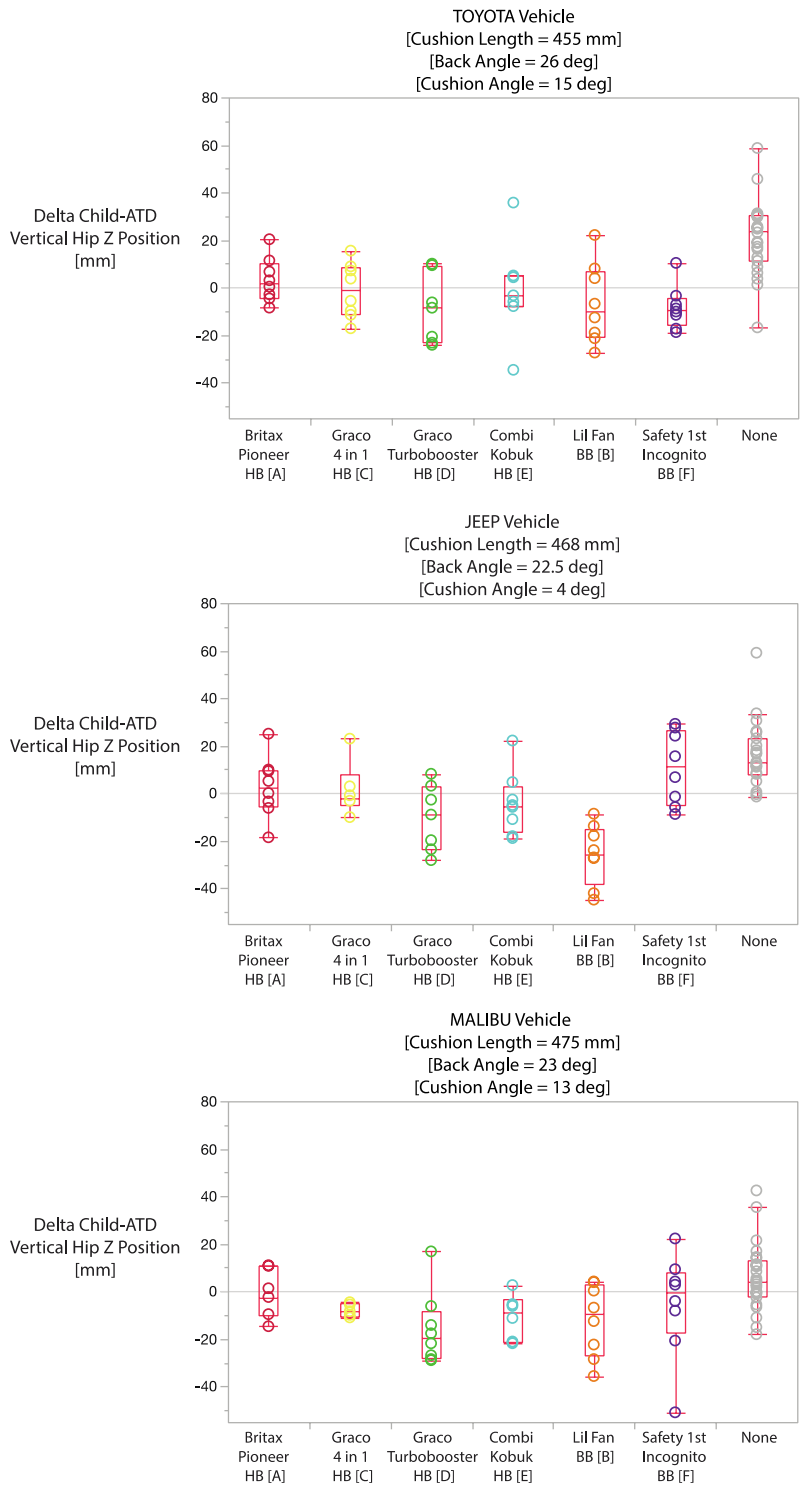


Figure 48. Comparison of vertical hip position (relative to H36YO) in vehicle conditions: Toyota, Jeep, and Malibu. A positive value indicates that the child's hip position is above the 6YO ATD.

Lower Extremity Posture Versus 6YO ATD

The knee position of the volunteers was observed to be forward of the 6YO ATD knee position. The top of Figure 49 illustrates the forward shift in child-ATD fore-aft knee X position across boosters, collapsed across the mockup and vehicle conditions, including the no-booster conditions, for all subjects. A negative value indicates that the child's knee is forward of the 6YO ATD knee. The overall mean forward shift of the child knee location relative to 6YO ranged from 48-82 mm. Across the mockup configurations, this forward shift in the horizontal knee location did not differ significantly between the boosters. However, pairwise comparison did result in significant differences between the lower height boosters [B and F] and the HB boosters for the Jeep vehicle condition ($p < 0.01$).

Vertical knee position was observed to vary with booster condition as shown in the lower part of Figure 49. A positive value indicates that the child's knee is above the 6YO ATD knee. The two lower height boosters (Lil Fan [B] and Incognito [F]) resulted in child lower extremity postures that were more closely associated with the ATD 6YO across the mockup and vehicle configurations. The overall mean of the vertical knee position was 2 mm lower and 10 mm higher than the ATD knee for the Lil Fan [B] and Incognito [F], respectively. As a result, the thigh angle of the ATD was observed to match that of the volunteers better in the two lower boosters compared to the taller boosters; the largest differences in vertical knee height were in the two combination boosters (A and C), which were on average 32 mm lower than the 6YO ATD knee.

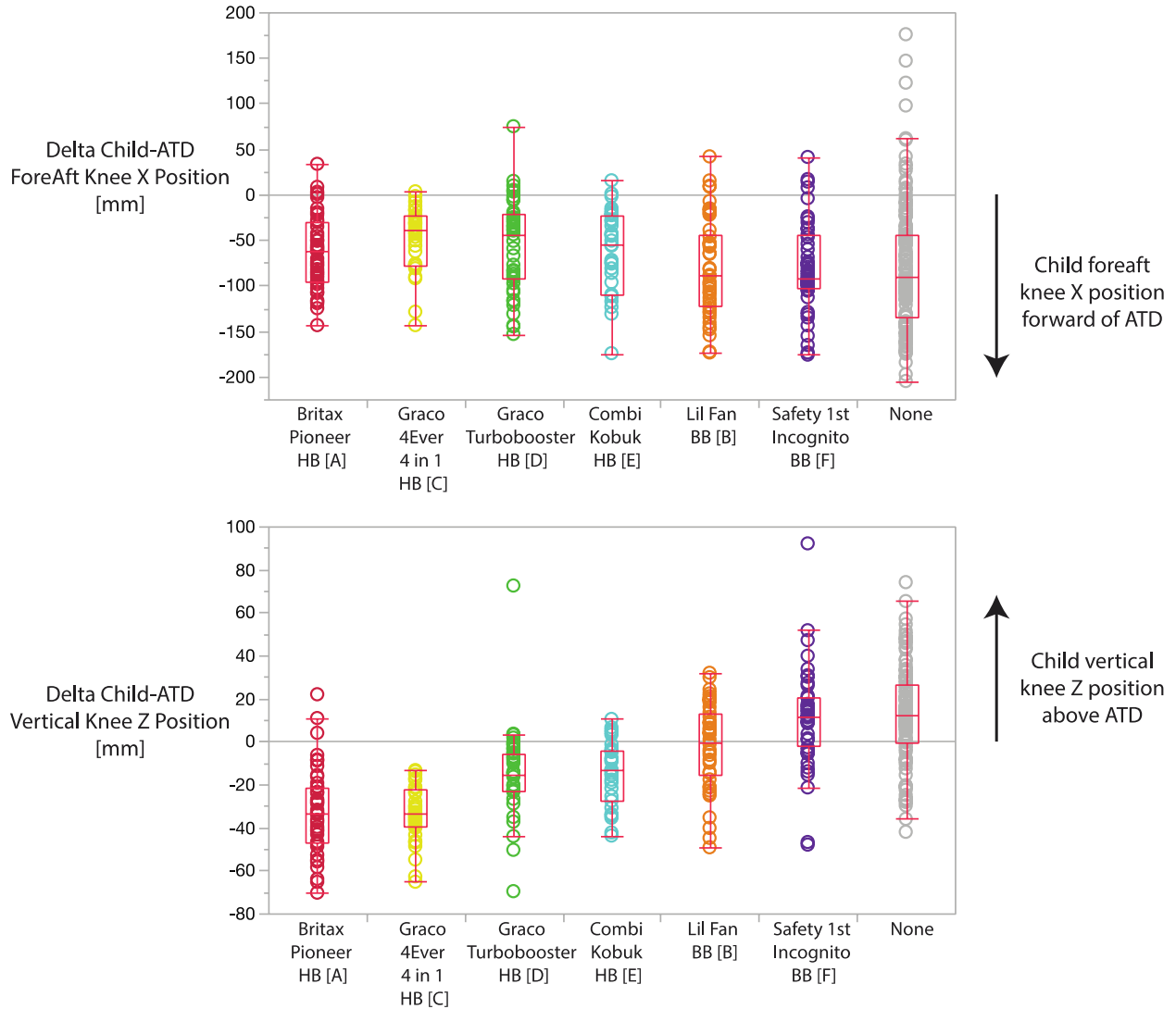


Figure 49. Difference in knee position (fore-aft X position, vertical Z position).

Figure 50 illustrates the range of included knee angles across all mockup and vehicle configurations. The filled circles correspond to the 6YO ATD. The knee angle of the 6YO ATD was generally at the higher end of the range measured in volunteers, particularly for the Incognito [F] and no-booster conditions.

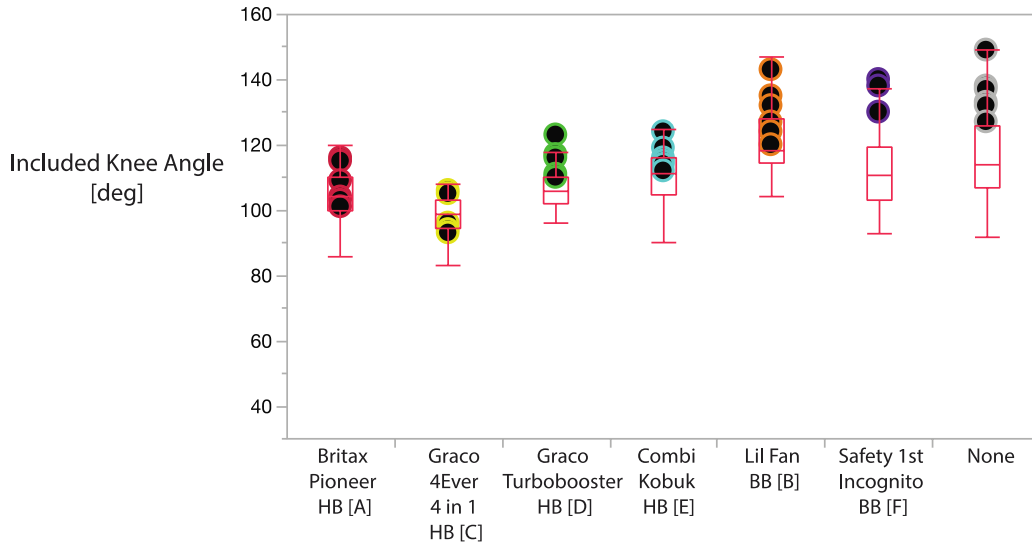


Figure 50. Distribution of the included knee angle. Box plots illustrate the distribution of the child lower extremity postures and color-coded filled circles overlay the included knee angle for the 6YO ATD installed in each booster, across the mockup and vehicle configurations.

Head CG Position Versus 6YO and 10YO ATD

Figure 51 shows the center of gravity location with respect to seat H-point for child and the 6YO and 10YO ATDs for all boosters in the mock up configurations. Positive vertical headCG indicates a head position upward, towards the roof. Positive fore-aft headCG indicates a head location rearward closer to the seat back. On average, the headCG of child volunteers seated in the lower height backless boosters (Lil Fan [B] and Safety 1st Incognito [F]) were 76 mm lower and 23 mm more rearward (towards than seat back) in comparison to the those in higher boosters. Across the mock up configurations, the range of headCG positions of the 6YO and 10YO ATDs (headCGX 135 -155 mm and headCGZ 440-530 mm) were reasonably associated with the overall range of the horizontal and vertical child headCG locations (headCGX 140 -185 mm and headCGZ 415-520 mm).

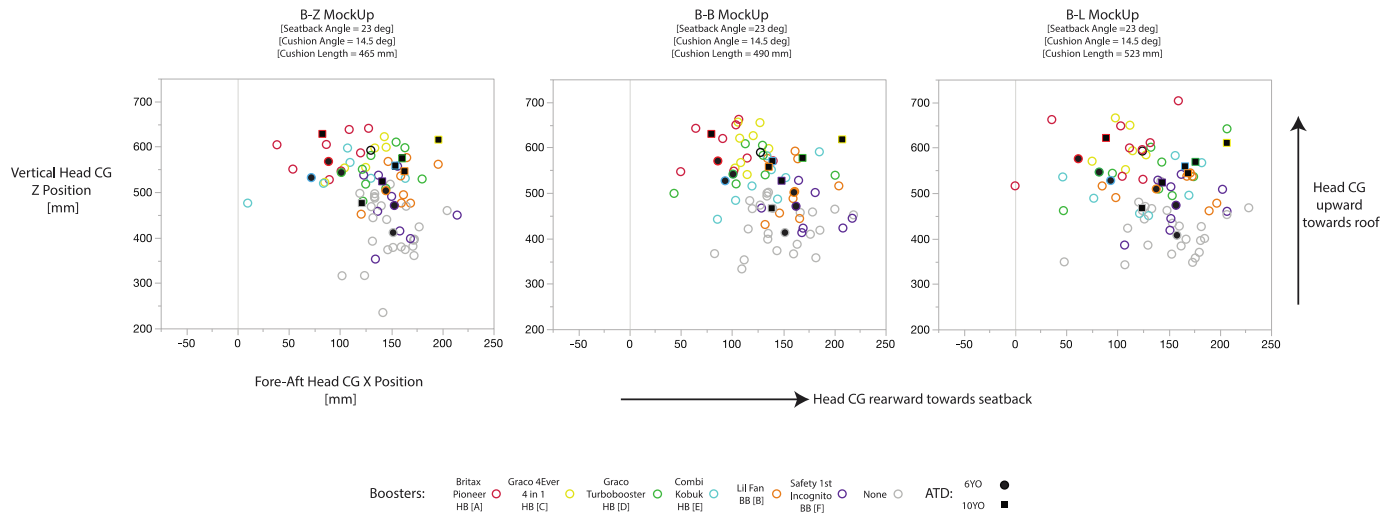


Figure 51. Location of the HeadCG of child participants and ATDs (6YO and 10YO) across all booster and mockup configurations. ATDs are coded by both booster and ATD.

Figure 52 shows the center of gravity location with respect to seat H-point for child and the 6YO and 10YO ATDs for all boosters and vehicle configurations. On average the headCG of child volunteers seated in the lower height boosters (Lil Fan [B] and Safety 1st Incognito [F]) were 84 mm lower and 78 mm more rearward (towards the seat back) in comparison to those in higher boosters. Across the vehicle configurations, installations of the 6YO and 10YO ATD resulted in headCG positions that were within the mean range of the child volunteers.

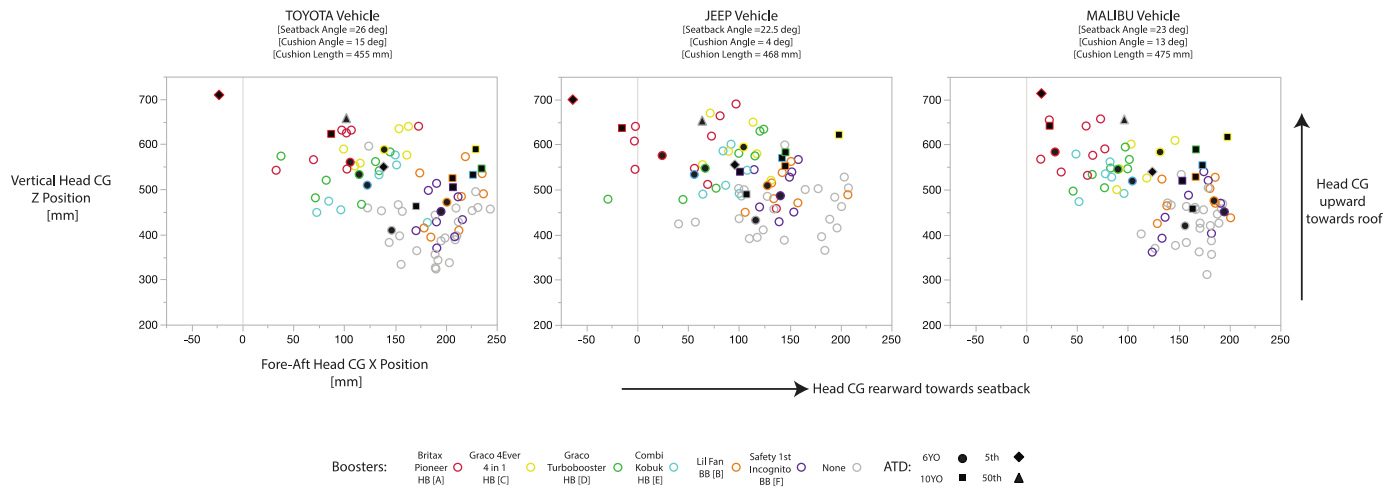


Figure 52. Location of the HeadCG of child participants and ATDs (6YO, 10YO, 5th, 50th) across all booster and vehicle configurations. ATDs are coded by both booster and ATD.

Installations of the 6YO, 10YO and 5th ATDs in the Britax Pioneer [A] high back booster, across all three vehicle configurations, resulted in head position that was quite high and forward. Examples are shown for each vehicle in Figure 53 through Figure 55.



Figure 53. 6YO, 10YO, and 5th ATDs on the Britax (A) (left to right) in Toyota



Figure 54. 5th on Britax (A) and 50th on seat in Toyota (better view of roof)



Figure 55. 6YO, 10YO, 5th ATDs on the Britax (A) and 50th on vehicle seat (left to right) in Jeep (vehicle with taller ceiling height)

Comparison Between Child and 6YO ATD Posture

On average, the lower height boosters resulted in child head postures that were 64 mm rearward and 82 mm lower than higher high back boosters. 6YO ATD head CG position was closely related to child head position as shown in Figure 56. Averaged across the Lil Fan [B] and Incognito [F] low height boosters and package conditions, child head CG position was 3 mm further rearward and 1 mm higher than the 6YO. The difference between child and ATD head CG position was only marginally increased for the high-back boosters. Table 22 presents the regression equations for head CG X and Z positions. Models are significant with $p < 0.0001$.

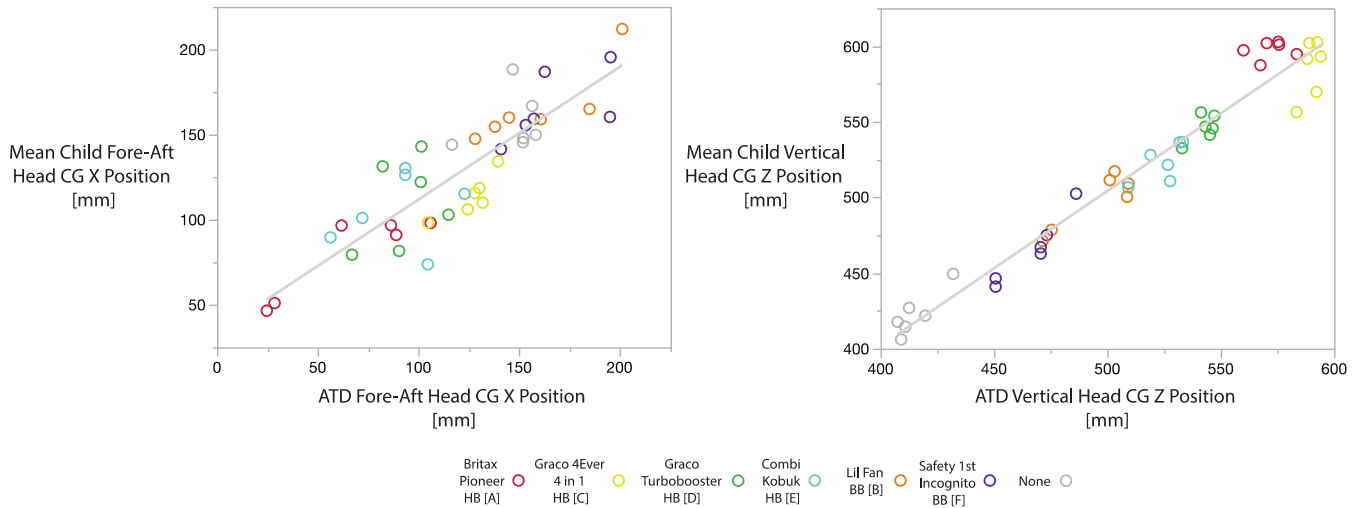


Figure 56. Association between the mean child head CG location and the 6YO ATD head CG location. Data points show the mean child head CG X and Z positions for each booster and package configuration.

Table 22. Regression results predicting mean child head CG position from 6YO ATD head CG.

	Regression Function	R ² Adj	RMSE
Head CG X Position	33.7 + 0.781*ATDHeadCGX	0.75	18.8
Head CG Z Position	-7.9 + 1.024*ATDHeadCGZ	0.95	13.2

Overall mean hip position of child volunteers seated in the lower height backless boosters was 34 mm rearward and 72 mm lower than children seated in the high back boosters. The association between the 6YO ATD and child hip postures are illustrated in Figure 57. On average, the mean child hip X position was 33 mm more rearward for the children seated in lower height backless boosters (B, F) than for the 6YO ATD. This could reflect a shift forward in the lower-height boosters relative to the bight at the intersection of the seat back and cushion, as well as different interaction between the vehicle seat back and child versus ATD. Nonetheless, ATD hip position was closely related to child hip position. Table 23 presents the regression equations for fore-aft and vertical hip X and Z positions. Models are significant with $p < 0.0001$.

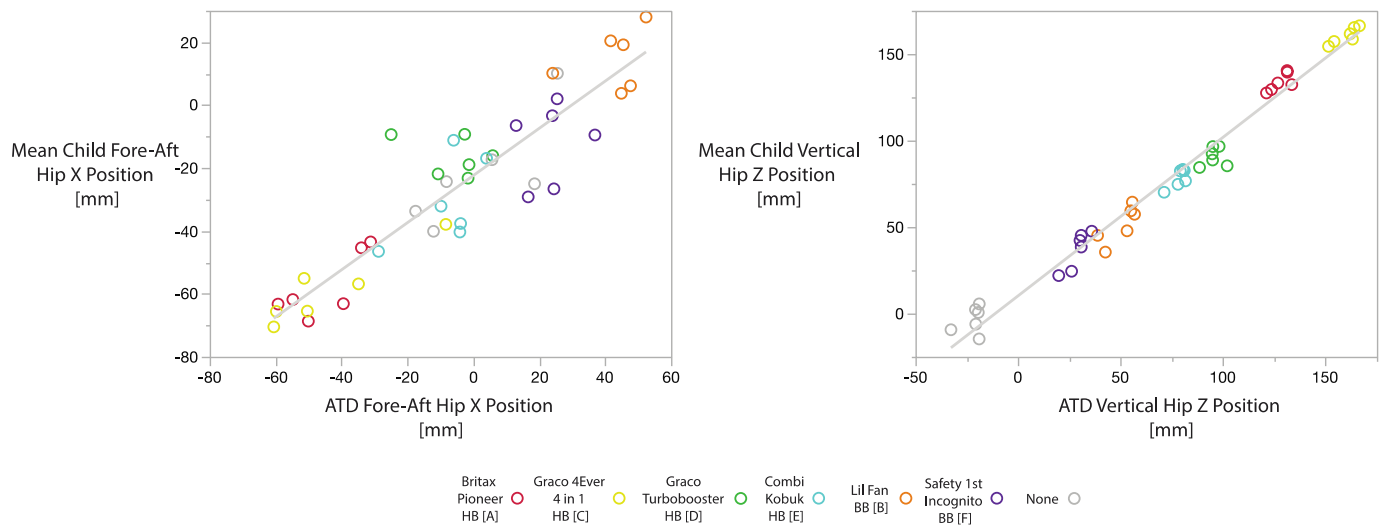


Figure 57. Association between the mean child hip X and Z position and the 6YO ATD hip. Data points show the mean child hip X and Z positions for each booster and package configuration.

Table 23. Regression results predicting mean child hip position from 6YO ATD hip position.

	Regression Function	R ² Adj	RMSE
Fore-Aft Hip X Position	-22.4 + 0.755*ATDmidHipX	0.83	10.9
Vertical Hip Z Position	10.208 + 0.917*ATDmidHipZ	0.98	7.3

Belt Fit

Lap Belt Fit

Figure 58 shows the fore-aft location of the top of the lap belt relative to the ASIS for the mockup conditions, while Figure 59 shows the same data for the vehicles. Values for the 6YO ATD align better with the volunteers than those for the 10YO ATD, which is reasonable given that most volunteers were smaller than the 10YO ATD. The lap belt was closest to the fore-aft position of the ASIS with the no-booster and Incognito, where no booster structure is present to shift the belt relative to the pelvis. Belt location generally varies more with child volunteers in these two conditions as well.

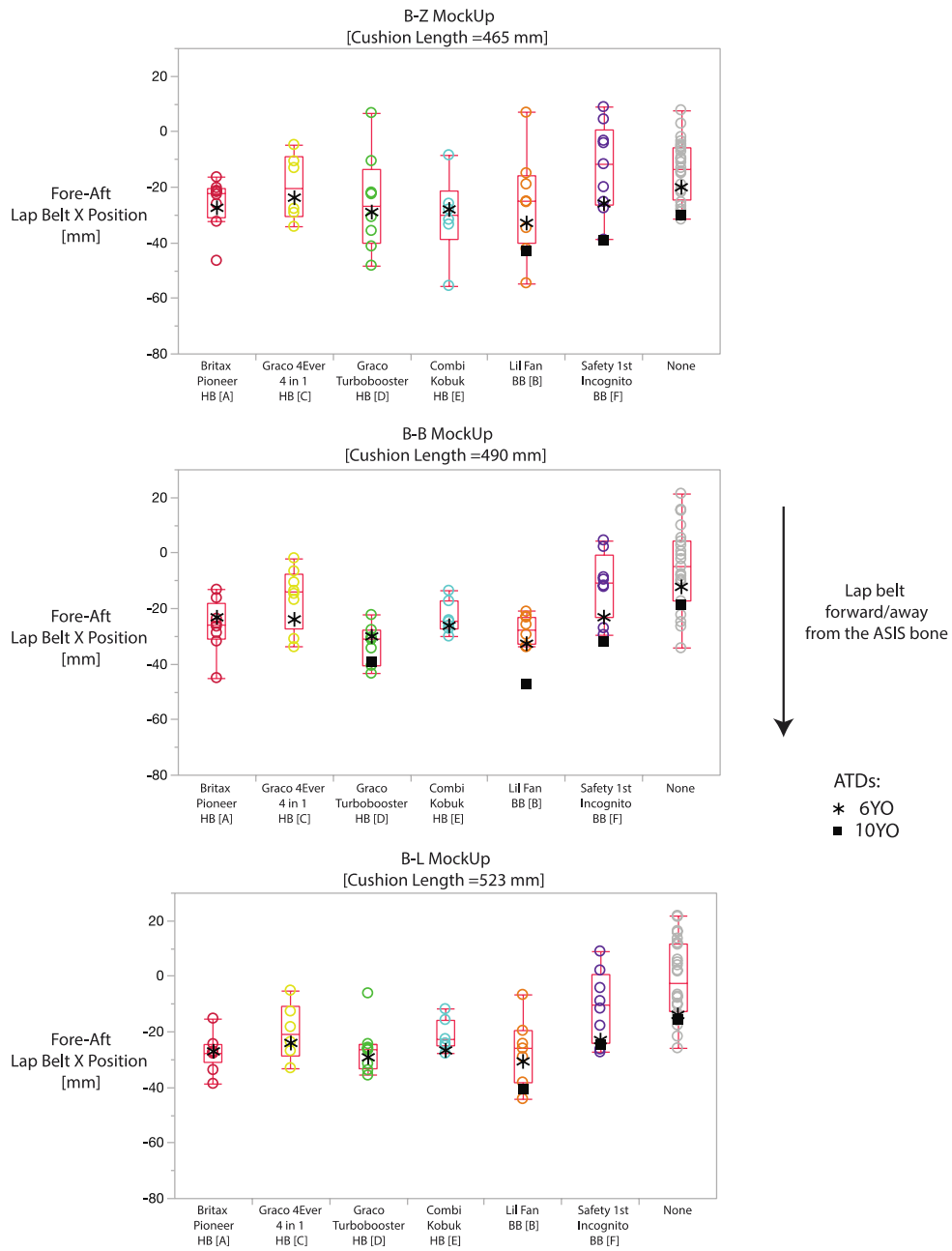


Figure 58. Box plots of fore-aft lap belt position in mockup conditions: B-Z, B-B, and B-L.

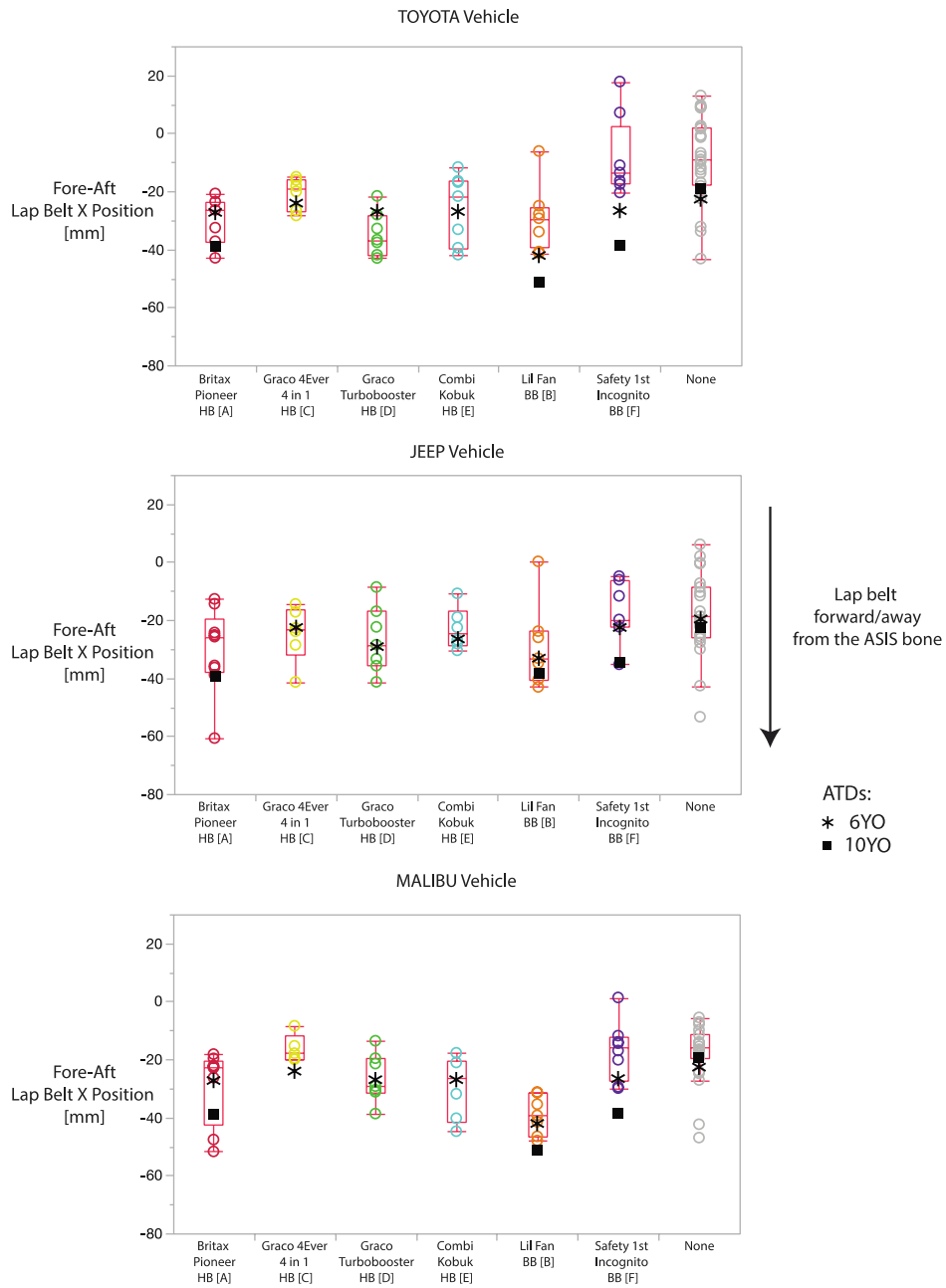


Figure 59. Box plots of fore-aft lap belt position in vehicle conditions: Toyota, Jeep, and Malibu.

The vertical position of the top of the lap belt relative to the ASIS is shown in Figure 60 for the mockup conditions and Figure 61 for the vehicles. The lap belt is higher relative to the ASIS on child volunteers than ATDs in all conditions, because the ASIS of the ATD is higher than the ASIS on a child. Differences between booster and no-booster conditions were larger in the ATD than the child volunteers.

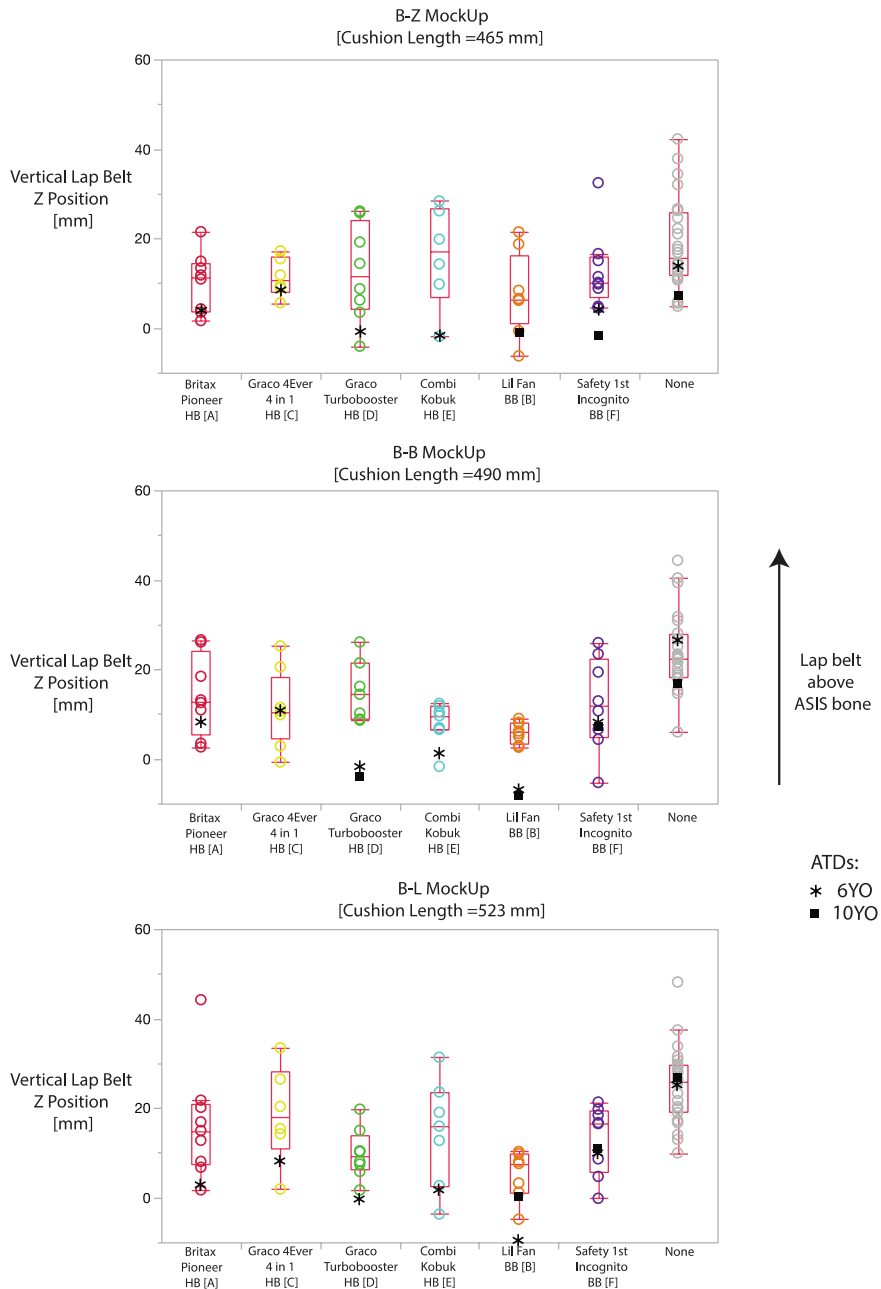


Figure 60. Box plots of the vertical lap belt position across all the boosters in mockup conditions: B-Z, B-B, and B-L.

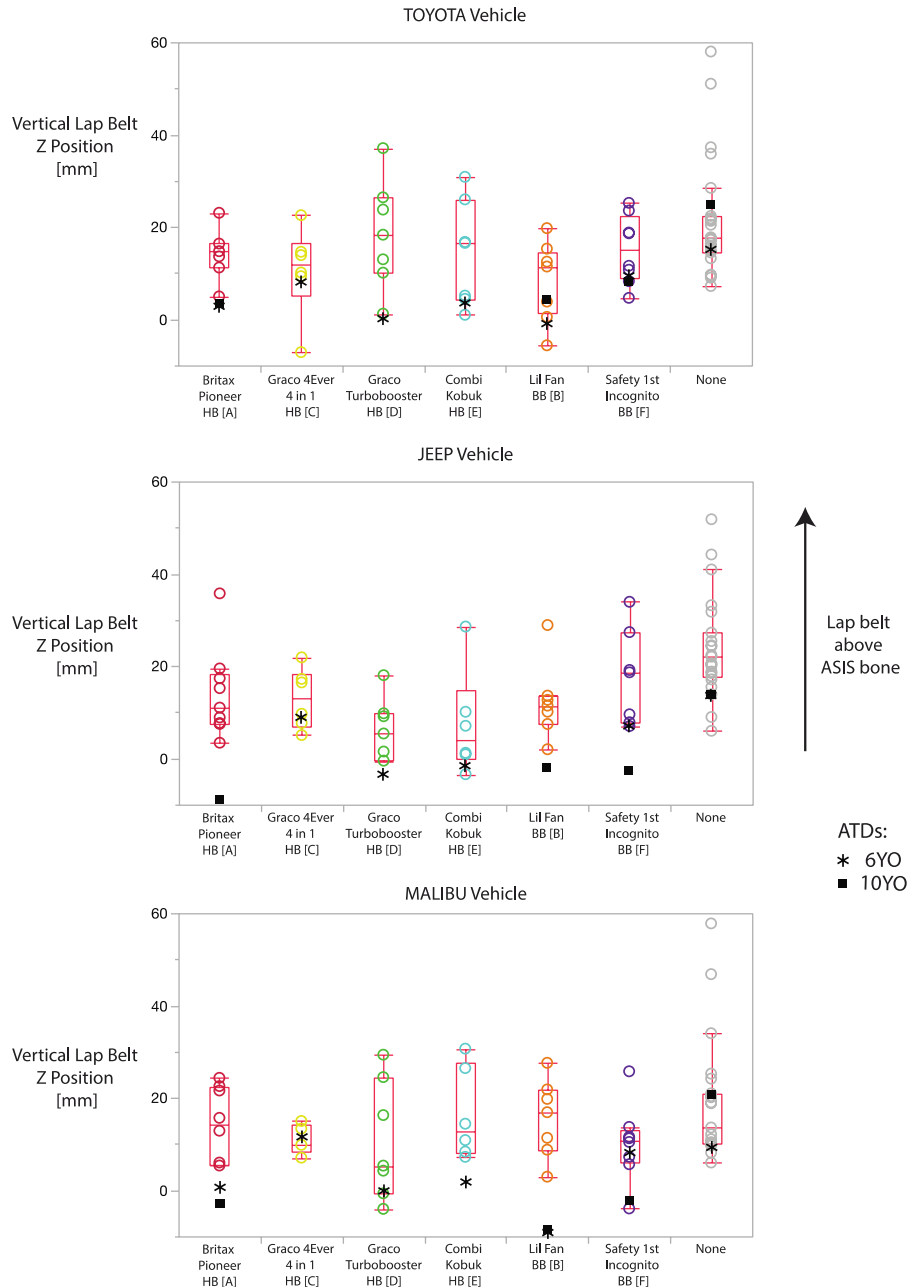


Figure 61. Box plots of the vertical lap belt position in vehicle conditions: Toyota, Jeep, and Malibu. A positive value indicates that the lap belt is above ASIS bone.

Figure 62 and Figure 63 plot the location of the top of the lap belt relative to the ASIS, compared to the 6YO and 10YO ATDs, respectively. The no-booster condition consistently has the highest location. Though the Lil Fan booster is lower, it has lap belt guides that keep the belt low and forward of the pelvis. The differences in slope of the ATD points of the 6YO and 10YO results from the ability of the 10YO pelvis to recline more.

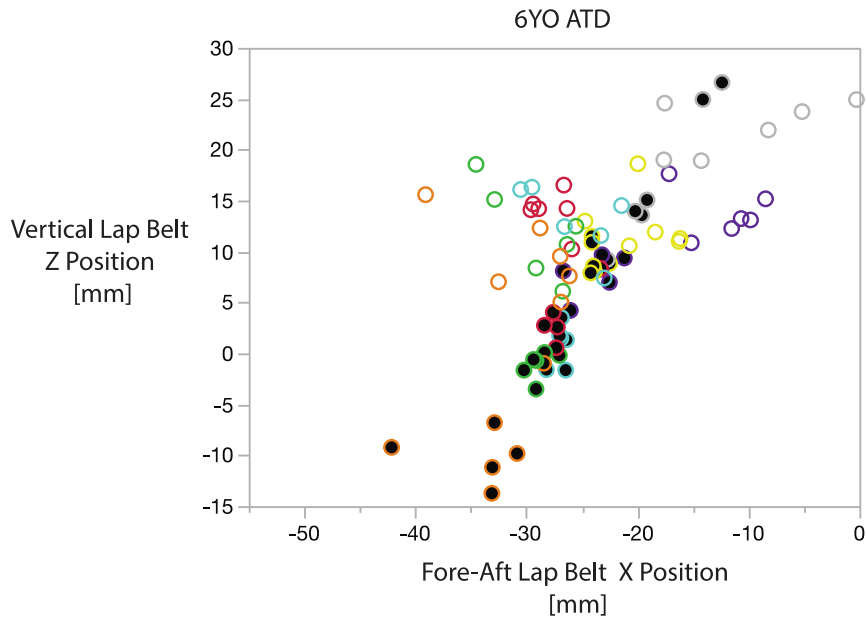


Figure 62. Lap belt position of volunteers relative to ASIS compared to 6YO ATD (filled circles.)

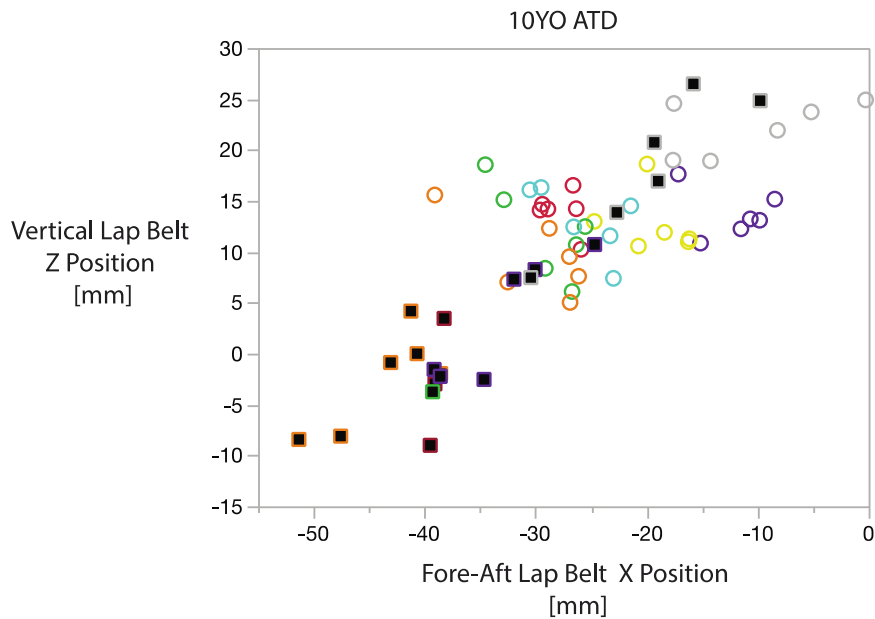


Figure 63. Lap belt position of volunteers relative to ASIS compared to 10YO ATD (filled squares).

Shoulder Belt Fit

The shoulder belt score quantifies the location of the inner edge of the belt relative to the torso centerline at the height of the suprasternale. Figure 64 shows the distribution of the shoulder score for the mockup conditions, while Figure 65 shows results for the vehicles.

For the volunteers, the shoulder belt was closest to the neck with the no-booster and Incognito for all conditions except the Jeep. The Lil Fan, Combi Kobuk, and Pioneer had the most outboard shoulder belt locations among volunteers, though it varies with the belt geometry across test conditions. For most conditions, the location of the shoulder belt on the 6YO ATD was closer to the neck than the volunteers, likely because of the non-realistic external contour of the ATD's neck; values for the 10YO were closer to those of the volunteers. The differences between the 6YO and the volunteers were larger in the vehicles than in the mockup conditions.

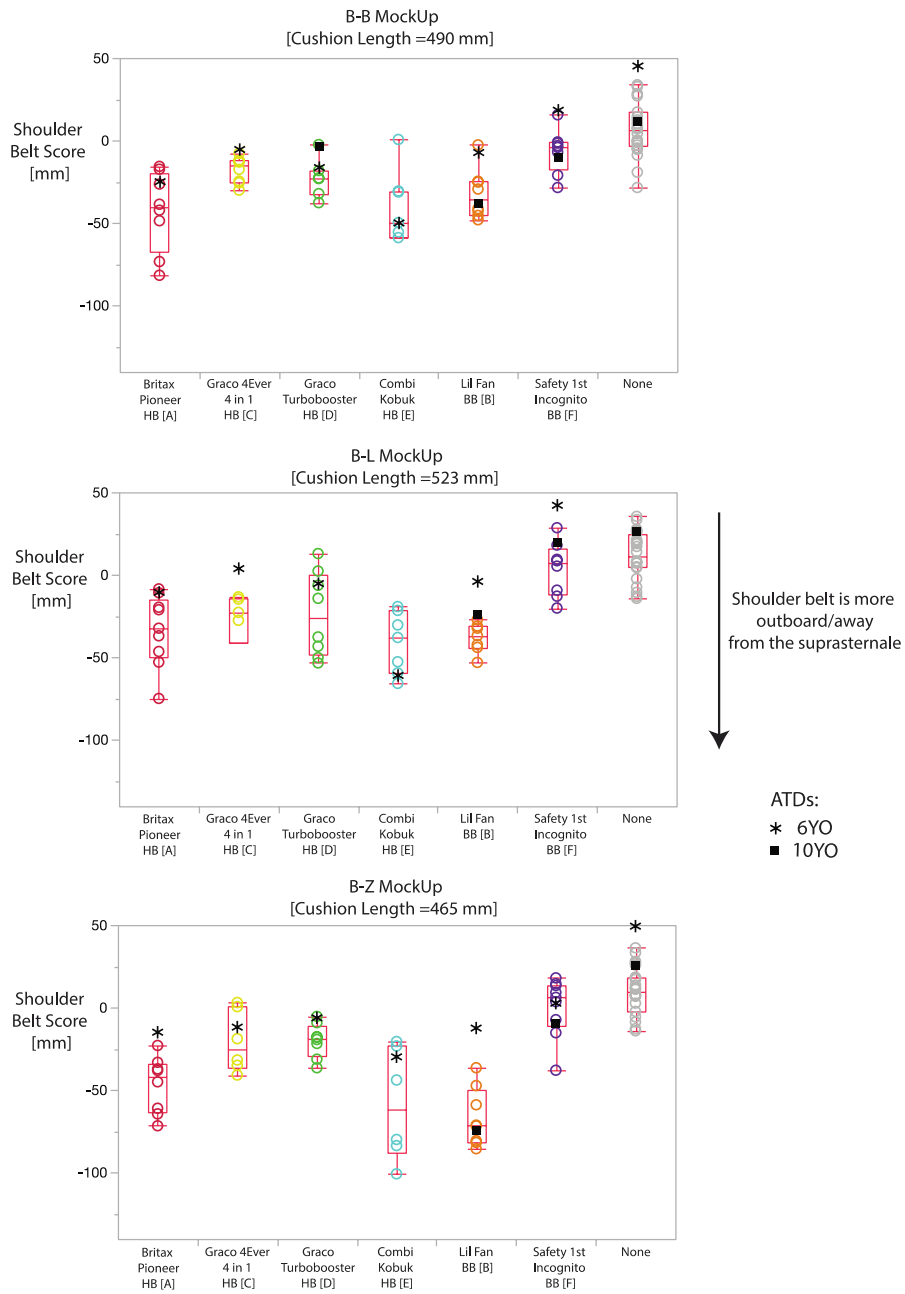


Figure 64. Distribution of the shoulder belt score (mm) across all the boosters in mockup conditions: B-Z, B-B, and B-L.

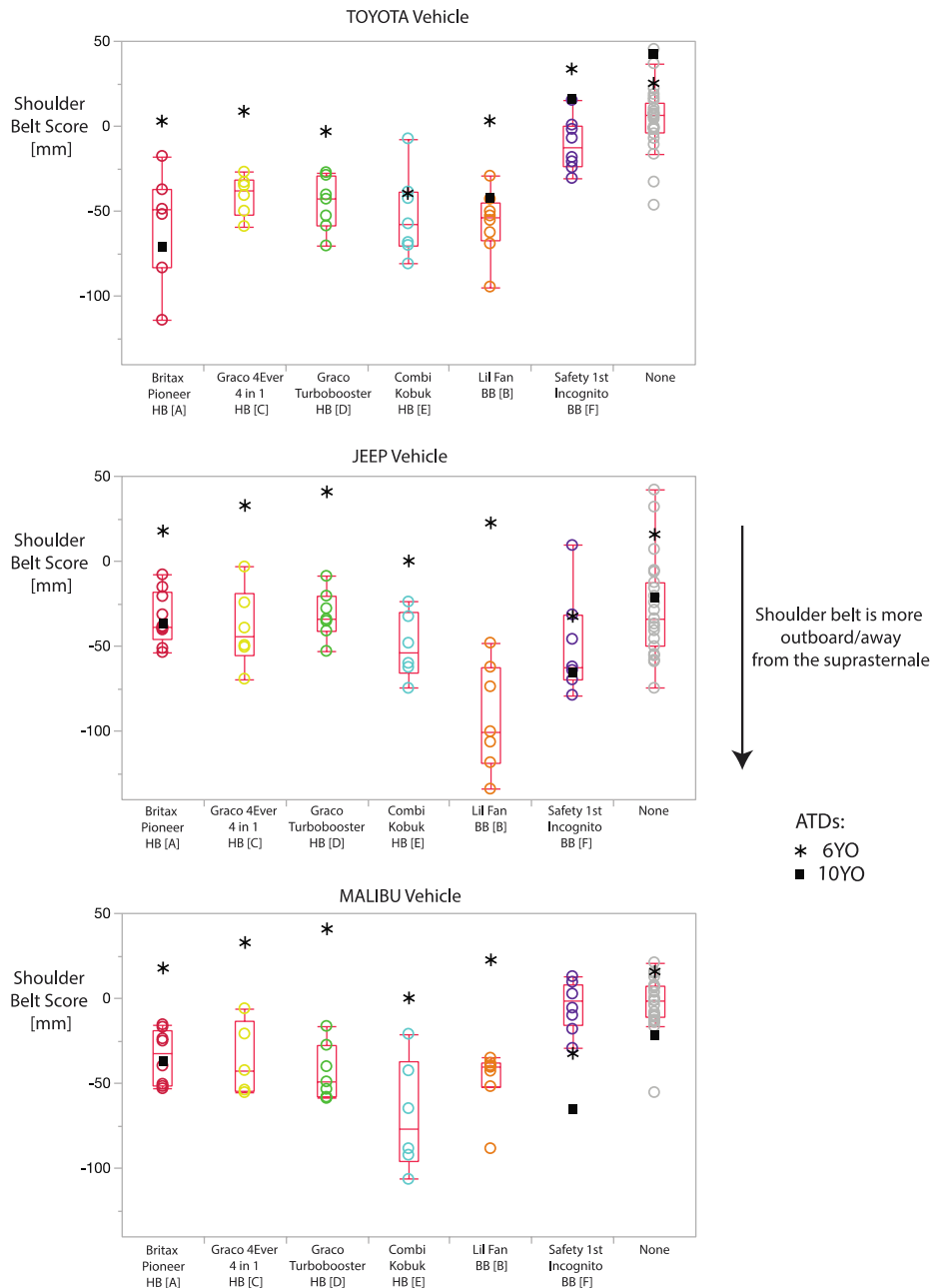


Figure 65. Distribution of the shoulder belt score (mm) across all the boosters in vehicle conditions: Toyota, Jeep, and Malibu.

DISCUSSION AND CONCLUSIONS

Volunteer Testing

Posture

When comparing the posture of children to ATDs in different boosters, our hypothesis was that children would slouch more in lower boosters compared to taller boosters. Taller boosters effectively shorten cushion length, and let a child's knees bend comfortably over the front of the booster. A low booster may not allow the child's knees to hang comfortably, possibly encouraging them to scoot forward to let their knees hang over the front edge of the vehicle seat.

The knee and hip positions of the child volunteers were consistently more forward of those measured on the 6YO ATD, indicating that they do slouch more. Differences in hip location were smaller in the vehicles compared to the mockup conditions, likely because of interactions with the seat package configurations, such as seat back and seat contours. The knee positions showed less variation among boosters than the hip positions, although the differences were smaller for knee and hip in the four taller boosters compared to the two low boosters and the no-booster condition. The included knee angle of the ATDs was always at the upper range of the knee angles measured in volunteers, particularly for the Incognito and no-boost condition. The vertical position of the hip was similar in between children and the ATD in most conditions, while the knee position of the kids was generally higher than the ATDs for the no-boost and Incognito but lower for the other boosters. Posture variability among volunteers was larger in the no-booster and Incognito conditions.

Data collected to compare the head CG position of the volunteers relative to the ATDs can be used to determine whether restrictions on how much a booster "boosts" are needed. Ideally, the head positions of children in boosters should be located where the head positions of adults are in a vehicle, to allow children to gain the most benefit from vehicle structures and curtain air bags that are evaluated relative to adult head positions. For the current study, we consider the head locations of the small female ATD and midsize male ATD as possible lower and upper bounds for child head position provided by a booster. While specifications for head restraints in the rear seat consider occupants the size of a 95th percentile male, designing boosters to place children no higher than the midsize male is more feasible and would minimize potential for roof loading in some crashes.

Reviewing the vehicle head CG position data in Figure 52 shows that the vertical location of the midsize male is near 650 mm in each vehicle, while the small female varies from 525 to 550 mm. Almost all of the volunteer head CGs measurements are below 500 mm in the no-boost and Incognito conditions; about half of the children seated in the Lil Fan booster are below this level, as well as some children using the Combi Kobuk and Graco TurboBooster. On the other hand, head CG location of the small female ATD seated in the Britax Pioneer (because a child with the stature and weight of the small female would be allowed to use this booster) is more than 100 mm forward and 50 mm above the head CG location of the midsize male. This booster may place a larger child closer to forward and roof structures than ideal.

Figure 66 plots the vertical head location of the child volunteers versus their stature. If a goal is to position the child’s head between 500 and 650 mm above the H-point to match the locations of small and midsize adults, a height range appropriate for each product is suggested in Table 24, together with the current range and conflicts highlighted in red text. The consistency in results between the vehicle and mockup data indicates that child restraint manufacturers could use a simulated vehicle seat (such as the FMVSS No. 213 bench) to check that their products place the heads of the ATDs at a location 500-650 mm above the seat’s H-point.

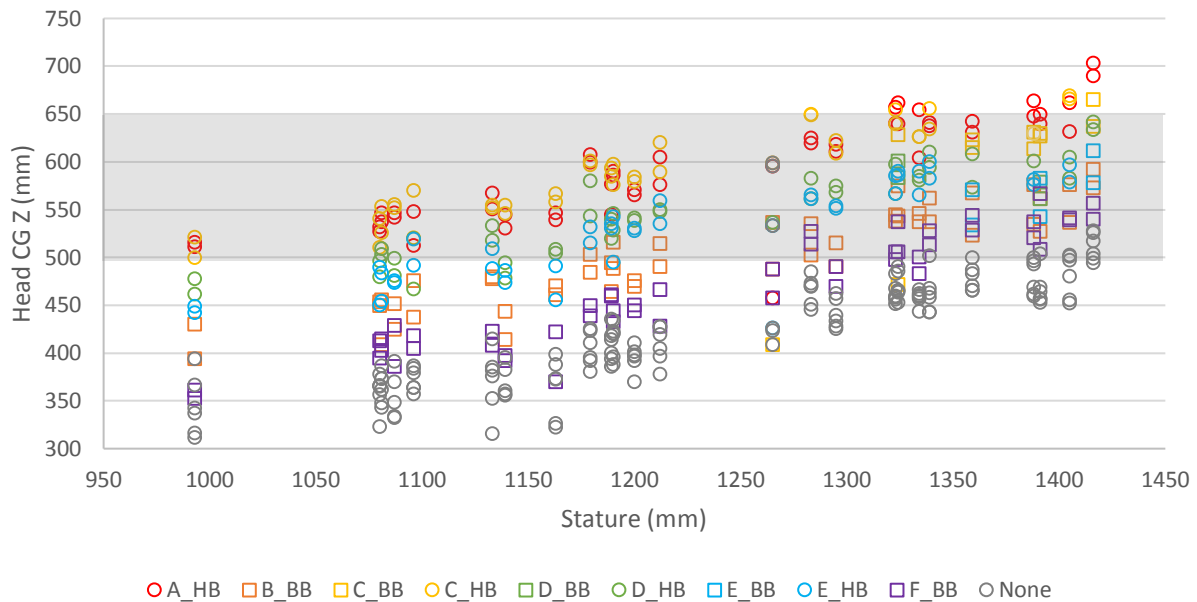


Figure 66. Head CG vertical location versus subject stature, relative to target zone defined by locations of small female and midsize male ATDs.

Table 24. Current and proposed allowable occupant height ranges for optimal head vertical location.

Booster	Current height range (mm)	Suggested height range (mm)
A Pioneer (highback)	1140-1500	1040-1350
B Lil Fan (backless)	1000-1450	1250-1400
C Graco 4 Ever (highback)	1000-1450	1000-1400
D Graco TurboBooster (highback)	965-1450	1050-1450
E Combi Kobuk (highback)	840-1450	1175-1450
F Incognito (backless)	<1525	1300-1450

Despite the differences in posture between the child volunteers and the ATDs, we were able to develop linear models that reasonably predict the location of the child’s head and hip based on the location of the 6YO ATD head and hip. Results shown in Figure 56 and Figure 57 indicate that the model’s predictive ability is similar for all boosters (regardless of boost level) and the no-booster condition. These models support the assertion that despite greater differences in posture between children and ATDs for lower boosters, the

current ATD seating procedure provides a reasonable representation of postures selected by child volunteers.

Belt fit

The belt fit data confirm the benefit provided by boosters, with the no-booster condition consistently having the highest lap belt placement relative to volunteers, as well as the shoulder belt position closest to the neck. The Incognito booster, which only provides about 45 mm of boost and has ineffective belt guides, has belt fit measures closest to the no-booster condition. Although the Lil Fan only provides about 75 mm of boost, it provides better lap belt fit through the design of the lap belt guides.

The comparison of volunteer and ATD belt fit measures highlights several differences. The shoulder belt measure always indicated that the belt is closer to the center of the ATD than the children, because the external contour of the ATD neck is not realistic. The lap belt measures exhibit more variability in children compared to ATDs; the higher degree of variability in the abdomen/pelvis surface of children, and their ability to shift, may contribute to these differences.

Dynamic Testing

Testing Conditions

Results are included from the first phase of the project conducted in 2015 during which the surrogate retractor was developed and initial candidate booster metrics were examined. However, the belt anchorage geometry was revised between the 2015 and 2018 versions of the test bench to more closely match the mean belt geometry seen in the US vehicle fleet. As shown in Figure 4, the decrease in distance between the lap belt anchors and the relocation of the shoulder belt anchor effectively bring the shoulder belt closer to the ATDs neck; the shoulder belt angle viewed from the front is 5 degrees steeper. When comparing tests without a booster run with the 2015 and 2018 benches, the head excursion was 90 mm higher in the 2015 version of the seat assembly. While the 2015 tests run with the surrogate retractor are included for comparison, measures collected in the initial phase of testing should not necessarily be expected to be consistent with the later tests because of the changes in belt anchorage geometry.

The knee-head excursion difference for the no-booster condition for the 6YO changed by 90 mm between the one test run in the 2015 series and the three tests run in the 2018 series. The shift in shoulder belt geometry increased the effect of the shoulder belt position relative to the lap belt position with regard to how it affects ATD kinematics. Use of a sliding latchplate rather than a locked latchplate may also have caused differences. The kinematics of the ATD without a booster on the 2018 version of the bench now exhibit submarining characteristics that would be expected if a 6YO child was not using a booster seat, so the most recent version of the bench may be more effective at identifying boosters that prevent submarining. However, it may possibly be more challenging for backless boosters to meet suggested criteria on the 2018 version of the FMVSS No. 213 sled seat assembly given the different shoulder belt geometry.

The surrogate retractor was initially designed to allow adjustment of the amount of shoulder belt spool-out, so it could be tuned so the ATD kinematics matched when using a production seat belt or the retractor. A final version of the retractor and procedure could

be designed to have only locking position so a consistent amount of spool-out is set for each test.

Knee and head excursions, as well as shoulder belt spool-out, were measured by digitizing initial and peak excursion images using a program called ImageJ, which can be used to calculate the distance between points on an image after calibration using a known reference distance on the image. Per NHTSA's request, the 2018 tests had additional targets and calibrations to allow use of TEMA software to measure excursions and displacements. We compared measurements of excursion using both methods for several tests and found good agreement. Because the FMVSS No. 213 peak head excursion criterion uses the leading edge of the head, rather than the head CG target to identify peak excursion, this may pose a challenge for the traditional TEMA analysis method as does target obscuration.

Repeatability

One objective of this project was to assess the repeatability of the test procedure using a variety of booster products and the surrogate retractor. For all measures, the variation between tests run with different boosters was greater than variation within boosters. In particular, the maximum difference in amount of spool-out was less than 10 mm for each set of matching tests; maximum difference in spool-out across all tests run in 2018 was less than 15 mm. This amount of spool-out variation provided by the surrogate retractor is substantially lower than the variability seen in production retractors.

Candidate booster metrics

Belt-positioning booster seats that are designed to meet current FMVSS No. 213 specifications demonstrate the ability to reduce risk of abdominal injury by 59 percent in motor-vehicle crashes (Arbogast, Jermakian, Kallan, & Durbin, 2009, Durbin, Elliott, & Winston, 2003). Thus the current booster performance metrics of head excursion, knee excursion, HIC (36), and 3 ms chest clip acceleration are partially effective in defining reasonable booster performance. However, a flaw in the current FMVSS No. 213 booster criteria is that all of the dynamic test measures can easily be met without using a booster. When reviewing the data in Figure 30 through Figure 32, the best results relative to the current criteria are achieved without a booster.

This finding is not consistent with the field data showing lower risk of injury when a booster is used. When considering candidates for booster metrics, our strategy focused on identifying measures that were related to booster design goals (raising the occupant and improving belt fit) and could not be met without a booster seat. In addition, we tried to identify measures correlated with good occupant kinematics. This includes the shoulder belt loading the ATD in the middle of the shoulder, not on the neck or falling off the arm. The torso should rotate pass vertical to allow good engagement of the shoulder belt and prevent the pelvis from sliding under the lap belt, and avoiding submarining kinematics where the knees have substantially higher excursions than the head.

Other researchers have attempted to measure loading to the pelvis using upper and lower ASIS load cells as a method for quantifying likelihood of submarining (Rouhana et al. 1990, Hagedorn and Stammen 2015, Jermakian and Edwards 2017). While we reviewed ASIS loads, they would not be able to identify if a booster initially routed the belt completely above the pelvis and over the abdomen, or if the booster shifted the lap belt

substantially forward on the thighs such that it allows forward motion of the pelvis before engaging. Both of these undesirable belt routings are found in a few 213-compliant products.

Neck axial force shows some correlation with targeted kinematics, as the test conditions where the shoulder belt was close to the neck generally had the highest measures of neck axial force, so a peak axial neck tension less than -2700 N might be considered a possible threshold. However, though based on limited biomechanical data and scaling, published values for allowable axial neck tension for the 6YO ATD are ~1800 N (Irwin, Prasad, and Mertz 1997); and nearly all current boosters would exceed this limit. Because field data do not identify high frequencies of cervical spine injury with booster seat use that would be predicted by the results of FMVSS No. 213 tests, neck measures have not been previously considered as potential booster metrics. So while neck axial loading corresponds with belt loading on the neck, the inconsistencies with suggested injury reference values that have been published may make it unsuitable for a potential booster metric.

Several static measurements related to belt fit and the amount of vertical boost provided by a product were also considered as candidate metrics. Most boosters with good kinematics also had reasonable lap and shoulder belt scores, but not all boosters with poor kinematics had poor belt fit scores. In some cases, the static position of the shoulder belt before the test indicated placement over the middle of the shoulder, but the booster design did not maintain the belt in that position under dynamic loading. The two products with the lowest amount of vertical boost produced submarining kinematics, but several other products with a substantial amount of boost also had submarining kinematics. However, requiring a minimum amount of boost (around 75 mm) would position children better relative to vehicle protection features such as curtain air bags and interior padding. Because the shapes and contours of boosters vary widely, it would be challenging to find a consistent way to define the amount of boost by measuring characteristics of the booster alone. Instead, we quantified boost for this project by measuring the location of the ATD H-point in the Z direction with a booster, and subtracting the location of the ATD H-point when seated on the FMVSS No. 213 bench without a booster.

When reviewing the kinematics of the no-booster conditions in Figure 67, the torso has not rotated past vertical because the shoulder belt loads the neck, while the knees have moved forward because the lap belt is loading the upper part of the pelvis. A candidate metric that quantifies this kinematic behavior is obtained by subtracting the knee excursion from the head excursion. For the 6YO, the knee-head value is about 140 mm with the no booster condition; we suggest a possible criterion of no more than 125 mm (to ensure that a booster is better [by ~10%], not just the same, as a no-booster condition.) For the 10YO, the no booster knee-head value is about 200 mm and suggested criterion is no more than 180 mm. An advantage of this metric is that it can be calculated simply using excursion measures that are already included in FMVSS No. 213 without additional instrumentation (and could be calculated on past test results).

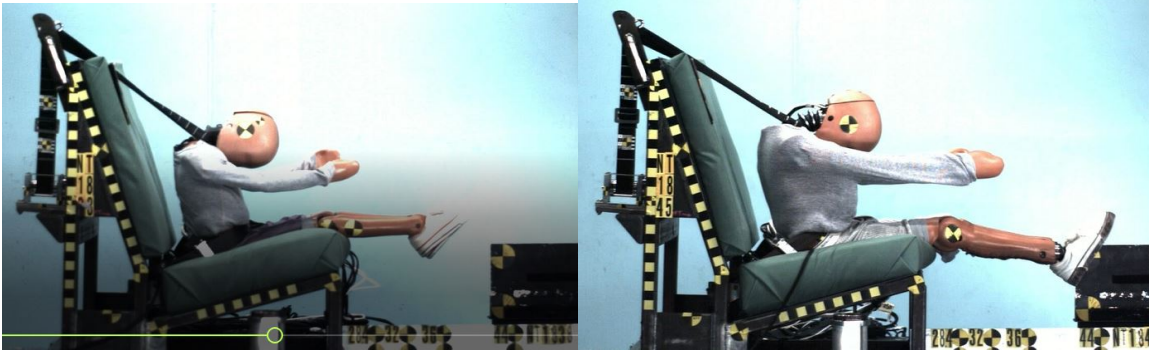


Figure 67. No-booster condition with 6YO (left) and 10YO (right) shows submarining tendencies on 2018 version of the bench.

A value that is closely correlated with the knee-head excursion is the maximum side-view thorax angle. This value is determined by measuring with an angular rate sensor in the ATD spine (at the same location as the thorax y-accelerometer), which is integrated to calculate rotation. We considered both change in thorax angle (peak change in the integrated signal) and the maximum thorax angle, where the initial angle between shoulder and hip is calculated from FARO Arm setup measurements. The maximum angle shows a better consistency with the knee-hip, and accounts for how the booster initially positions the ATD thorax. Maximum thorax angle could also be a good measure for describing desirable kinematics, with a suggested threshold of at least 5 degrees forward of vertical for the final angle. This measure could also identify cases of rollout where the shoulder belt falls off the shoulder onto the arm; for the tests in this series it would correspond to a value beyond 35 degrees past vertical. The disadvantage of this metric is the additional sensor required, as well as the ability to digitize the initial angle with a FARO Arm. Since the measure is closely correlated with knee-head, it may not add additional value.

Another metric associated with desirable kinematics is the lumbar moment about the Z-axis, which corresponds to twisting of the torso relative to the pelvis. For the cases where the belt loads the neck, the peak value of Lumbar MomentZ is positive; for the cases where the belt rolls off the shoulder, the peak value for the 6YO is greater than -10 Nm. The 10YO data show similar patterns. There are no published injury thresholds for lumbar moment for the child ATDs, so use of this as a performance measure would not pose any conflicts with suggested injury criteria. Based on the results of the current test series, a lumbar MomentZ value of -5 to -10 Nm for the 6YO and -10 to -20 Nm for the 10YO would result in kinematics where the shoulder belt loads the center of the ATD's shoulder. These thresholds would need to be transposed if the shoulder belt was positioned on the left shoulder rather than the right. The lumbar ForceY could also be used as a criteria, as it is closely related to the lumbar MomentZ; a possible threshold for both ATDs would be 250 to 1000 N based on the range of values associated with desirable kinematics shown in Figure 38 and Figure 40. However, the repeatability of the peak lumbar MomentZ is better than the lumbar ForceY.

In addition to dynamic testing, Canada requires boosters to pass a compression test (see Section 4 of CMVSS test method 213.2), which verifies a booster's ability to resist downward loading that will discourage submarining of the occupant under the lap belt. In this quasi-static test, a preload of 175 N is applied to the center of the seating area of the

booster using a 203 mm flat circular indenter. The vertical position of the indenter after preload is defined as the initial position. Then the downward load is increased to 2250 N and the downward displacement of the indenter is recorded. If the displacement exceeds 25 mm, the booster fails the test. Inflatable boosters and boosters made of Styrofoam (both of which can meet the current FMVSS No. 213 requirements) do not pass this test, so the compression test could be considered as an additional requirement for evaluating boosters.

The current metrics used to assess boosters in FMVSS No. 213 are HIC (36ms), head excursion, knee excursion, and 3 ms chest clip acceleration. On the one hand, boosters designed to meet these measures have led to products that have reduced risk of injury in the field. On the other hand, these metrics tend to have their lowest values when no booster is used. If you were trying to design a product to minimize all these currently used measures, the no booster condition would produce the best results. Additional measures to ensure boosters do not allow occupant submarining and encourage good shoulder belt routing, such as the proposed knee-head excursion and lumbar MomentZ criteria, should be considered to guide future booster designs.

REFERENCES

- 49 CFR Part 571 (Docket No. NHTSA–2014–0012), RIN 2127–AK95, in FR 79, No. 18, Tuesday, January 28, 2014; Federal Motor Vehicle Safety Standards; Child Restraint Systems, Child Restraint Systems—Side Impact Protection, Notice of proposed rulemaking. Available at <https://www.govinfo.gov/content/pkg/FR-2014-01-28/pdf/2014-01568.pdf>
- American Academy of Pediatrics. (2017). Car Seats: Product Listings for 2017. (Web page of healthychildren.org). Itasca, IL: Author. www.healthychildren.org/English/safety-prevention/on-the-go/Pages/Car-Safety-Seats-Product-Listing.aspx
- Arbogast, K. B., Jermakian, J. S., Kallan, M. F., & Durbin, D. R.. (2009). Effectiveness of belt positioning booster seats: An updated assessment. *Pediatrics*, *124*:1281-1286
- Beck, B., Brown, J., & Bilston, L. E. (2012). *Objective measures for determining submarining and abdominal injury in Hybrid III crash test dummies*. Proceedings of the 2012 International IRCOBI Conference on the Biomechanics of Injury, September 12-14, 2012; Dublin, Ireland
- Belwadi, A., Duong, N., Fein, S., Maheshwari, J., & Arbogast, K. (2018). *Efficacy of booster seat design on the response of the Q6 ATD in simulated frontal sled impacts*. Protection of Children in Cars, 15th Annual Proceedings, December 7-8, 2017, Munich.
- Bilston, L. E., & Sagar, N. (2007). Geometry of rear seats and child restraints compared to child anthropometry. *Stapp Car Crash Journal*, *51*:275-98.
- Durbin, D. R., Elliott, M. R., & Winston, F. K. (2003). Belt positioning booster seats and reduction in risk of injury among children in vehicle crashes. *Journal of the American Medical Association*, *289*(21): 2835-2840.
- Ebert, S. M., Klinich, K. D., Manary, M. A., Malik, L. A., & Reed, M. P.. (2018, April). *Toddler lowerextremity posture in child restraint systems* (Report No. DOT HS 812 470). Washington, DC: National Highway Traffic Safety Administration. Available at www.nhtsa.gov/sites/nhtsa.dot.gov/files/documents/11710_toddlerlowerextremityposture_040218-v3-tag.pdf
- Hagedorn, A., & Stammen, J. (2015, January). *Comparative evaluation of 6-year-old Hybrid III and DAPRR prototype ATD abdomen/pelvis components* (Report No. DOT HS 812 088). Washington, DC: National Highway Traffic Safety Administration. Available at https://one.nhtsa.gov/DOT/NHTSA/NVS/VRTC/bio/812088_ComparativeEvaluationHybrid-III.pdf
- Huang, S., & Reed, M. (2006). *Comparison of child body dimensions with rear seat geometry* (SAE Technical Paper 2006-01-1142). Warrendale, PA: SAE International. doi:10.4271/2006-01-1142.

- Insurance Institute for Highway Safety. (2014, September). Booster seat belt fit evaluation protocol (version III). Ruckersville, VA: Author. Available at https://avtodeti.ru/UserFiles/File/organizations/IIHS/IIHS_booster_protocol_2014_EN.pdf
- Irwin, A., Prasad, P., & Mertz, H. J. (1997). *Injury risk curves for children and adults in frontal and rear collisions*. Proceedings of the 41st Stapp Car Crash Conference. Warrendale PA: Society of Automotive Engineers,
- Jermakian, J. S. & Edwards, M. A., (2017). *Kinematics comparison between the Hybrid III 6 year-old with standard pelvis and modified pelvis with gel abdomen in booster sled test* Paper No. IRC-17-38). Proceedings of the 2017 IRCOBI Conference, September 13-15, 2017, Antwerp, Belgium..
- Jones, M. H., Klinich, K. D., Ebert, S. M., Malik, L., Manary, M. A., & Reed, M. P. (2015) A pilot study of toddler anthropometry and posture in child restraint systems. *Proceedings of the 2015 Association for the Advancement of Automotive Medicine Scientific Conference, October 5, 2015, Philadelphia, PA.*
- Kim, K. H., Jones, M. J. H., Ebert, S. M., Malik, L., Manary, M. A., Reed, M. P., & Klinich, K. D. (2015, December). *Development of virtual toddler fit models for child safety fit design* (Report No. UMTRI 2015-38). Washington, DC: National Highway Traffic Safety Administration. Available at <https://deepblue.lib.umich.edu/bitstream/handle/2027.42/136629/UMTRI-2015-38.pdf?sequence=1&isAllowed=y>
- Klinich, K. D., Benedetti, M., Manary, M. A., & Flannagan, C. A. (2016) Rating child passenger safety laws relative to best practices for child occupant protection *Traffic Injury Prevention, 18*(4):406-411. doi: 10.1080/15389588.2016.1203427.
- Klinich, K. D., Reed, M. P., Ebert, S. M., & Rupp, J. D. (2013, December). *Effects of realistic vehicle seats, cushion length, and lap belt geometry on child ATD kinematics* (Report No. DOT HS 811 869). Washington, DC: National Highway Traffic Safety Administration. Available at https://one.nhtsa.gov/DOT/NHTSA/NVS/Crashworthiness/Child%20Safety%20Crashworthiness%20Research/FX_Real_V_Seats_Cushion_Length_Lap_Belt_Geom_Chld_ATD_Kinematics_811869.pdf
- Klinich, K. D., Reed, M. P., Ebert, S. M., & Rupp, J. D. (2014) Kinematics of pediatric crash dummies seated on vehicle seats with realistic belt geometry, *Traffic Injury Prevention, 15* (8): 866-74.
- Klinich, K. D., Reed, M. P., Ritchie NL, Manary, M. A., Schneider LW, Rupp JD (2008, September). *Assessing child belt fit, Volume II: Effect of restraint configuration, booster seat designs, seating procedure, and belt fit on the dynamic response of the Hybrid III 10YO ATD in sled tests* (Report No. UM-2008-49-2). Washington, DC: National Highway Traffic Safety Administration. Available at <https://deepblue.lib.umich.edu/bitstream/handle/2027.42/64460/102443.pdf?sequence=1>

- Klinich, K. D., Ritchie, N., Manary, M. A., & Reed, M. P. (2010) Development of a more realistic pelvis for the Hybrid III 6YO ATD. *Traffic Injury Prevention, 11*(6):606-12
- Klinich,, K. D., Reed, M. P., Hu, J., & Rupp, J. D. (2014, July) *Assessing the restraint performance of vehicle seats and belt geometry optimized for older children*. (Report No. DOT HS 812 048). Washington, DC: National Highway Traffic Safety Administration. Available at www.nhtsa.gov/sites/nhtsa.dot.gov/files/812048_resraint-performance-seatbelt-older-kids.pdf
- Klinich,, K. D., Reed, M. P., Manary, M. A., Orton, N. R., & Rupp, J. D. (2011, November). *Optimizing protection for rear seat occupants: assessing booster performance with realistic belt geometry using the Hybrid III 6YO ATD* (Report No. UM-2011-40). Washington, DC: National Highway Traffic Safety Administration. Available at <https://deepblue.lib.umich.edu/bitstream/handle/2027.42/90973/102860.pdf?sequence=1&isAllowed=y>
- Li, H. R., Pickrell, T. M., & KC, S. (2016, September). The 2015 National Survey of the Use of Booster Seats (Report No. DOT HS 812 309). Washington, DC: National Highway Traffic Safety Administration. Available at <https://crashstats.nhtsa.dot.gov/Api/Public/ViewPublication/812309>
- Manary, M. A., Klinich, K. D., Boyle, K. J., Orton, N. R., Eby, B., & Weir, Q. (2016, January) Development of a *Surrogate Shoulder Belt Retractor for Sled Testing* (Report No. UMTRI-2016-21). Washington, DC: National Highway Traffic Safety Administration. Available at <https://deepblue.lib.umich.edu/bitstream/handle/2027.42/140786/UMTRI-2016-21.pdf?sequence=1&isAllowed=y>
- National Highway Traffic Safety Administration. (2014, February 16). Laboratory Test Procedure for FMVSS No. 213, Child Restraint Systems (Test No. TP-213-10). Washington, DC: Author. Available at <https://one.nhtsa.gov/staticfiles/nvs/pdf/TP-213-10.pdf>
- Reed, M. P. & Klinich, K. D. (2016). Predicting vehicle belt fit for children ages 6-12, *Traffic Injury Prevention, 17*(1):58-64. doi: 10.1080/15389588.2015.1040877
- Reed, M. P., Ebert, S. M., Klinich, K. D., & Manary, M. A. (2008, September). *Assessing child belt fit, Volume I: Effects of vehicle seat and belt geometry on belt fit for children with and without belt-positioning booster seats* (Report No. UMTRI- 2008-49-1). Washington, DC: National Highway Traffic Safety Administration. Available at <http://mreed.umtri.umich.edu/mreed/pubs/UMTRI-2008-49-1.pdf>
- Reed, M. P., Ebert, S. M., & Jones MLH (2017, February). Vehicle occupant nationality study: Japanese (Report UMTRI-2017-3). Ann Arbor, MI: University of Michigan Transportation Research Institute.
- Reed, M. P., Ebert, S. M., Sherwood, C. P., Klinich, K. D., & Manary, M. A., (2009). Evaluation of the static belt fit provided by belt-positioning booster seats *Accident Analysis and Prevention, 41*:598-607.

- Reed, M. P., Ebert-Hamilton, S. M., Klinich, K. D., Manary, M. A., & Rupp, J. D. (2013). Effects of vehicle seat and belt geometry on belt fit for children with and without belt positioning booster seats *Accident Analysis and Prevention*, 50:512-522. doi:10.1016/j.aap.2012.05.030
- Reed, M. P., Ebert-Hamilton, S. M., Manary, M. A., Klinich, K. D., & Schneider, L. W. (2005). A new database of child anthropometry and seated posture for automotive safety applications (Technical Paper 2005-01-1837) *SAE Transactions: Journal of Passenger Cars - Mechanical Systems*, Vol. 114.
- Reed, M. P., Ebert-Hamilton, S. M., Manary, M. A., Klinich, K. D., & Schneider L. W. (2006). Improved positioning procedures for 6YO and 10YO ATDs based on child occupant postures (Technical Paper 2006-22-0014). *Stapp Car Crash Journal*, 50:337-388.
- Reed, M. P. & Ebert-Hamilton, S. M. (2013). Distribution of belt anchorage locations in the second row of passenger cars and light trucks. *SAE International Journal of Transportation Safety*. 10.4271/2013-01-1157.
- Rhule, D., Rhule, H., & Donnelly, B. (2005, June). The Process of Evaluation and Documentation of Crash Test Dummies for Part 572 of the Code of Federal Regulation. (Paper Number 05-0284 presented at 19th Annual ESV Conference, June 6-9, 2005, Washington, DC. Available at <http://citeseerx.ist.psu.edu/viewdoc/download?doi=10.1.1.621.5617&rep=rep1&type=pdf>
- Rouhana, S. W., McCleary, J. D., & Jedrzejczak, E. A. (1990). Assessing submarining and abdominal injury risk in the Hybrid III family of dummies: Part II - Development of the small female frangible abdomen (SAE Technical Paper No. 902317). *Proceedings of the Thirty-Fourth Stapp Car Crash Conference*, November 4-7, 1990, Orlando, FL. Warrendale, PA: SAE International.
- Society of Automotive Engineers. (2008). SAE Recommended Practice J2732, Motor vehicle seat dimensions.. Warrendale, PA: SAE International.
- Summers, L. K. (2015a, March 11). Child Frontal Impact Sled-Feb 2015. In Docket No. NHTSA-2013-0055-0002. Washington, DC: National Highway Traffic Safety Administration. Available at www.regulations.gov/document?D=NHTSA-2013-0055-0002
- Summers, L. K. (2015b, July 29). Memorandum re: Modifications of the Preliminary Drawings of an Upgraded Standard Seat Assembly to Evaluate Child Restraint Systems. In Docket No. NHTSA-2013-0055-0008. Washington, DC: National Highway Traffic Safety Administration. Available at www.regulations.gov/document?D=NHTSA-2013-0055-0008
- Summers, L. K. (2015c, August 21). Updated Preliminary Drawings (V2) of an Upgraded Standard Seat. In Docket No. NHTSA-2013-0055-0015. Washington, DC: National Highway Traffic Safety Administration. Available at www.regulations.gov/contentStreamer?documentId=NHTSA-2013-0055-0015&attachmentNumber=1&contentType=pdf

Transport Canada. (2010). CMVSS 213-Child Restraint Systems. Ottawa, Ontario, CA:
Author. www.tc.gc.ca/eng/acts-regulations/regulations-sor2010-90.htm

APPENDIX A

Instructions for surrogate retractor use

Surrogate Retractor User Instructions

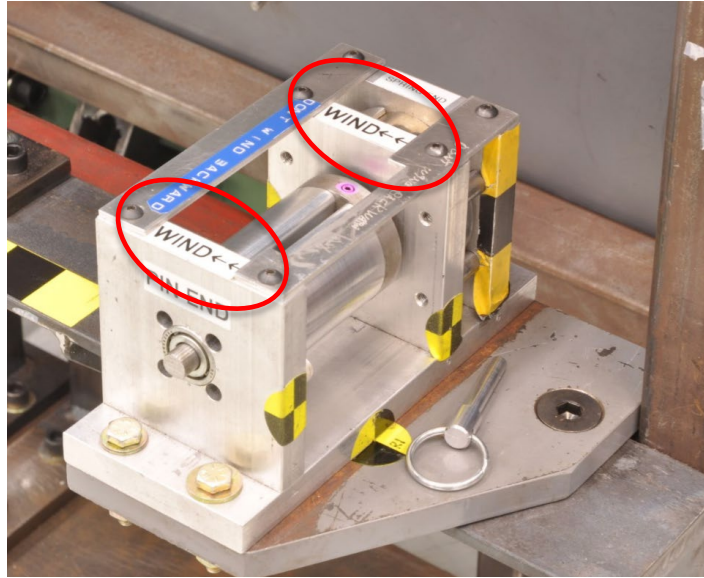
1. When the retractor is assembled, the spring should be installed coiled in the clockwise direction when looking at the spring end of the retractor with the cover off. The inner end of the spring should be punched and bolted to the spring-side shaft of the retractor. The outer end of the spring is bolted to the housing tube.



2. Loosely route the belt webbing through the belt path to restrain the ATD by passing through the D-ring, across the ATD chest, through the inboard lap belt webbing anchor and to the outboard lap belt webbing anchor.



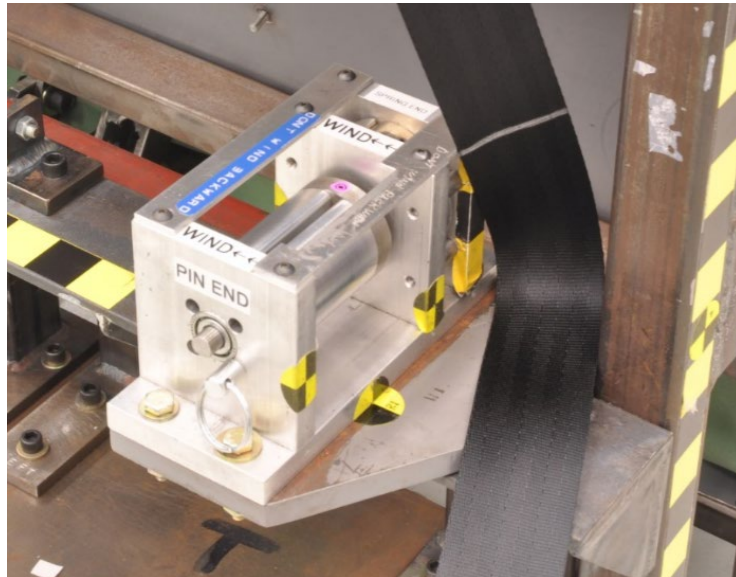
3. To tension the retractor, the user should only rotate the spindle in the direction indicated by the arrows on the top of the retractor assembly. See assembly drawings for more details.



4. Mount the retractor assembly at mid height on the back of the test bench, at approximately the same vertical height as the tether anchor. The surrogate retractor should be oriented with the long axis of the spindle aligned with the direction of impact and the spring end of the retractor facing forward and the pin end of the retractor facing rearward. The surrogate retractor should be mounted under the D-ring to be used, and located so that the webbing path will be vertical between the retractor and the D-ring.



5. Turn the spindle 10 half turns (5 full rotations) to create the 213-specified belt tension. Note that the user should only turn the spindle in the direction indicated by the arrow on top of the retractor hardware, so that the spring will work correctly and not break. Once you have completed winding, pin the retractor using any pin slot. This will prevent rotation of the spindle while the belt is threaded through the retractor.



6. Thread the shoulder belt end of the webbing through the 3-bar clip so it is about 15 inches from the end of the webbing. Mark the webbing about 250 mm (10 inches) from the end.



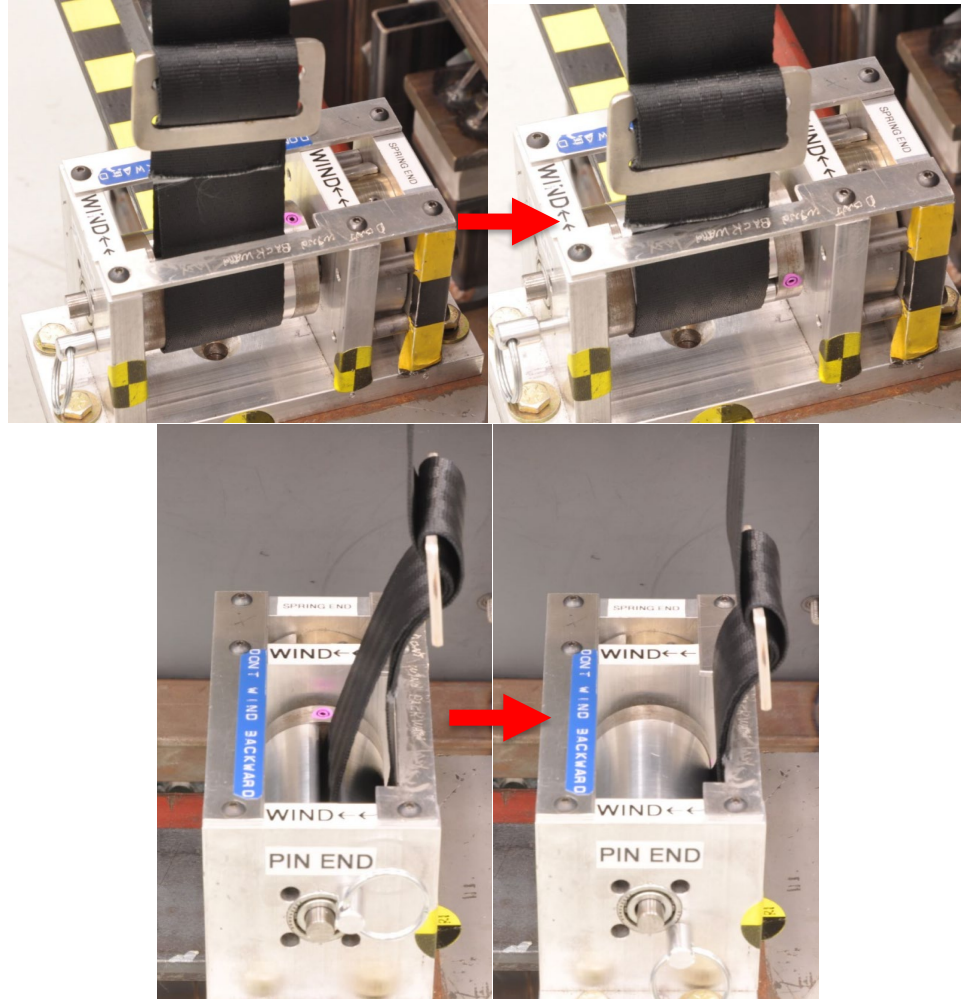
7. Thread the end of the webbing down through the split drum of the surrogate retractor until the 250 mm mark is visible. Then direct the webbing tail under the top framing bracket along the right side of the spindle.



8. Route the webbing through the 3-bar clip, leaving about 5 inches of webbing tail. Route the tail end of the webbing back through the clip to lock it.

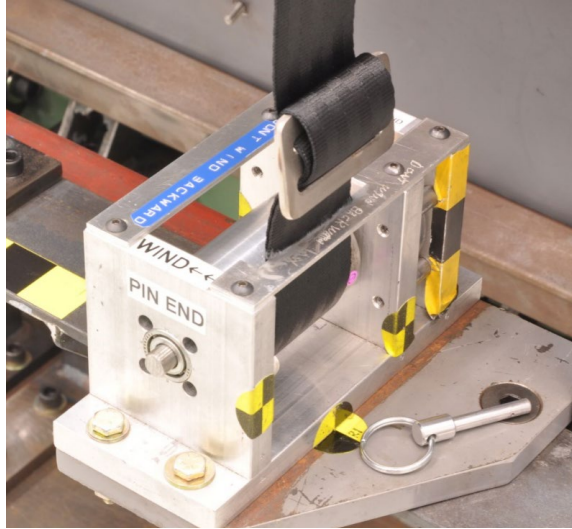


9. Hold the belt webbing above the 3-bar clip. Unpin the surrogate retractor and allow 50 mm (2 inches) of the webbing to wind back on the spindle by allowing the spindle to rotate one-quarter of a turn. (Note: the spring tension will turn the spindle opposite to the arrow direction, but this ok.) The quarter-turn change is represented in the photos below by the movement of the pink dot from the top to the right side of the spindle. Re-pin the retractor using any slot.



10. Secure the webbing at the outboard lap belt anchor, removing all excess belt from the system without shifting the ATD position.

11. Unpin the surrogate retractor just before the test. Check that the spindle of the surrogate retractor does not rotate when the pin is removed.



APPENDIX B

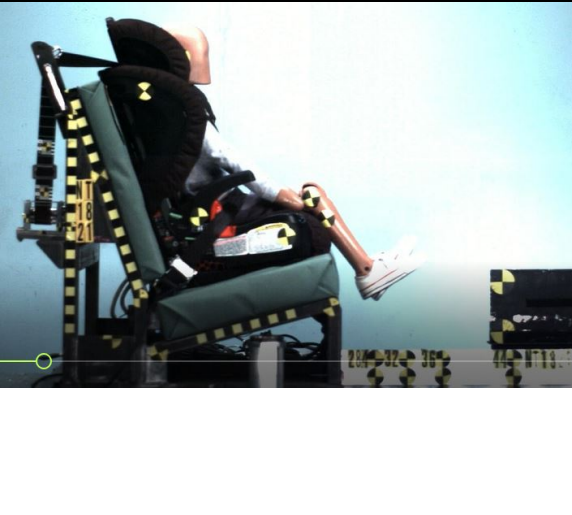
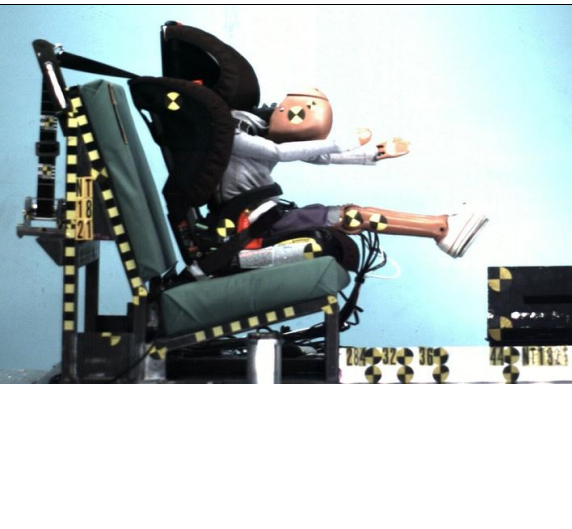
Examples for each ATD/CRS pairing

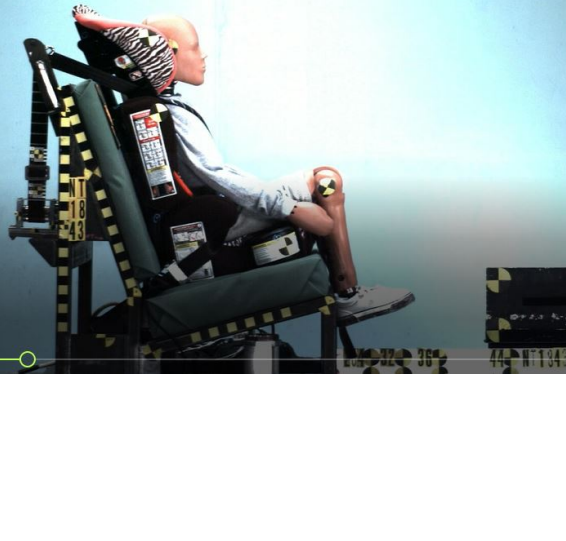
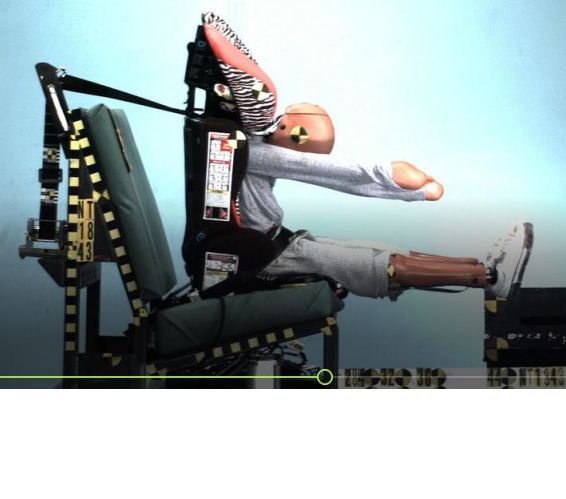
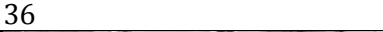
Images at initial position and maximum head excursion from overhead and right side cameras

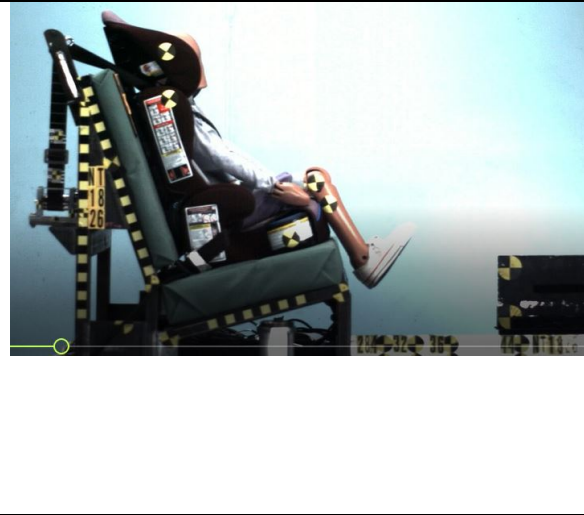
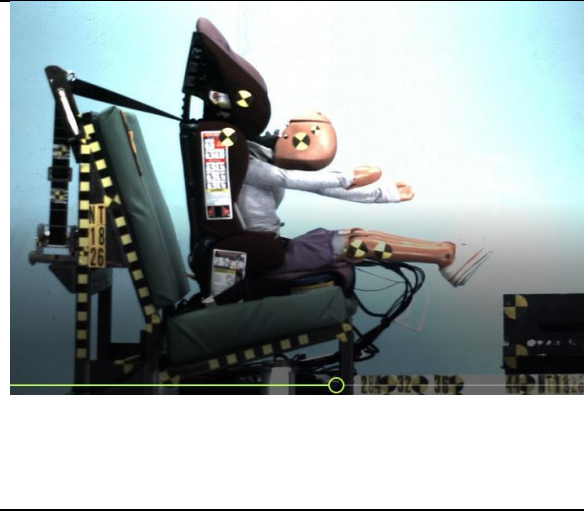
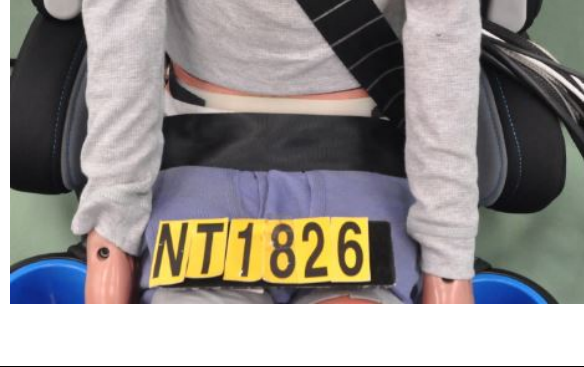
Pre-test photos of shoulder belt and lap belt fit

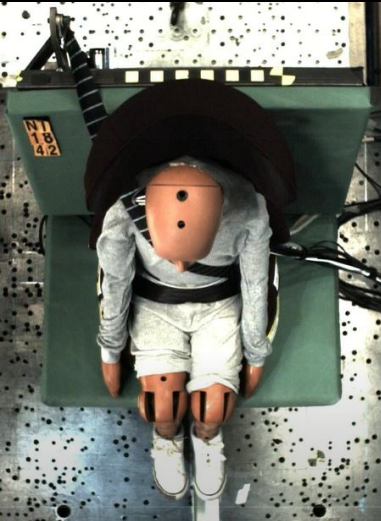
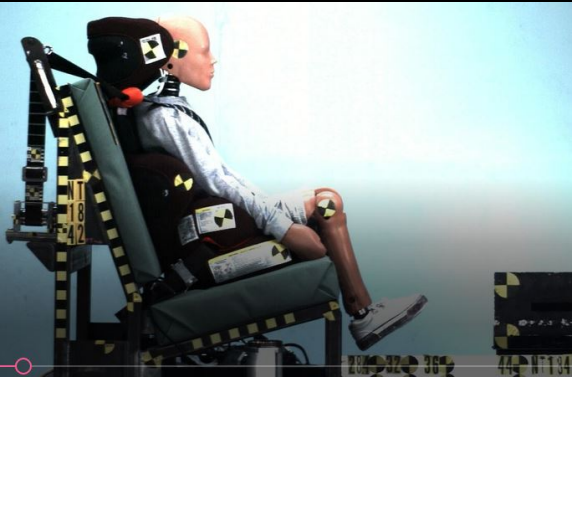
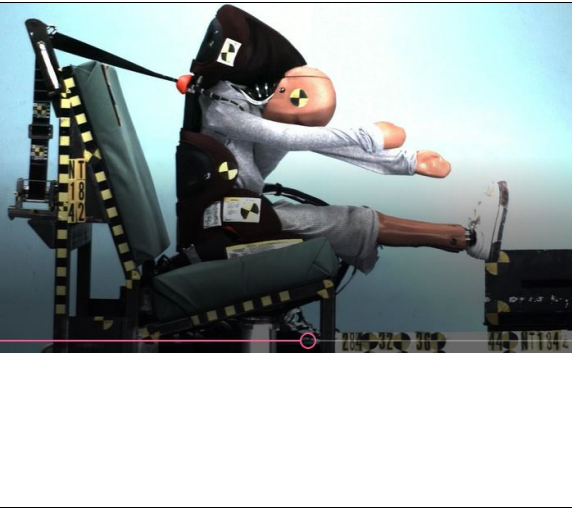
Shoulder belt score and lap belt score

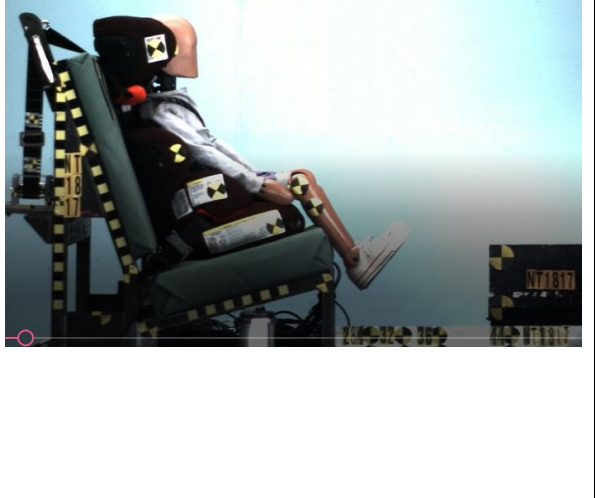
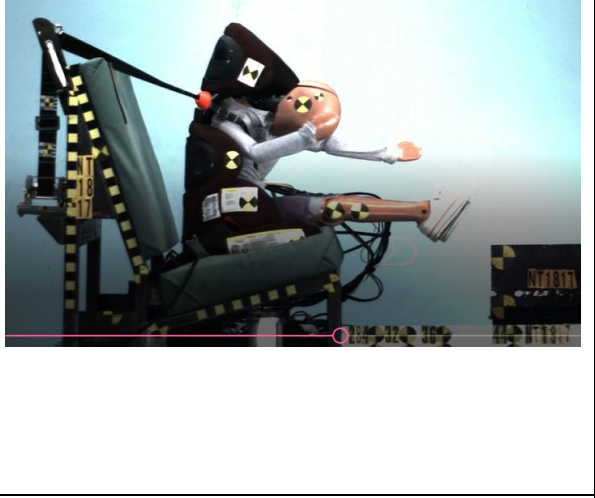
6YO	NT1815	Aidia Pathfinder
T0		
Tmax		
SBS	19	LBS Mean
	19	15.4
		

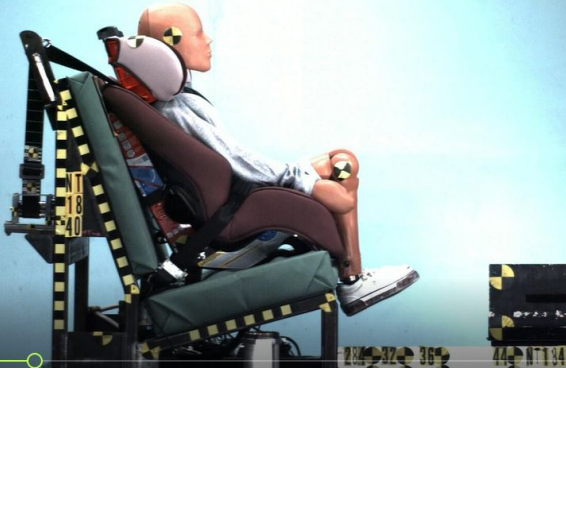
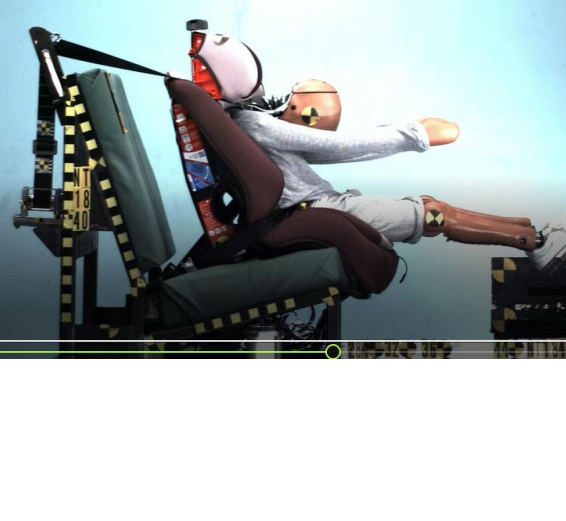
6YO	NT1821	Britax Pioneer
T0		
Tmax		
SBS	19	LBS Mean 21.5
		

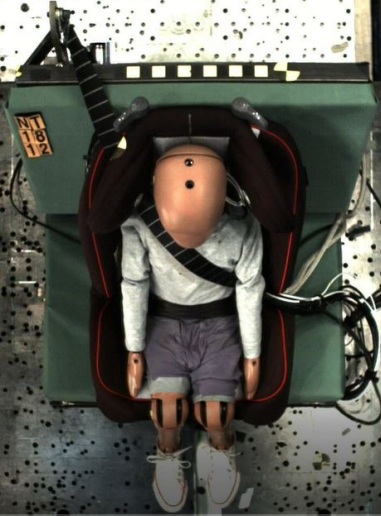
10YO	NT1843	BabyTrend Hybrid 3-in-1
T0		
Tmax		
SBS	36	LBS Mean
36		

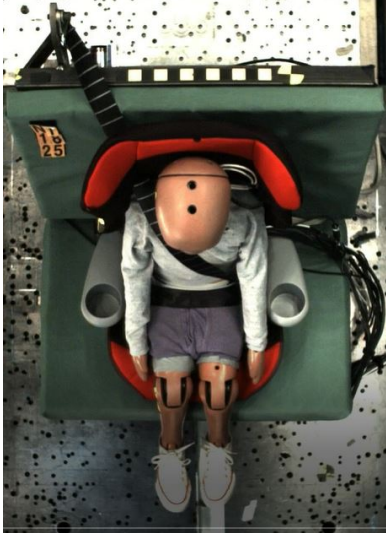
6YO	NT1826	BabyTrend Hybrid 3-in-1
T0		
Tmax		
	SBS	LBS Mean
	27	16
		

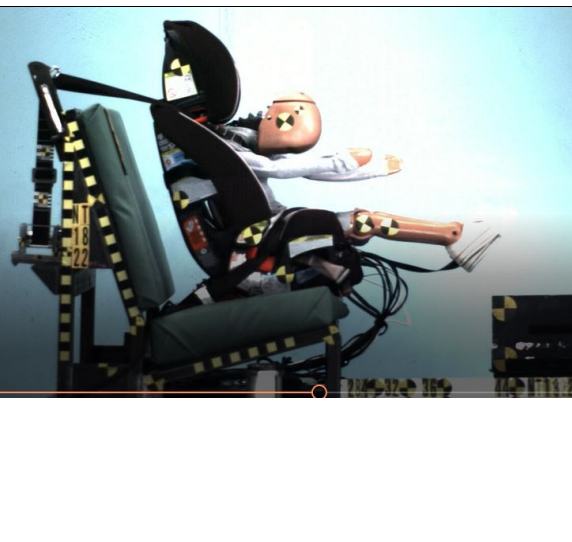
10YO	NT1842	Combi Kobuk
T0		
Tmax		
SBS	44	LBS Mean
44		42
		

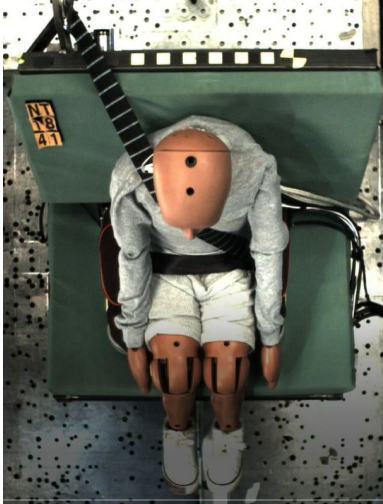
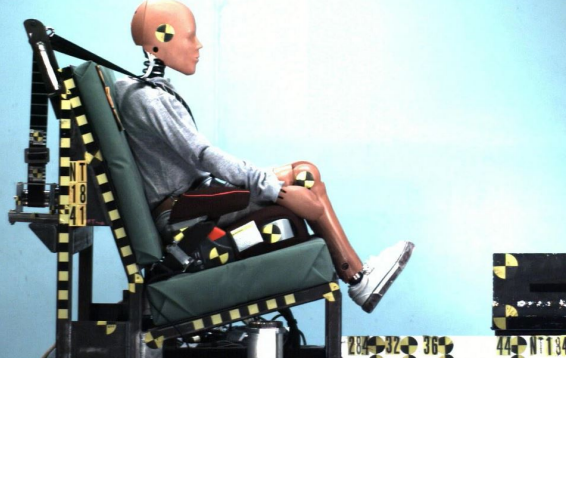
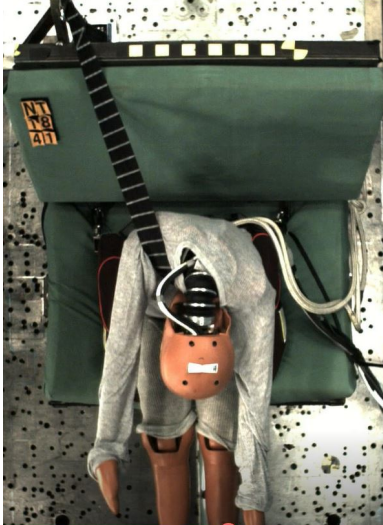
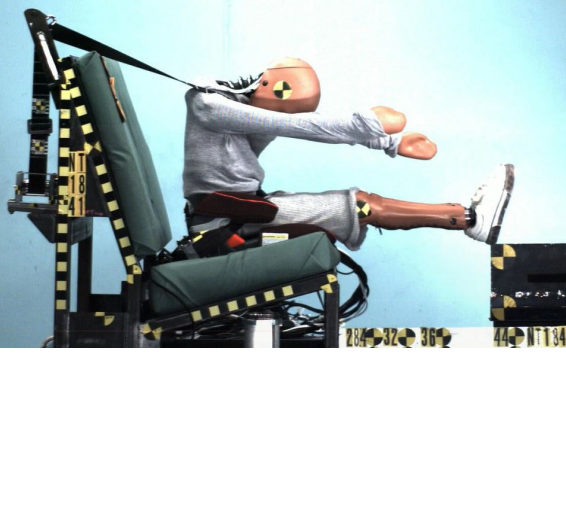
6YO	NT1817	Combi Kobuk
T0		
Tmax		
SBS	23	LBS Mean
		

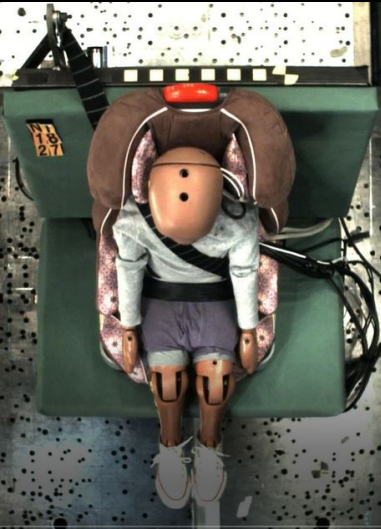
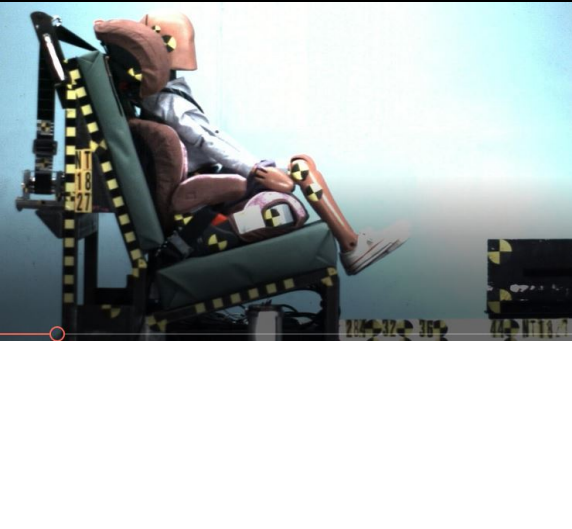
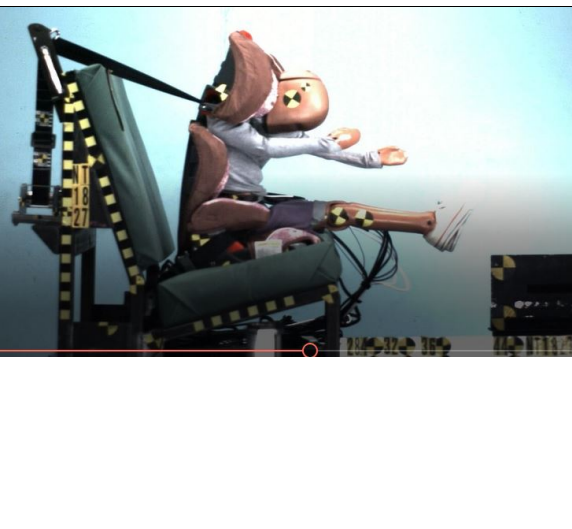
10YO	NT1840	Cosco Easy Elite
T0		
Tmax		
SBS	5	LBS Mean
	5	13
		

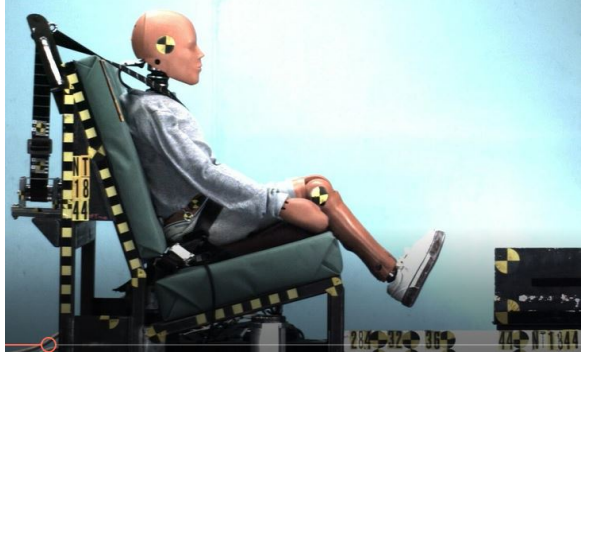
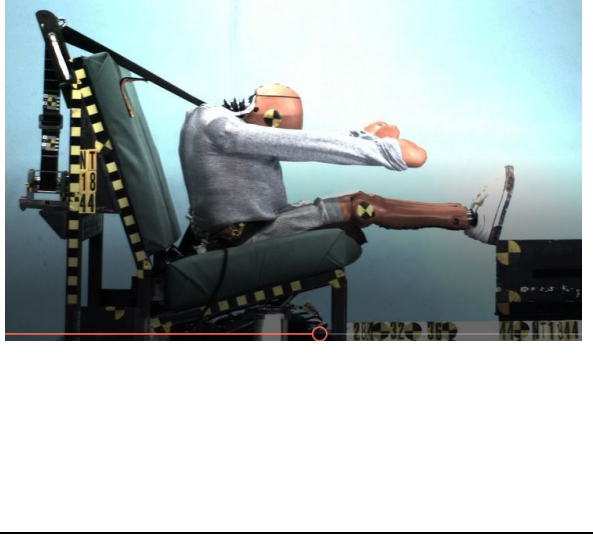
6YO	NT1812	Cosco Easy Elite
T0		
Tmax		
	SBS	LBS Mean
	0.2	8
		

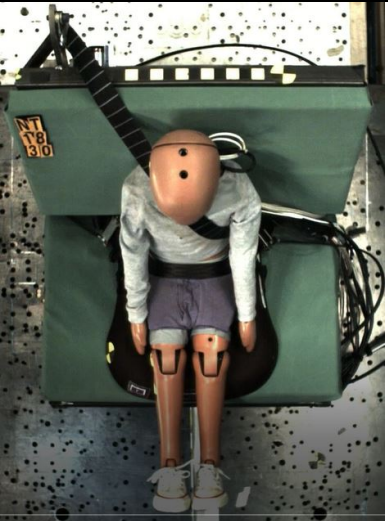
6YO	NT1825	Evenflo Amp HB
T0		
Tmax		
	SBS	LBS Mean
	23	24
		

6YO	NT1822	Graco 4Ever
T0		
Tmax		
	SBS	LBS Mean
	8	14
		

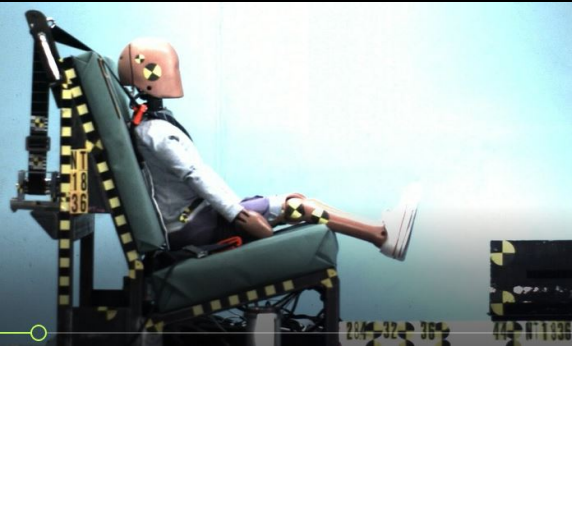
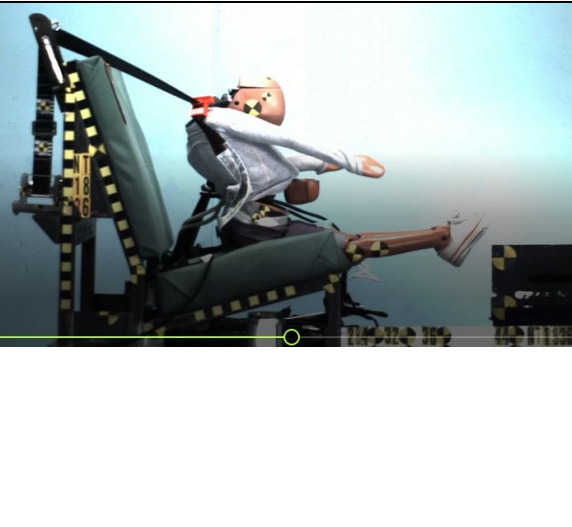
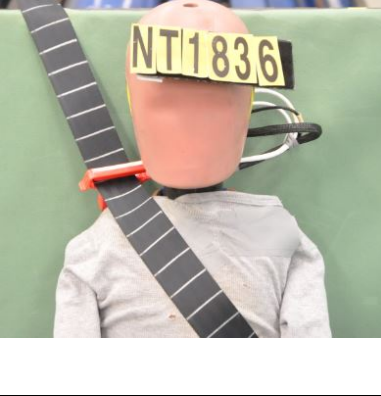
10YO	NT1841	Graco TurboBooster BB
T0		
Tmax		
	SBS	LBS Mean
	30	39
		

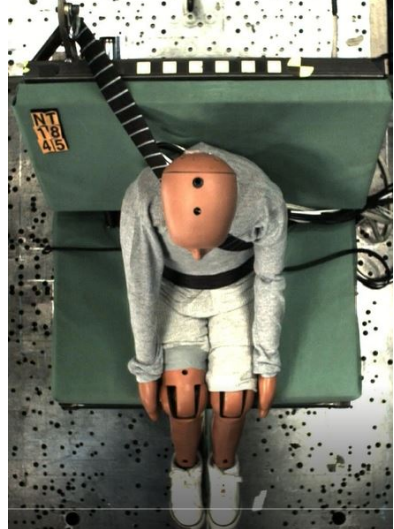
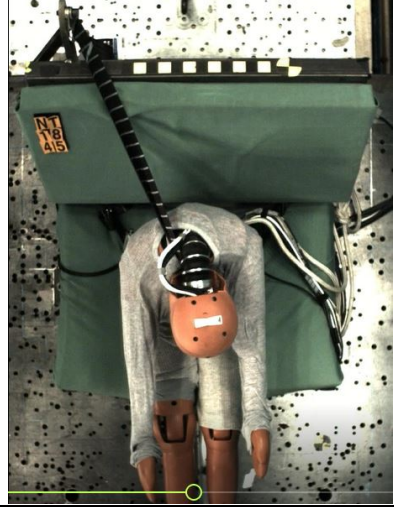
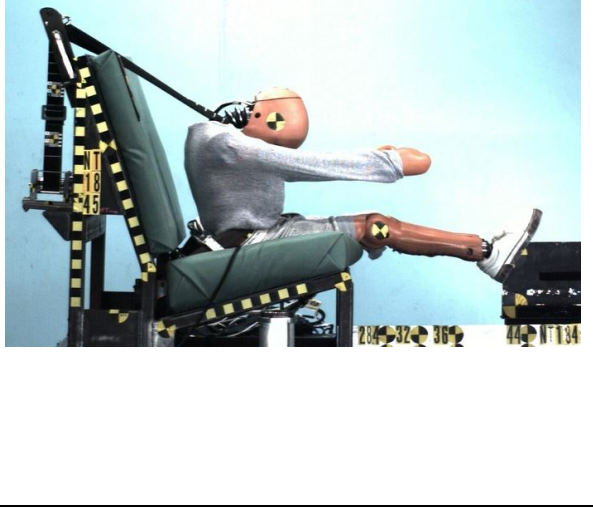
6YO	NT1827	Graco TurboBooster HB
T0		
Tmax		
	SBS	LBS Mean
	23	19
		

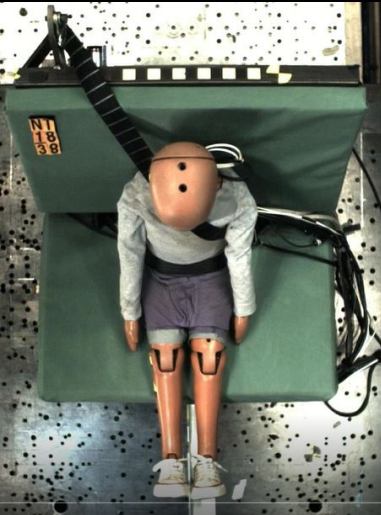
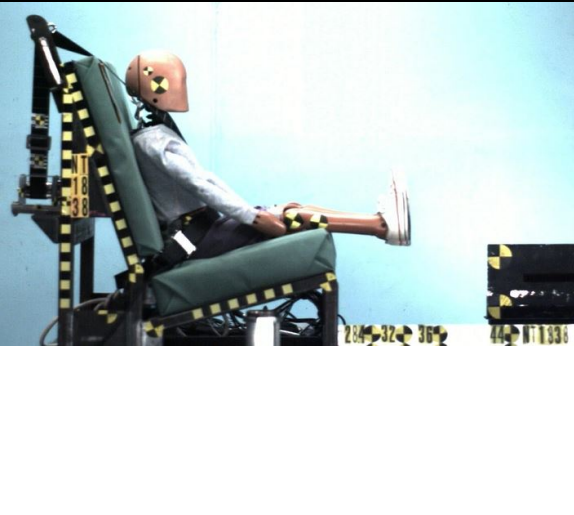
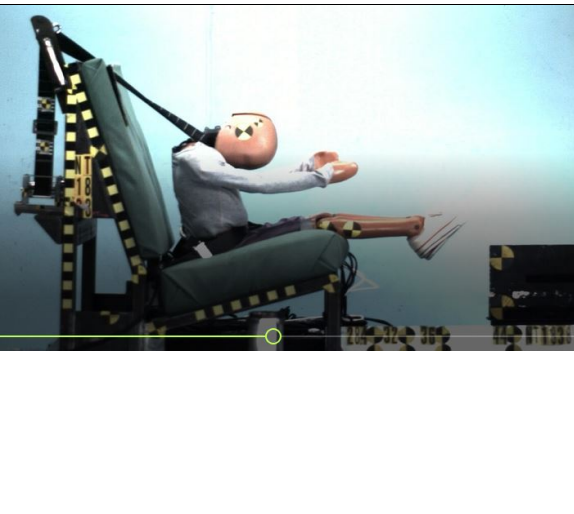
10YO	NT1844	Incognito
T0	 <p>Front view of the crash test dummy NT1844 at time T0. The dummy is seated in a green seat, wearing a grey long-sleeved shirt and white shorts. A black seatbelt is visible across its chest. The dummy's head is positioned forward, and its arms are at its sides.</p>	 <p>Side view of the crash test dummy NT1844 at time T0. The dummy is seated in a green seat, wearing a grey long-sleeved shirt and white shorts. A black seatbelt is visible across its chest. The dummy's head is positioned forward, and its arms are at its sides.</p>
Tmax	 <p>Front view of the crash test dummy NT1844 at time Tmax. The dummy is seated in a green seat, wearing a grey long-sleeved shirt and white shorts. A black seatbelt is visible across its chest. The dummy's head is tilted back, and its arms are raised.</p>	 <p>Side view of the crash test dummy NT1844 at time Tmax. The dummy is seated in a green seat, wearing a grey long-sleeved shirt and white shorts. A black seatbelt is visible across its chest. The dummy's head is tilted back, and its arms are raised.</p>
SBS	-24	LBS Mean
	 <p>Close-up front view of the crash test dummy NT1844. The dummy is wearing a grey long-sleeved shirt and a black seatbelt. A yellow identification tag with the number 'NT1844' is visible on the dummy's chest.</p>	 <p>Close-up side view of the crash test dummy NT1844. The dummy is wearing a grey long-sleeved shirt and a black seatbelt. A yellow identification tag with the number 'NT1844' is visible on the dummy's chest.</p>

6YO	NT1830	Incognito
T0		
Tmax		
	SBS	LBS Mean
	-25	9
		

6YO	NT1829	Lil Fan
T0		
Tmax		
	SBS	LBS Mean
	23	9
		

6YO	NT1836	Mifold
T0		
Tmax		
	SBS	LBS Mean
	9	46
		

10YO	NT1845	None
T0		
Tmax		
SBS	-23	LBS Mean
		4
		

6YO	NT1838	None
T0		
Tmax		
	SBS	LBS Mean
	-35	6
		

APPENDIX C

Posture Comparisons: Mockup and Vehicle Configurations Compared to 6YO

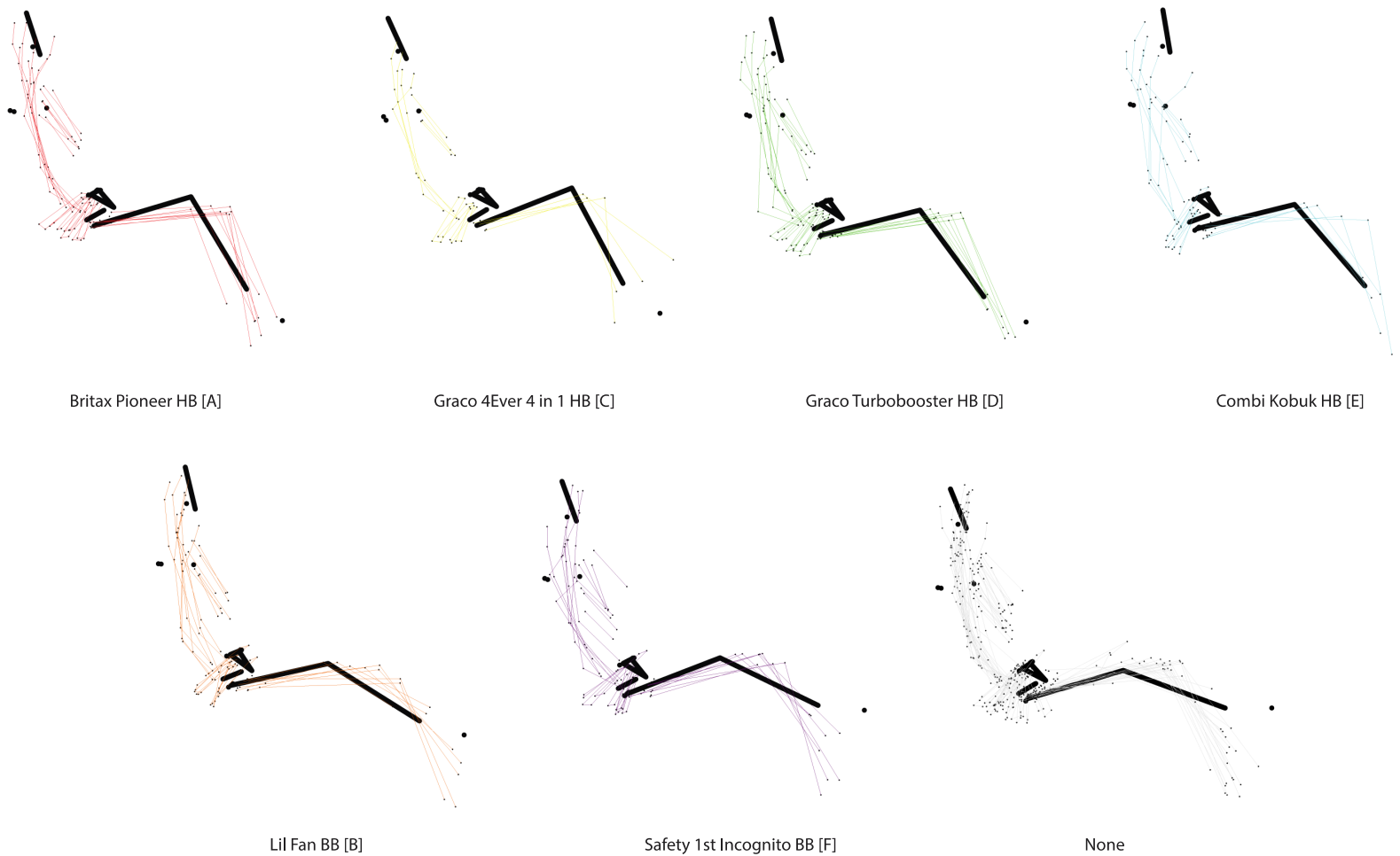


Figure C1. Comparison of postures of child volunteers overlaid and expressed w.r.t 6YO ATD across all booster configurations in B-Z mockup. Cushion Length = 465 mm; Seat back angle = 23-deg; Cushion angle = 14.5-deg.

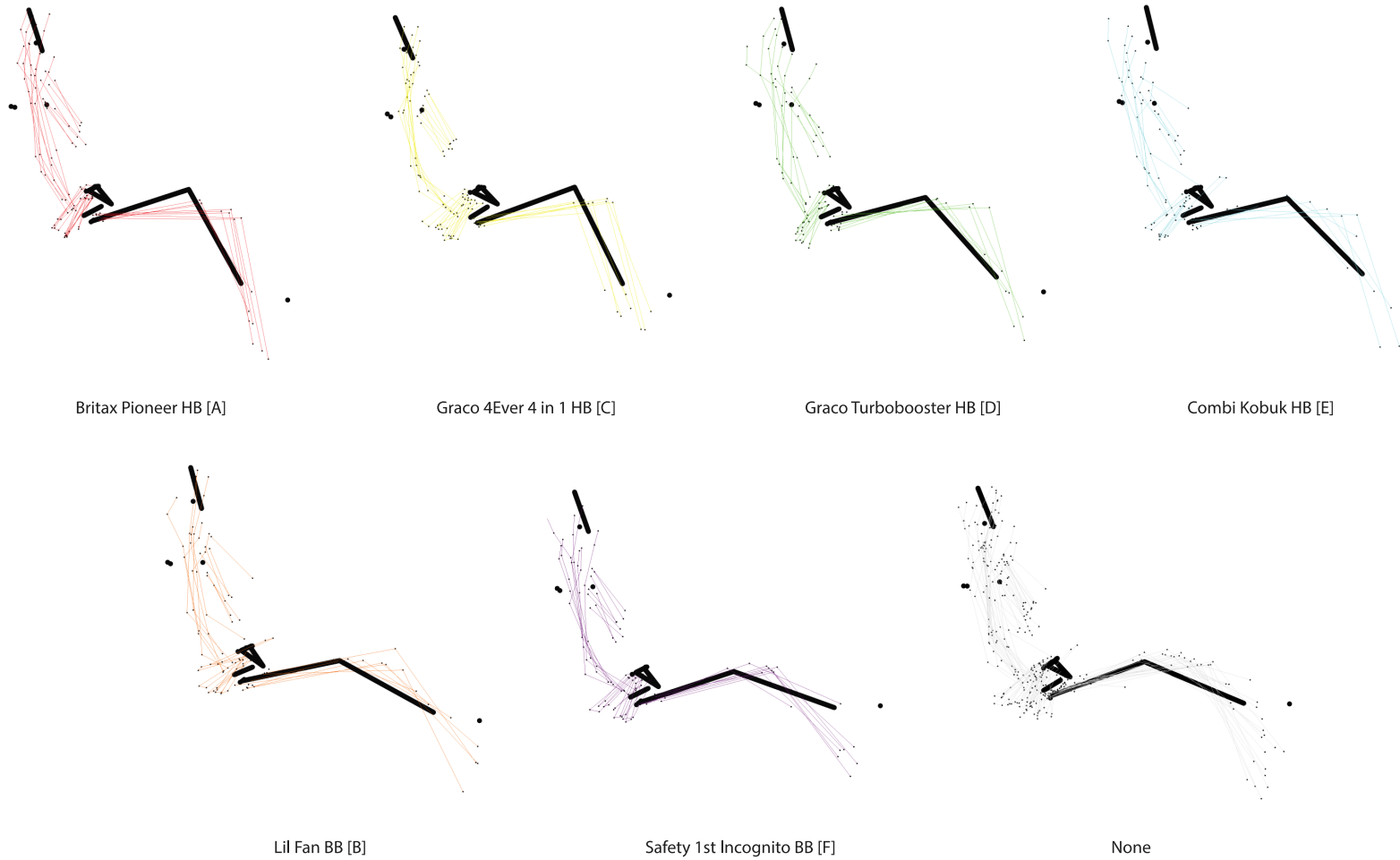


Figure C2. Comparison of postures of child volunteers overlaid and expressed w.r.t 6YO ATD across all booster configurations in B-B mockup. Cushion Length = 490 mm; Seat back angle = 23-deg; Cushion angle = 14.5-deg.

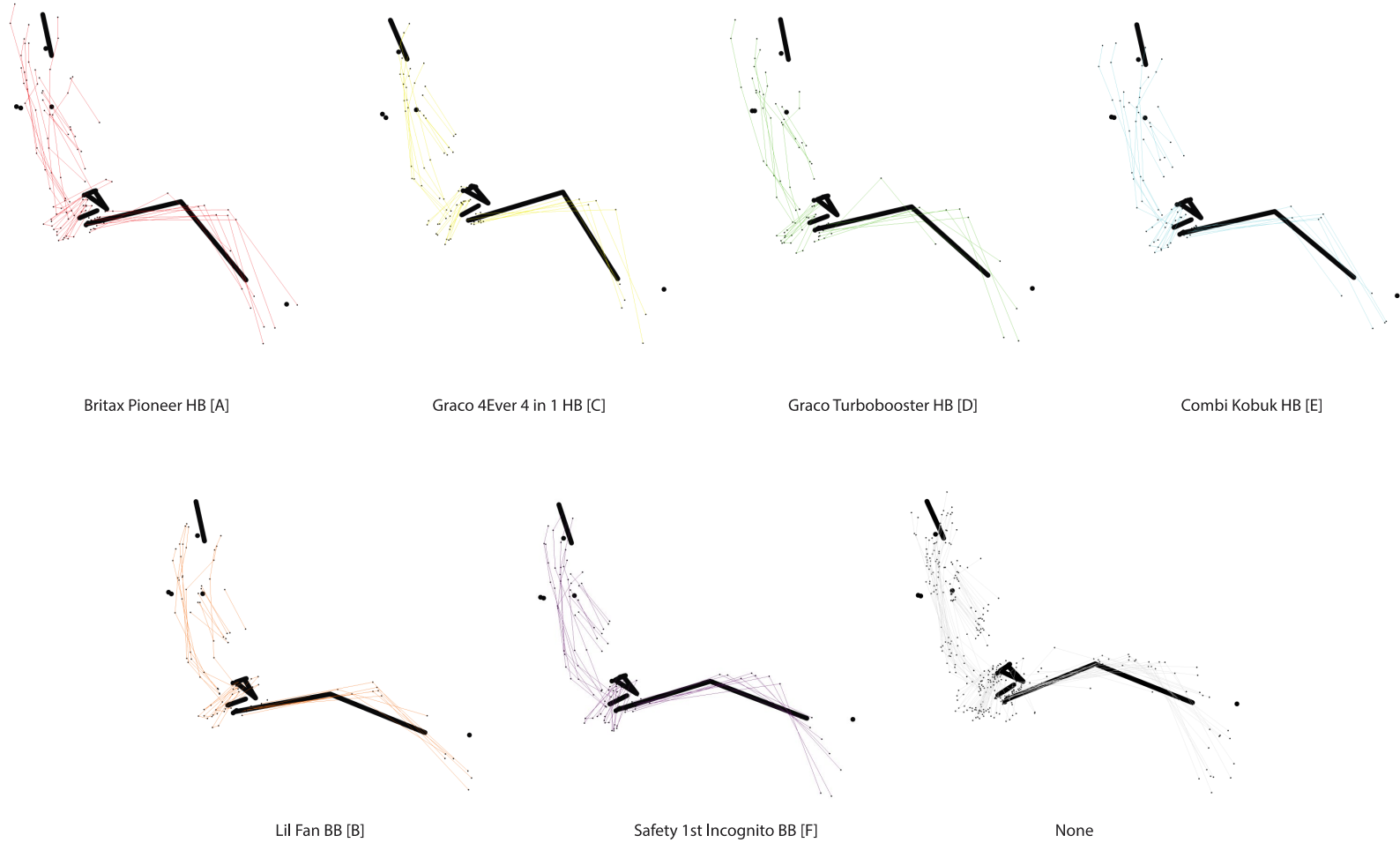


Figure C3. Comparison of postures of child volunteers overlaid and expressed w.r.t 6YO ATD across all booster configurations in B-L mockup. Cushion Length = 523 mm; Seat back angle = 23-deg; Cushion angle = 14.5-deg.

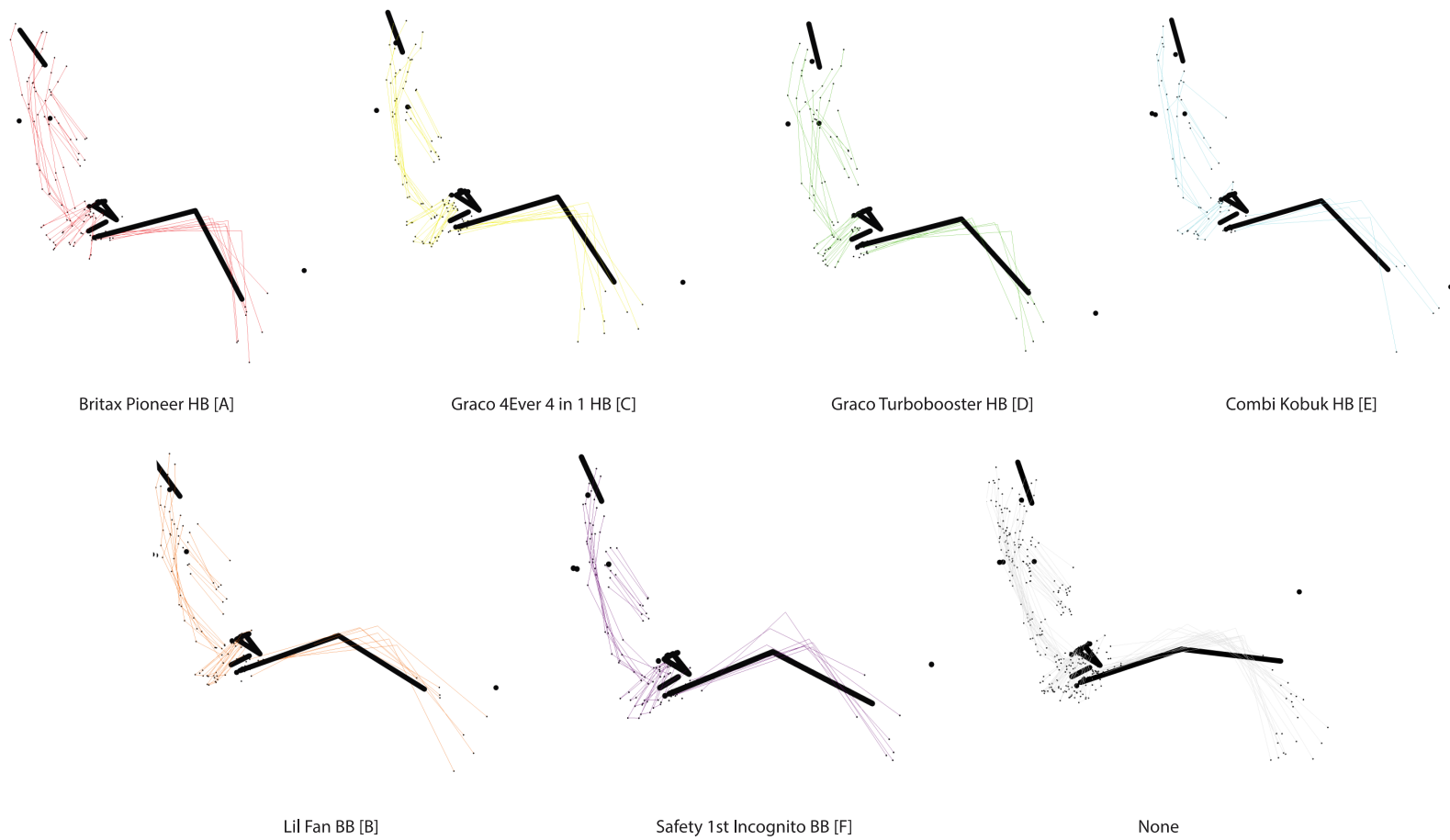


Figure C4. Comparison of postures of child volunteers overlaid and expressed w.r.t 6YO ATD across all booster configurations in TOYOTA vehicle. Cushion Length = 455 mm; Seat back angle = 26-deg; Cushion angle = 15-deg.



Figure C5. Comparison of postures of child volunteers overlaid and expressed w.r.t 6YO ATD across all booster configurations in JEEP vehicle. Cushion Length = 468 mm; Seat back angle = 22.5-deg; Cushion angle = 4-deg.

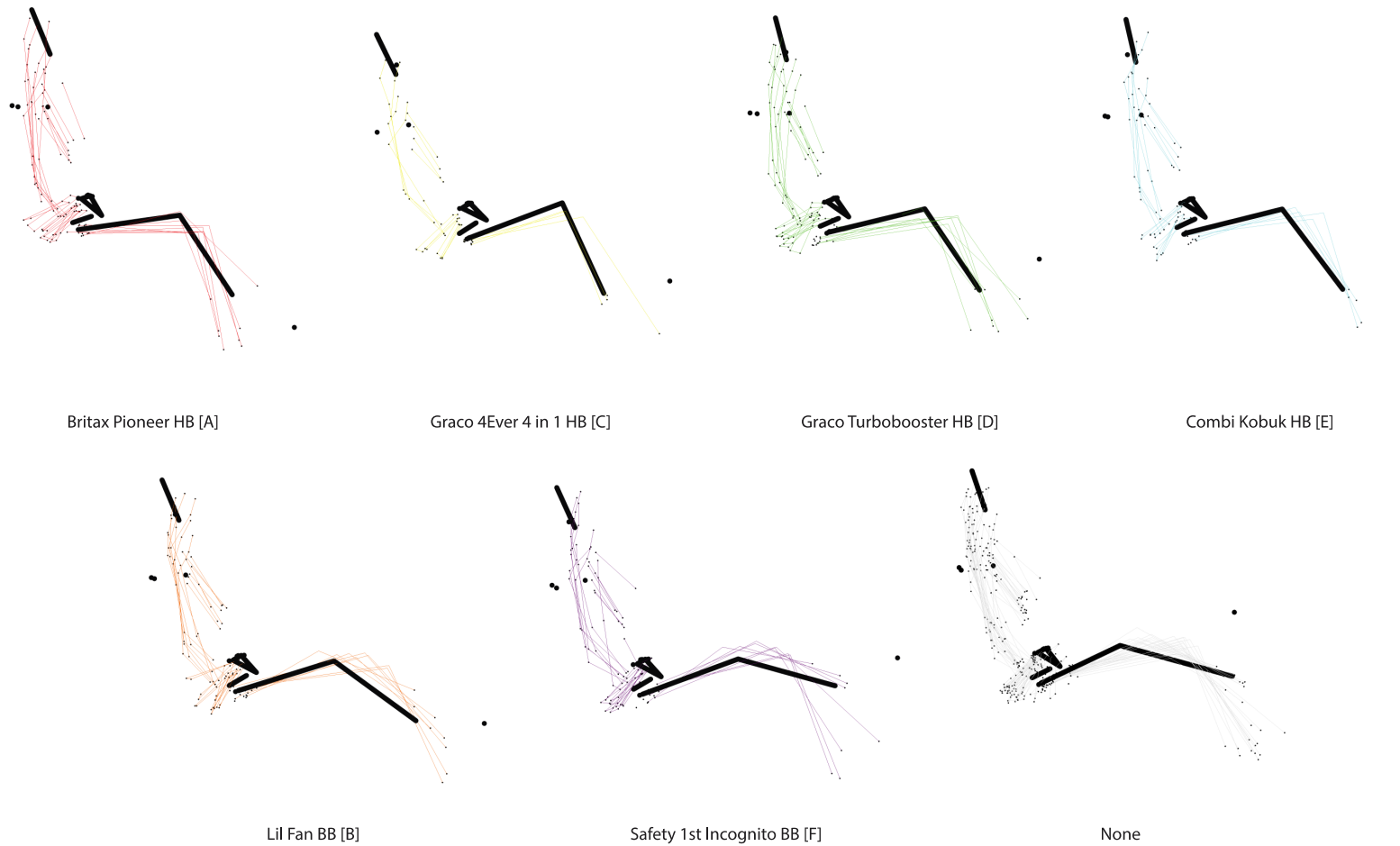


Figure C6. Comparison of postures of child volunteers overlaid and expressed w.r.t 6YO ATD across all booster configurations in MALIBUU vehicle. Cushion Length = 475 mm; Seat back angle = 23-deg; Cushion angle = 13-deg.

Posture Comparisons: Mockup and Vehicle Configurations Compared to 10YO and Small Female
6YO: solid black
10YO: solid gray
Small female: dashed gray

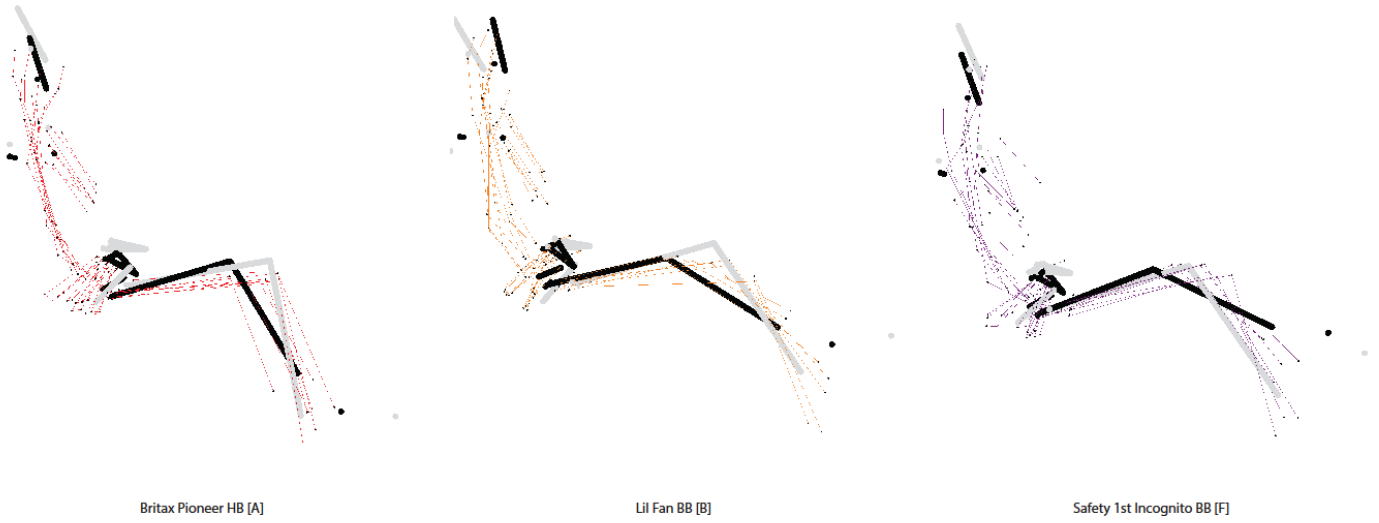


Figure C7. Comparison of postures of child volunteers with 10YO and small female across applicable booster configurations in B-Z mockup. Cushion Length = 465 mm; Seat back angle = 23-deg; Cushion angle = 14.5-deg.

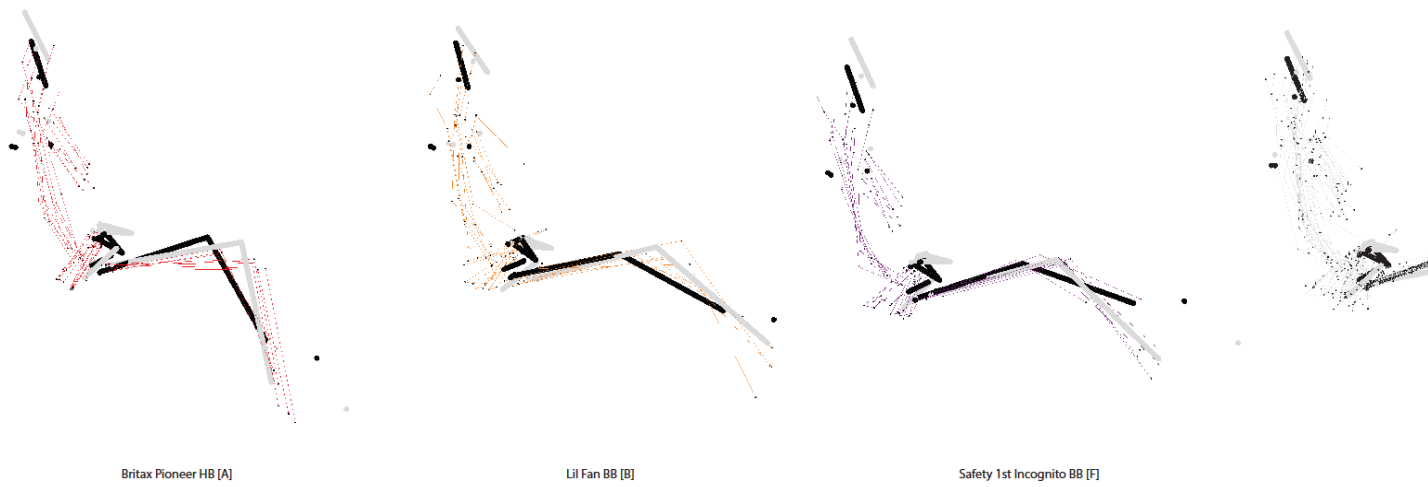
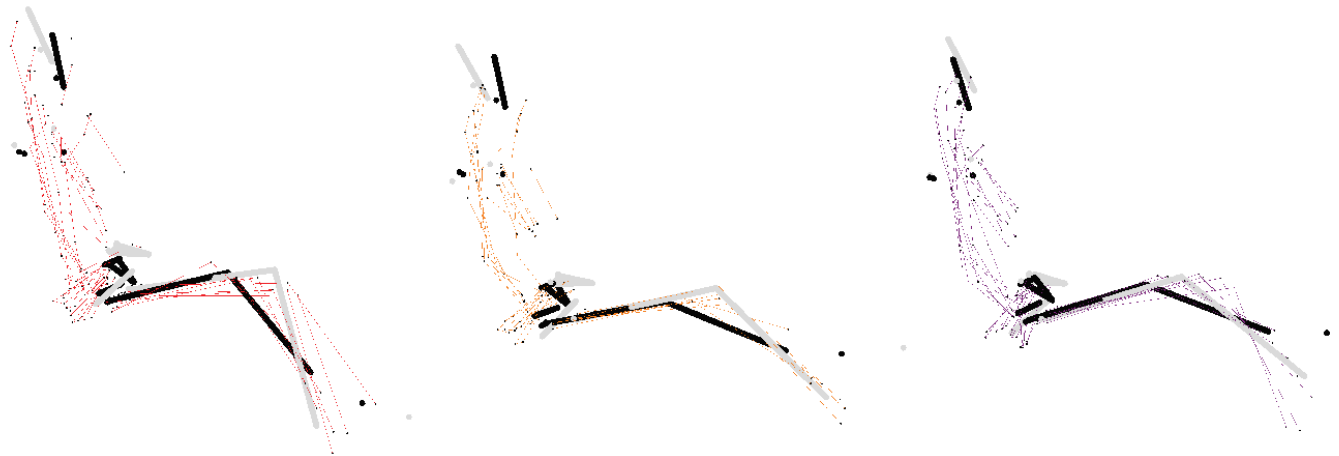


Figure C8. Comparison of postures of child volunteers with 10YO and small female across applicable booster configurations in B-B mockup. Cushion Length = 490 mm; Seat back angle = 23-deg; Cushion angle = 14.5-deg.

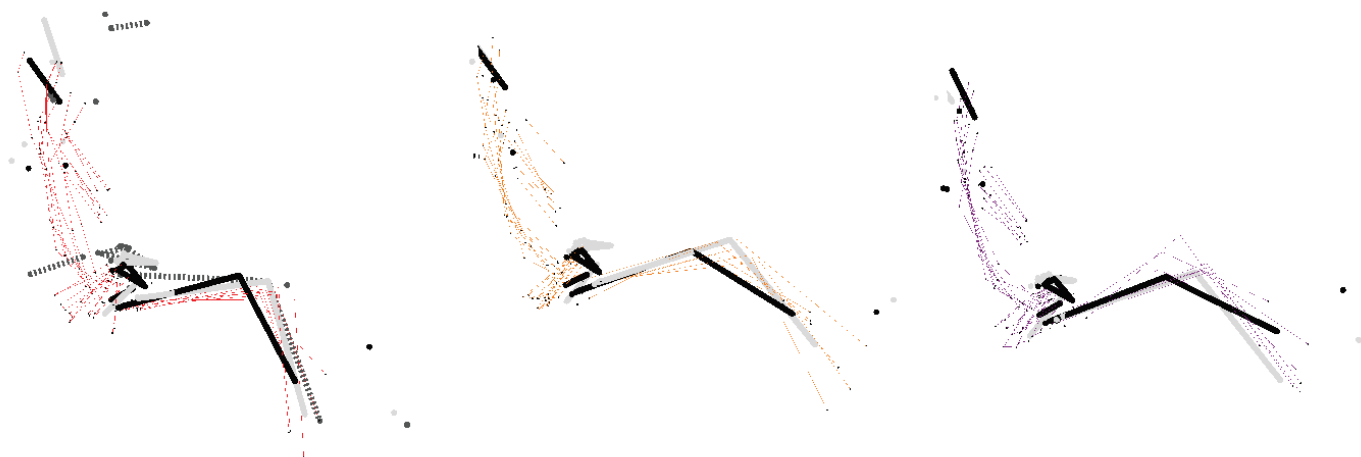


Britax Pioneer HB [A]

Lil Fan BB [B]

Safety 1st Incognito BB [F]

Figure C9. Comparison of postures of child volunteers with 10YO and small female across applicable booster configurations in B-L mockup. Cushion Length = 523 mm; Seat back angle = 23-deg; Cushion angle = 14.5-deg.

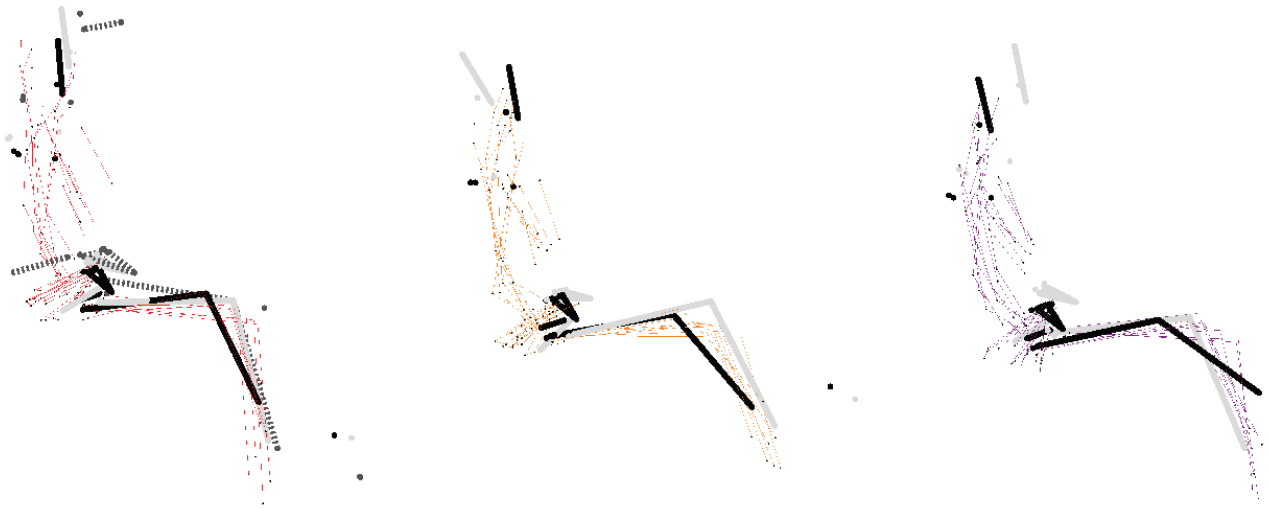


Britax Pioneer HB [A]

Lil Fan BB [B]

Safety 1st Incognito BB [F]

Figure C10. Comparison of postures of child volunteers with 10YO and small female across applicable booster configurations in TOYOTA vehicle. Cushion Length = 455 mm; Seat back angle = 26-deg; Cushion angle = 15-deg.

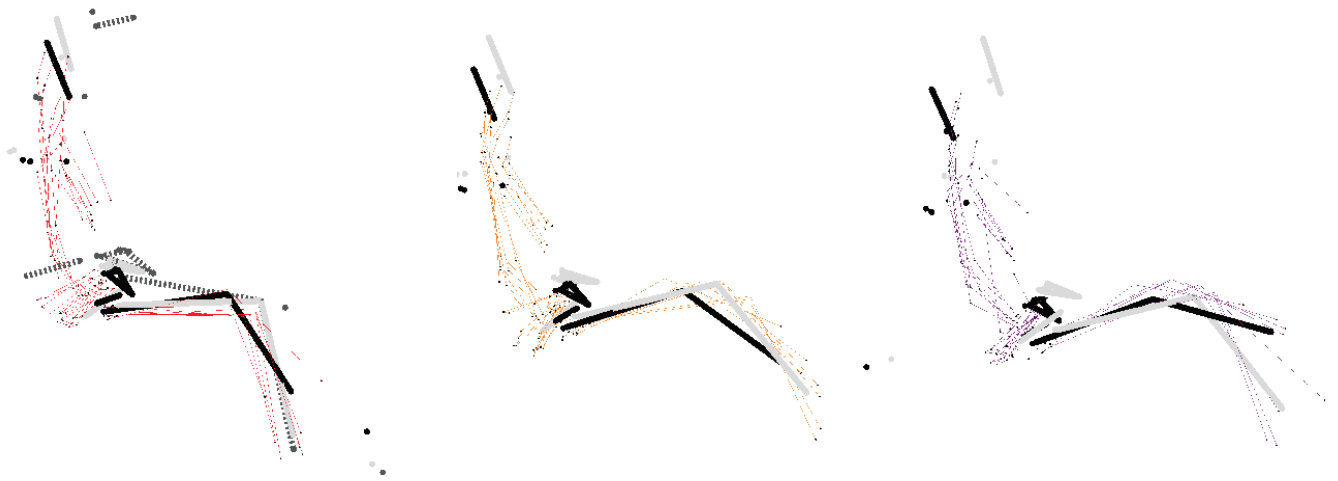


Britax Pioneer HB [A]

Lil Fan BB [B]

Safety 1st Incognito BB [F]

Figure C11. Comparison of postures of child volunteers with 10YO and small female across applicable booster configurations in JEEP vehicle. Cushion Length = 468 mm; Seat back angle = 22.5-deg; Cushion angle = 4-deg.



Britax Pioneer HB [A]

Lil Fan BB [B]

Safety 1st Incognito BB [F]

Figure C12. Comparison of postures of child volunteers with 10YO and small female across applicable booster configurations in MALIBUU vehicle. Cushion Length = 475 mm; Seat back angle = 23-deg; Cushion angle = 13-deg

DOT HS 812 919
April 2020



U.S. Department
of Transportation
**National Highway
Traffic Safety
Administration**

